Open-Mold Polyurethane Injection Bonding Process for Modular Exterior Automotive Parts

Experimental Verification of a Subframe for a Carbon Fiber Reinforced Plastic Roof with Class-A Surface Finish

Julia Sothmann

20.12.2017

TU Delft

Delft
University of
Technology

Open-Mold Polyurethane Injection Bonding Process for Modular Exterior Automotive Parts

Experimental Verification of a Subframe for a Carbon Fiber Reinforced Plastic Roof with Class-A Surface Finish

MASTER OF SCIENCE THESIS

For obtaining the degree of Master of Science in Aerospace Engineering at Delft University of Technology

Julia Sothmann

20.12.2017

Faculty of Aerospace Engineering · Delft University of Technology

Delft
University of
Technology

DELFT UNIVERSITY OF TECHNOLOGY
FACULTY OF AEROSPACE ENGINEERING
DEPARTMENT OF AEROSPACE STRUCTURES AND MATERIALS

GRADUATION COMMITTEE

Dated: <u>20.12.2017</u>

Chair holder:

_____

Committee Chair, Ir. Jos Sinke

Committee members:

_____

Dr.ir. J.M.J.F. (Julien) van Campen

_____

Dr. Hans Poulis

_____

Dipl.-Ing. (FH) Rainer Hauk

_____

Fourth Committee Member

Restriction Note / Sperrvermerk

Die vorliegende Arbeit enthält firmeninterne Informationen und vertrauliche Daten des Unternehmens Mercedes-AMG GmbH, Affalterbach und gegebenenfalls von mit Mercedes-AMG im Sinne von §15 AktG verbundenen Unternehmen.

Sie darf aus diesem Grunde nur zu Prüfungszwecken verwendet und ohne ausdrückliche Genehmigung durch Mercedes-AMG (Leiter des betreuenden Fachbereichs, mindestens Führungskraftebene 3) weder Dritten zugänglich gemacht, noch ganz oder in Auszügen veröffentlicht werden.

Dies gilt für eine Dauer von 5 Jahren, es sei denn der Leiter des betreuenden Fachbereichs hält eine vorzeitige Veröffentlichung wegen der Qualität der firmeninternen Information und vertraulichen Daten für unbedenklich und bestätigt dies schriftlich.

Affalterbach, 20.12.2017

_____

Julia Sothmann

Für die Hochschule/Universität:

_____

Dr.ir. J.M.J.F. (Julien) van Campen

Abstract

The development and production of carbon fiber reinforced plastic exterior parts with Class-A surface finish in the automotive industry comes with a few challenges. Next to the structural design of the components, the surface quality, the joining technique and the Mercedes-AMG specific factory integration into the worldwide production lines of the Daimler AG need to be considered. The aim of this thesis was to qualify an in-house developed open-mold polyurethane injection bonding (OMPURIB) process to form and bond a subframe structure in one process to the inside of a carbon fiber reinforced plastic (CFRP) roof with Class-A surface finish. This subframe is required to bridge the Z-offset between CFRP roof and roof frame, which is used for both the panoramic roof of greater thickness as well as the thinner CFRP roof.

The polyurethane (PUR) subframe is ought to replace the current solution of a bonded CFRP subframe to offer more design flexibility for prospective roof designs with a potential of higher complexity. For the PUR subframe material and structure the same principle requirements hold as for the CFRP subframe. The main requirement is the bridging of the Z-offset using a hard material that can keep its structural integrity without causing print-through on the CFRP roof with Class-A surface finish. Additionally, the PUR has to adhere to both, the CFRP roof and the assembly adhesive used to bond the sub-assembly to the BIW, with at least 95% cohesion failure. Lastly, the lap-shear strength of the PUR should not be lower than the lap-shear strength of the assembly adhesive, even after aging, to guarantee the latter being the weak link.

The qualification was done by means of experimental material and process verification in close collaboration with the adhesives team at Daimler AG Sindelfingen. Fundamental tests were performed to analyze the bond properties, such as adhesion and lap-shear strength, depending on various pre-treatments and aging conditions. Subsequently, process and print-through tests were used for process assurance and the inspection of the surface quality. The latter were performed on flat plate specimens before the process application was tested on an actual Mercedes-AMG GT R CFRP roof.

The outcomes of this research project are bond properties using a process specific PUR material for CFRP-PUR-Steel(e-coated) bonds such as lap-shear strength, specimen stiffness

and adhesion, depending on the applied pre-treatments and experienced aging conditions. It was found that the PUR material complies with the material profile of requirements . The lap-shear strength is obtained in any case, whereas for sufficient adhesion pre-treatments are vital. The CFRP substrate has to be treated abrasively and a thin layer of primer has to be applied. For the application of the assembly adhesive, the PUR surface has to be sanded first, where the adhesion of different assembly adhesives varies with the hardening time of the PUR. An approach independent of the used assembly adhesive is a change of PUR mixing ratio from 100:58 to 100:64. Moreover, important observations with regards to profile variations during process optimization. The variation in width, height and angle along the edges, as well as the bottom shape are dependent on the tool and adherend respectively. The only process-driven factor is the thickness of the bulk and the slope shape, which are dependent on the injection rate and application speed, as well as the tilting direction of the mixing (and dispensing) head and the mold tool. It was found that the process is applicable for the roof application, but still requires fine tuning to optimize the PUR surface. During print-through tests of various thicknesses and an overmolded crash bar, the examination showed that print-through is dependent on the structural design. For the various thicknesses print-through along the bond line only appears for bond lines greater than 15 mm, which can be reduced if the transition between PUR and CFRP substrate is designed smoother (no 90° angle). Looking at the steel crash bar samples no bond line print-through was visible, but slight warping of the CFRP plate caused by differences in thermal expansion between the three materials and moisture absorption. The effect could be less when examining assembly parts with higher flexural rigidity.

The final experiment was the process application onto a Mercedes-AMG GT R CFRP roof based on a CAD design, including the integration of spacers. This test proved the applicability of the process onto a CFRP roof including functional integration. Process-related and print-through related the subframe passed the first examination. Further testing in the final vehicle assembly, as well as dynamic testing and weathering on an actual vehicle need to be performed as the final steps of the technology qualification.

Subsequently to the experimental verification of the technology, possibilities for industrialization were considered. A market analysis was performed and considerations were made for possible technology transfer to different vehicle parts as well as different industries. It was found that the technology as discussed in this thesis does not exist on the market yet and leaves room for further applications. Therefore a patent was requested. Once patented, the technology can be presented to the suitable supplier, determined in the supplier strategy trade-off. Lastly, a cost analysis was performed and the PUR subframe costs were compared to the CFRP subframe cost. Replacing the current subframe solution results in a total saving of 167.68€(56%) per unit.

Acknowledgements

This thesis contains the research work I carried out at the Aerospace Structures and Materials department. It concludes my seven month of research at Mercedes-AMG GmbH and Daimler AG and is the final milestone of my long journey at TU Delft. During the six years I spent at TU Delft, I did not only build up my knowledge in aerospace engineering, but also met a lot of great people and gained valuable overseas experience.

I would like to thank everyone who contributed to this thesis and my successful completion of my study. Special appreciation goes to my supervisors Dr.ir. J.M.J.F. (Julien) van Campen and Dipl.-Ing. (FH) Rainer Hauk for the opportunity and the assistance during the research execution and writing of this thesis. Further thanks go to the adhesives research team at Daimler AG Sindelfingen, without whom I would have not been able to perform my work and who helped me to extend my knowledge on adhesives.

Moreover, I would like to thank everyone who was part of my journey and led me to become the person who I am today. Finally, my sincerest gratitude goes out to my parents for their life-long encouragement. They give me the pushes I need to go beyond myself and always support me in good and bad times, even when I am at the other end of the world.

<div align="right">

Julia Sothmann
Affalterbach, December 2017

</div>

Table of Contents

Nomenclature

List of Symbols

Abbreviations

AF	Adhesion Failure
AHS	Alternating Heat Climate Storage
AMG	Mercedes-AMG
B	Blank
BIW	Body-In-White
CAD	Computer-Aided Design
Cata	Cataplasm Storage
CCH	Condensation Atmosphere with Constant Humidity Storage
CF	Cohesion Failure
CFRP	Carbon Fiber Reinforced Plastic
CTE	Coefficient of Thermal Expansion
DoE	Design of Experiments
G	Gaseous
GFRP	Glas Fiber Reinforced Plastic
IM	Injection Molding
L	Liquid
LRIM	Liquid Reaction Injection Molding
MF	Mixed Failure
OEM	Original Equipment Manufacturer
OFAT	One-Factor-At a-Time
OMPURIB	Open-Mold Polyurethane Injection Bonding
P	Primer

POM	Polyoxymethylene
PP	Peel-Ply
PT	Print-Through
PUR	Polyurethane
RH	Relative Humidity
RIM	Reaction Injection Molding
RRIM	Reinforced Reaction Injection Molding
RTM	Resin Transfer Molding
S	Sanded
S	Solid
SA	Standard Atmosphere
SF	Substrate Failure
SRIM	Structural Reaction Injection Molding
TAE	Trial And Error
UV	Ultra-Violet
WST	Window Spray Technology

Greek Symbols

α	Coefficient of Thermal Expansion
Δ	Difference
ϵ	Strain
γ	Shear Angle
κ	Curvature
μ	Poisson Ratio
σ_s	Shrinkage Stress
σ_{te}	Thermal Expansion Stress
τ	Shear Stress
τ_B	Lap-Shear Strength

Latin Symbols

| F_{max}	Maximum Recorded Force
I	Second Moment of Area
M_B	Bending Moment
T	Temperature
t	Time
T_g	Glass Transition Temperature
A	Bond Area
E	Young's Modulus
F	Breaking Force
G	Shear Modulus
l	Length

Chapter 1

Introduction

Automotive Original Equipment Manufacturers (OEM's) always compete for the most customers to get the biggest profit. They either try to attract the customers by offering the best performing engine, the sleekest design and by offering lightweight solutions. In the sportscar business, in which Mercedes-AMG (further abbreviated as AMG) is established, customers spare no expenses to own the fastest and best looking vehicles.

AMG is not only known for their high performance motors, but also for the implementation of a fair amount of lightweight interior, exterior and BIW features to increase the car's performance even more. While doing so, AMG is restricted in their body-in white (BIW) design freedom because the majority of their cars is based on BIW of the Daimler AG's series vehicles. Even for the vehicles that are AMG only, like the AMG GT, and therefore not limited by the BIW structure of a Daimler version, one significant restriction holds. The final vehicle assembly is always done within a Daimler production plant. This usually does not pose any problems for metal parts, which are part of the BIW, but for mounted parts, like composite or plastic parts. Looking at a roof, which is in the focus of this thesis work, the full solid (metal) roof is already welded to the BIW at the suppliers assembly plant and undergoes the same assembly steps as the Daimler cars. For panoramic roofs and carbon fiber reinforced plastic (CFRP) roofs though the assembly process looks different. Since multiple different materials need to be joined, thermal joining is not an option, which is why the roofs are adhesively bonded in a separate assembly line or step. Moreover, this step can only be done after the BIW has gone through its surface treatment, because the E-coat and lacquering processes for the BIW reach temperatures of up to $190°C$, which would degrade the assembly adhesive and the substrate material itself. Therefore the two modular roofs are assembled as part of the final vehicle assembly.

The panoramic glass and CFRP roof share one BIW version, which is a modification to the full solid roof BIW. For the panoramic glass roof the modification is required mainly because of its extra weight and the difference in crash behavior. The result is an additional inner roof frame, which is welded to the outer roof frame and onto which the panoramic glass roof is bonded. Figure 1.1 shows a section of the BIW of the AMG GT R including the CFRP roof.
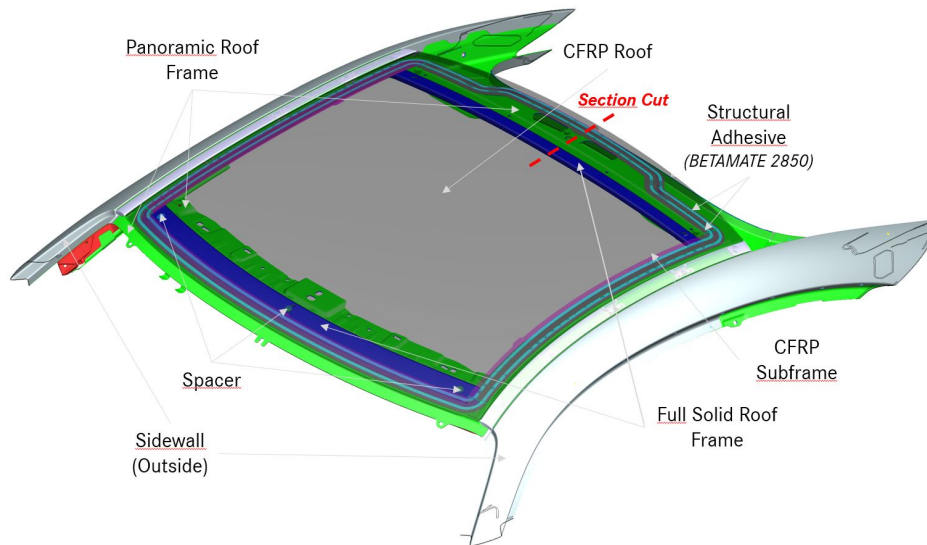
Figure 1.1: Section of the AMG GT R BIW including the CFRP roof

The same BIW version as for the panoramic glass roof is used for the CFRP roof. Because the number of CFRP roof units is extremely low (compared to the other roof types), the costs and logistics expenditure would be tremendous to implement another assembly line for such small quantities. Therefore the same assembly adhesive, the same gripper and same tact time as for the panoramic glass roof need to be considered for the CFRP roof.

Looking at the two modular roof types, which are depicted in Figure 1.2, it quickly becomes apparent that the CFRP roof is much thinner than the panoramic glass roof and requires a subframe to bridge the thickness difference, the Z-offset to the roof frame.

(a) AMG GT glass roof

(b) AMG GT R CFRP roof with subframe
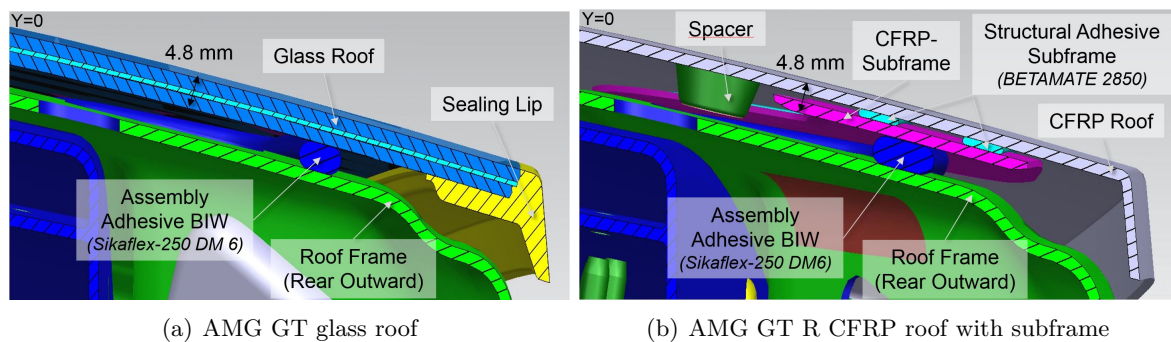
Figure 1.2: Section cut of the assembled panoramic glass and CFRP roof to the inner roof frame (cross-section at Y=0 as indicated in Figure 1.1)

The current solution, shown in Figure 1.2(b), is a bonded CFRP subframe. With increasing complexity of the future roofs (i.e. implementation of an embossing or change in roof flange design) the required subframe design (i.e local variations in thickness) will also become more complex. Using a CFRP frame, the production can therefore very quickly become an expensive process. Therefore the choice was made to use a smart multi-material solution, which offers more design freedom and keeps the costs low. At Daimler AG Sindelfingen the

adhesives team was already working on an open-mold polyurethane injection bonding process (OMPURIB), using special BASF polyurethanes, to replace the roof trim by a shadow gap with a sealing lip as depicted in Figure 1.3 [1, 2].
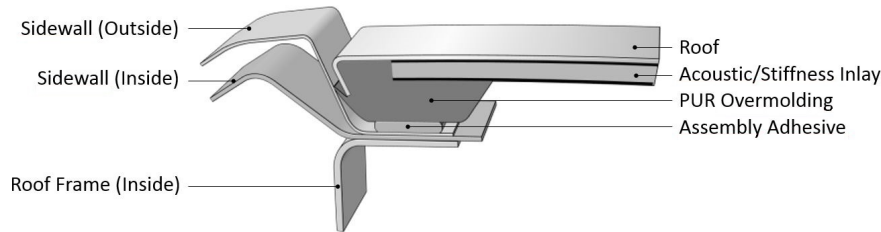
Figure 1.3: Shadow gap concept as developed by the adhesives research team at Daimler AG Sindelfingen

As they proved the process feasibility, it was decided together with the developers of the shadow gap concept, to take the application another step further and develop a way to make use of the process for the CFRP roof concept. For the CFRP roof subframe the OMPURIB process is used to form a subframe structure while simultaneously bonding it to the inside surface of the roof. The sub-assembly is then transported to the Daimler production plant where it is bonded to the BIW by applying assembly adhesive onto the subframe surface.

The main function of the subframe is the bridging of the Z-offset with a support structure that can be bonded to the roof frame. It is a requirement that the PUR subframe offers the same structural integrity as the CFRP subframe and that the material does not cause any print-through on the Class-A roof surface, neither after process application nor due to environmental effects.

The implementation of the new subframe offers great benefits for AMG. Not only does it give more design freedom for more complex designs, but it also has the potential to reduce the cost of the subframe structure by approximately 50%. Since this exact process has not been used anywhere else yet, the process technology has a great potential for patenting and further use in the automotive and other engineering industries.

1.1 Research Objective

As a result of the motivation stated in the previous section, the objective of the research is to develop a way to use OMPURIB to integrate a local or circumferential 3D subframe profile to the inside of a visible CFRP roof with Class-A surface finish. The subframe has to offer a hard and durable support structure for the assembly of the roof to the roof frame, which is used for both, the thicker panoramic glass roof and the CFRP roof. This combines the determination of mechanical properties of the PUR and the optimization of the material application process to the inside surface of different CFRP roofs. The research will be performed by means of experimental tests. Fundamental studies on flat plate specimens (lap shear, peel, and print-through) need to be performed for material and process qualification. Moreover, the process is ought to be qualified on the CFRP roof of the AMG GT R including functional integrations. The final goal is to achieve a use of OMPURIB as a supporting subframe for a visible CFRP roof assembly in series production.

To solve the above mentioned research objective, the following research questions need to be answered during the research.

1. In what way can the roof subframe itself and joining of the CFRP roof to the roof frame be improved?

    (a) Where does the need for a subframe originate from?
    (b) What is the current solution applied by AMG?
    (c) What are the major disadvantages of the current solution?
    (d) What are the requirements for the adapter structure?

2. What research has already been performed on OMPURIB and similar technologies?

    (a) What applications is OMPURIB already used for and what further applications has it been tested for?
    (b) What patents exist within or outside the corporation?
    (c) Which similar technologies are already used for similar purposes and could give additional improvement potential?

3. What is the working principle of the OMPURIB process?

    (a) What are the material restrictions and requirements for processing?
    (b) What are the design restrictions for the PUR component, substrate and tools?
    (c) What is the cycle time of the application process?
    (d) Which parameters of the machine can be tuned to change the outcome?

4. What tests should be performed?

    (a) Which tests are most useful to gain the best knowledge about the procedure and material behavior?
    (b) How should the tests be set up and performed? What are the standards?
    (c) Where can the tests be performed?
    (d) How many test repetitions should be performed?
    (e) Will the tests be performed on specimen/coupons or actual parts?

5. What needs to be done to be able to use the OMPURIB process?

    (a) How fast can and should the material be injected (i.e. curing time, void inclusion)?
    (b) What adhesive strength does the PUR have on CFRP?
    (c) Is it necessary to redesign (parts of) the roof (e.g. flanges) or the roof frame?

6. What needs to be included when looking at industrialization and cost analysis for this product?

(a) Is the use of OMPURIB for this approach certifiable/ does it comply with all restrictions and load cases?

(b) What is the plant invest?

(c) What are the material cost of the new compared to current subframe design?

(d) What are the manufacturing cost of the new compared the current subframe design?

(e) How should the collaboration model be set up in terms of commercialization, transfer, etc. for AMG?

7. What recommendations can be drawn on the optimal use of OMPURIB?

1.2 Thesis Structure

The following chapters discuss the work performed to answer the research questions and achieve the research objective.

First and foremost, Chapter 2 gives an insight into the most important information on adhesive bonding it demonstrates possible surface pre-treatments for composite adherends. Furthermore, it describes the envisaged material test methods, before it the chapter is concluded by the presentation of a strong process analysis tool, the design of experiments (DoE). This chapter as well as Chapter 3 are a repetition of the literature study, which was written to support the research work.

Chapter 3 gives a review of the previously performed work on PUR injection techniques and provides information on the manufacturing and assembly of visible CFRP roofs in the automotive industry.

The approach that was taken to work towards the research goal is subsequently described in Chapter 4. It lays out the planning and preparation that had to be done before the experiments could be started.

Following the experiment design, the experiment execution is presented in Chapter 5. It contains a demonstration of the test equipment and material, followed by the fundamental experiments to analyze the material and bond properties, the process and print-through tests and finally the application test on the AMG GT R roof.

For AMG's cost and logistic planning, an industrialization and cost analysis was performed and is presented in Chapter 6. It includes the performed market analysis and the determined technology transfer potential for other applications. Moreover, it lays out an analysis of the most beneficial supplier strategy for AMG and entails a cost calculation of the PUR subframe with a comparison to the current CFRP design.

In the final chapter, Chapter 7, all outcomes of the research project are discussed and concluded. Subsequently, based on these results, recommendations for the completion of the qualification process and future work are drawn.

Chapter 2

Fundamental Principles

The researched process is an open mold injection bonding process, where a polyurethane part is formed and simultaneously joined to a structure. Even though only one adherend is involved, the working principle of joining is still based on common adhesive bonding. Therefore a broad overview of adhesive bonding is given in this chapter. Moreover, common pretreatments for increased adhesion on CFRP structures and suitable material test methods for the research work are discussed. Finally, the chapter concludes with a process analysis tool, the design of experiments, used for a smart setup and design of the experiments.

2.1 Adhesive Bonding

Following the most important definitions related to adhesive bonding, the working principle as well as the different adhesive categories are explained in this section. Moreover, the most important characteristics to analyze an adhesive are described.

2.1.1 Important Definitions

This section describes the most important definitions associated with adhesive bonding. The designation, as used in the definitions, is done according to engineering standards and will be used throughout the whole document.

Adhesive
As defined in DIN EN 923 an adhesive is a 'non-metallic substance capable of joining materials by surface bonding (adhesion), and the bond possessing adequate internal strength (cohesion)' [3]. Usually the naming of an adhesive is done based on the main functional group or the adhesive's physical origin. This process is not fully fixed, which is why some adhesive are also named according to less significant factors.

Adherend
An adherend, also called substrate, is a body to which the adhesive is applied to connect it to another body [3].

Adhesion and Adhesion Zone

Adhesion is generally described by Wu as 'the state in which two dissimilar bodies are held together by intimate interfacial contact such that mechanical force or work can be transferred across the interface' [4]. The more precise description can be drawn from the chemical behavior.

The adhesion zone describes the interface where the adhesive bonds onto the substrate, as shown in Figure 2.1, where the adhesion forces act. Adhesion forces are caused by molecular interactions between dissimilar substances, such as electrostatic (due to unequal charge) or micro-mechanical (due to roughened surfaces) forces between the substrate surface and the adhesive. Adhesion therefore describes the attraction between the two substances (adhesive and adherend) that make physical contact [5].

Cohesion and Cohesion Zone

Cohesion denotes the internal strength of an adhesive. It is prescribed by cohesive forces acting in the cohesive zone, also visible in Figure 2.1, within the adhesive bulk.
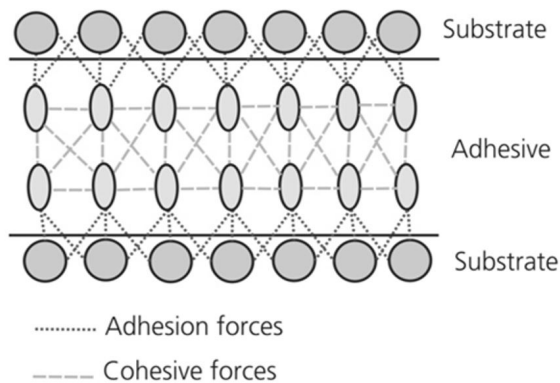
Figure 2.1: Forces in an adhesive bond between 2 substrates [5]

These forces are caused by chemical bonds between atoms of the adhesive and intermolecular reactions between the molecules within the adhesive. Examples of intermolecular forces are hydrogen bonds or van der Waals forces, which act between molecules of the same substance [6]. They therewith create an internal coherence within the adhesive itself. The mechanical properties of the cured adhesive as well as the flow properties in an uncured state are determined by these internal forces and are usually defined by the manufacturer of the adhesive [5].

For a proper bond it is important that it fails under cohesive fracture, within the adhesive, and not between substrate and adhesive, as the maximum bond load is determined by the adhesive strength, which is related to the cohesion zone [5].

Print-Through

For bonded surfaces which are exposed to the human eye, it is important that no print-through of the bond line is visible on the outside surface at the part's operating temperatures. The effect where the bond line creates a visible distortion on the other side of the substrate is called print-through or synonymous read-through. It is always caused by residual stresses in the bond which are further described in Section 2.1.2 'Stresses in Adhesive Bonds' and can have three major causes [7]. Print-through can emerge during the process due to the temperature and pressure applied while applying the adhesive or due to different adhesive thicknesses and stiffness jumps due to abrupt thickness variations. A second cause can be customer load cases, such as UV rays or high temperatures where the difference in thermal expansion between the adhesive and the adherend (or two adherends) can cause stresses within the adhesive, leaving

a print on the outside. And finally print-through can result from the material properties. Examples are moisture absorption and shrinkage. Print-through is related to the mechanical properties of the adhesive and the adherends, but should generally be denoted as a process and operating phenomenon.

2.1.2 Principle of Adhesive Bonding

The basic working principle and bond layout, in terms of adhesion and cohesion zones, were already explained in Section 2.1.1. This section highlights additional factors that are important for the understanding of adhesive bonding. First, the requirements for a good bond are explained, followed by a representation of the common stresses in adhesive bonds. Finally, the benefits and challenges of adhesive bonding and the resulting application fields are depicted.

Requirements for a Durable Adhesive Bond

The requirements one needs consider when a high bond quality is desired are as follows [8].

1. ***The right choice of adhesive.***
   There is a broad selection of adhesives on the market, which makes it important to carefully choose the right one based on the performance specifications and the bonding process. Typical influencing factors are required strengths and stiffness, shear modulus, operating temperatures and chemical resistance. There are many more factors, which are dependent on the joint design and location of the joint. For example, as shown in Figure 2.2, the choice between a brittle and elastic adhesive can already make a huge difference in the stress-strain behavior and following the stress distribution within a single lap-joint.

2. ***A good joint design.***
   A joint is designed to achieve the maximum strength in the joint. In adhesive bonds the stresses act over the bond area and not over a single point as in fasteners. Therefore the design of a bonded joint should minimize stress concentrations and create a rather continuous stress distribution. More about the stress distribution in joints is explained in Section 2.1.2.

3. ***A clean contact surface and surrounding.***
   If the adherend's surface is contaminated with dirt, oil and other substances, these substances form weak boundary layers of the surface and prohibit bonding between the adhesive and adherend. The adhesive bonds to the weak boundary layer instead, which decreases the adhesion forces and therewith results in a weak bond. Therefore it is important to clean the contact surfaces adequately before the adhesive application. Possible cleaning methods for CFRP are depicted in Section2.2. A clean surrounding also helps to prevent re-contamination of the surfaces.

4. ***Good surface wetting.***
   Surface wetting describes the process where the adhesive spreads over the adherend and replaces air and other gases to form a continuous interfacial contact between adhesive and adherend. Important influencing factors of surface wetting are surface tension and

surface energy. The adhesive molecules are held together by cohesive forces. Although they balance each other out in the inside, they create a resulting adhesion force on the surface in the direction of the bulk of the material. These forces create a surface tension and the energy needed to overcome the surface tension is the surface energy. In order for the adhesive to properly wet the substrate surface it has to have a lower surface energy than the substrate. Treatments to increase the substrate surface energy are mentioned in Section 2.2.
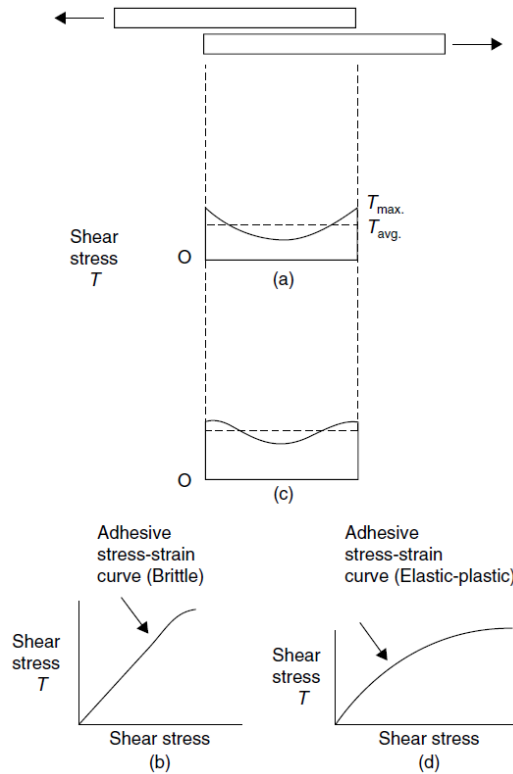
Figure 2.2: The stress distribution in a single lap joint over its overlap length using a) brittle and b) elastic adhesive. b) and d) show the corresponding stress-strain curves of the brittle and elastic material [8]

Proper wetting can be measured by the contact angle between the surface tension tangential of the adhesive (between liquid (L) and gaseous (G) state) and the surface tension of the adherend (between solid (S) and (G) state), as displayed in Figure 2.3. The balance between the different surface tensions and the interface tension between the two is achieved in point A.
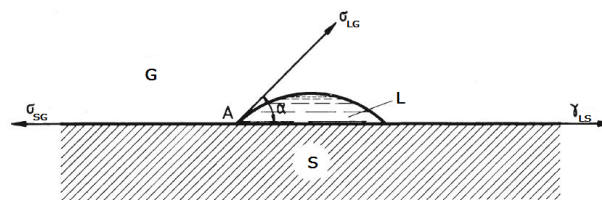
Figure 2.3: Surface tension and interface tension during wetting [9]

A contact angle of zero or near-zero is desired for good wetting, as indicated in Figure 2.4. Only if the contact angles are low, interactions between the dipols of the adhesive and adherend molecules can occur to achieve the lowest energy state for the particles.
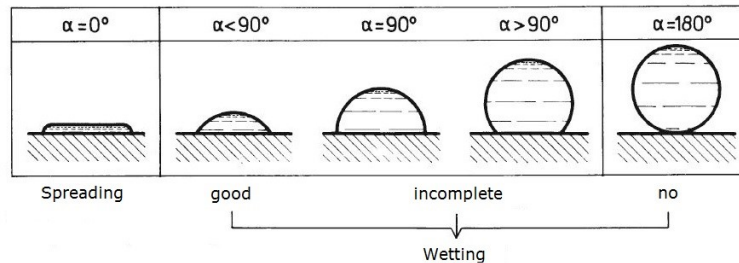
Figure 2.4: Coherence between contact angle and wetting behavior of an adhesive [9]

Once the lowest energy state is reached, the potential energy between the particles is minimal and they do not move away from each other anymore. The second requirement for low contact angles is a low adhesive viscosity. A low viscosity facilitates a high degree of movability of the adhesive molecules, which aids the achievement of a low energy state and therewith improves the wetting of the substrate [9].

5. ***The optimal process for the chosen adhesive.***
   Lastly, it is important to assure the correct application and curing process for the chosen adhesive. Some adhesives require applied temperature or heat in order to cross-link properly, others need cooling. The joining setup should therefore incorporate all the necessities. Moreover, the curing time needs to be preconceived, such that the part is not removed before the bond is not strong enough for handling.

Once these requirements are met, a good bond can be assured.

Stresses in Adhesive Bonds

Adhesive bonds are popular because of their uniform stress distribution over the joint width. In comparison rivets and other fasteners introduce stress concentrations around the hole edges as shown in Figure 2.5, which makes them less suitable for joints that experience shear stresses [10].
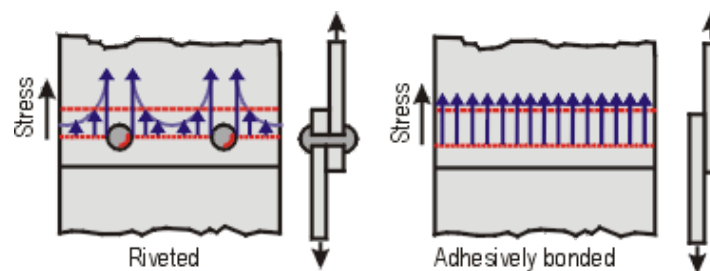
Figure 2.5: Stress distribution over joint width for a) a riveted and b) an adhesively bonded joint [10]

Along the overlap length, the length direction in a single lap joint, the stress distribution follows a bathtub curve as depicted in Figure 2.2. The stress is higher at the edges of the bond, which indicates a lower resistance to peel. A rather inconvenient behavior of adhesive bonds is the buildup of residual stresses due to various causes. These residual stresses can be negligibly small for thick adherends, but can cause print-through on thinner adherends of certain material type. In very adverse situations residual stresses can even cause a decrease in bond strength.

Common reasons for residual stresses are differences in thermal expansion coefficient between the adherends and adhesive or between dissimilar adherend materials. Moreover, residual stresses can be caused by shrinkage of the adhesive or temperature differences in the adherends during the application and curing process. Finally, temperature changes and other environmental effects can have an influence on the cured adhesive during operation [9].

Residual Stresses due to Differences in Thermal Expansion Coefficient
When the temperature increases, the materials expand by their coefficient of thermal expansion (α). As discernible from Table 2.1, the thermal expansion coefficients can vary a lot. Aluminum has a coefficient almost twice as large as steel and four times as large as carbon fiber reinforce epoxy. Its coefficient is about 4 times lower than of polyurethane though. From this results that the materials expand differently at the same temperatures. If the materials are bonded together, the difference in thermal expansion ($\Delta\alpha$) causes stresses between the adherends and adhesive. They can be a result of $\Delta\alpha$ between adhesive and adherend, but also if the adherends are of dissimilar material. The stress magnitude depends on the chosen material combination.

Table 2.1: Coefficients of Thermal Expansion (CTE) for research relevant materials (Data extracted from Table 5.2 in [9])

Material	**CTE** (α) $[10^{-6}K^{-1}]$
Aluminum	23.5
Steel (unalloyed or low-alloy)	10-14
Steel (high-alloy)	13-19
Carbon Fiber Reinforced Epoxy (quasi-isotropic)	5
Polyurethane	110-210

The calculation of stress due to thermal expansion (σ_{te}) is done using Eq. 2.1, which uses the Young's modulus (E) of the adhesive, the thermal expansion factors (α) of adhesive and adherend and the change in temperature (ΔT) [9].

$$\sigma_{te} = E_{adhesive} \left(\alpha_{adhesive} - \alpha_{adherend} \right) \Delta T \tag{2.1}$$

For a more exact calculation one also needs to consider the expansion in the bonds latitude, which is done by the use of the Poisson ratio (μ), as displayed in Eq. 2.2.

$$\sigma_{te} = \frac{E_{adhesive}}{1 - \mu_{adhesive}} \left(\alpha_{adhesive} - \alpha_{adherend} \right) \Delta T \tag{2.2}$$

The above mentioned equations assume a $\Delta\alpha$ only between adhesive and adherends of the same material and an ideally elastic behavior of the adhesive, having an invariant α. In real life

the adhesive behaves elastic-plastic, where α is dependent on the temperature. This method is conservative and overestimates the residual stresses. Additionally, a constant E-Modulus is assumed, which is only valid if the considered temperature lies below the glass transition temperature of the material (T_g), where the material turns from solid to rubbery and loses its integrity. Above the T_g the residual stresses cannot build up because the increased movability of the molecules relieves the stresses. For this reason Eq. 2.1 and Eq. 2.2 can only be used for adhesives with high glass transition temperatures.

It can also happen that the adherends are of dissimilar material. In that case the $\Delta\alpha$ between the adherend materials causes an additional relative elongation between the adherends. The highest residual stresses act at the overlap edges in that case and need to be counterbalanced by the adhesive. Only adhesives which show an elastic-plastic behavior can counterbalance those stresses, which shows the importance of the ability of relaxation of the adhesive. Good relaxation behavior is only achieved if the adhesive has time to cure and cool, and is not cooled abruptly .

Differences in thermal expansion coefficient can cause a decline in the joint's performance. One result can be fracture of the adherends, if the adherend's strength is not sufficient to withstand the built up stresses or if the adhesive has no room to expand to counterbalance the changes in elongation. Moreover, if improper surface pre-treatment was performed, the bond can fail in adhesion, because the stresses in the interface are too large and the bond strength in the adhesion zone too low. Another sign of too high residual stresses are micro-cracks in the adhesive and in the interface zone.

To prevent the above mentioned failures, the following points should be considered. An adhesive with a low shear modulus (G) should be used, the use of primers and adhesion agents with a high deformability should be added in a surface pre-treatment and fillers could be added to the adhesive to modify it such that it has a thermal expansion coefficient which is between the ones of the two adherends [9].

Residual Stresses due to Shrinkage
Another cause for residual stresses in the adhesive can be shrinkage. Shrinkage can get really problematic if bond gaps of high thickness compared to the adherend thickness are used, as commonly used in the automotive industry for bonding of a CFRP roof, bonnet or trunk lid. There are three phases to describe the shrinkage behavior [9]:

1. ***Thermal Expansion***
   During the heating phase the adhesive expands, because the movement of its molecules increases (see Figure 2.6 curve A-B).

2. ***Shrinkage during reaction***
   During the reaction phase the monomers react to polymers and the secondary bonds of the monomers change to covalent bonds within the polymer. These stronger bonds in the polymers decrease the distance between the molecules and therewith increase the density of the polymer. With increasing density the volume decreases, resulting in a shrinkage of the adhesive (see Figure 2.6 curve B-C).
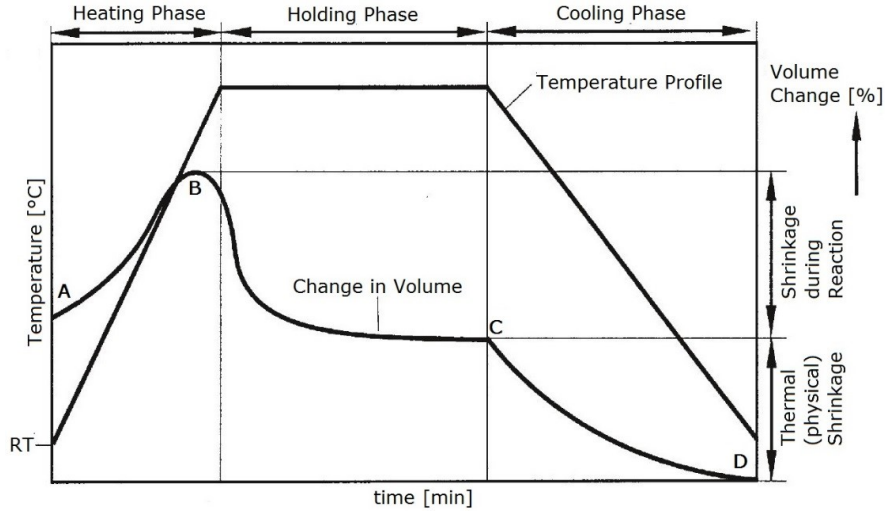
Figure 2.6: Schematic of the adhesive shrinkage due to temperature and chemical reaction [9]

3. ***Thermal (physical) shrinkage***

   Once the polymers are fully cured and are cooled below their T_g, their inter-molecular movement decreases and the adhesive volume shrinks. The effect is like the opposite of the first phase (see Figure 2.6 curve C-D).

Further reasons for shrinkage can be the release of small molecules separated during polycondensation processes or as emissions, like remaining solvents, additives or other low-molecular weight compounds. The residual stress due to shrinkage (σ_s) can be computed using Eq. 2.3.

$$\sigma_s = E_{adhesive} \left(\epsilon_{tot} - \alpha_{adherend} \Delta T \right) \tag{2.3}$$

where $\epsilon_{tot} = \epsilon_{reaction} + \epsilon_{cooling}$ and where $\epsilon_{cooling} = \alpha_{adhesive} \Delta T$.

By substituting the above, the stress can generally be calculated using Eq. 2.4.

$$\sigma_s = E_{adhesive} \left(\epsilon_{reaction} + \left(\alpha_{adhesive} - \alpha_{adherend} \right) \Delta T \right) \tag{2.4}$$

The above stated equation represents ideally even shrinkage, which in real life can be unevenly distributed. It still gives a good estimation of the residual stresses.

Shrinkage can cause print-through, but usually does not cause residual stresses of levels where the adhesive bond strength reduces. This only happens in rare cases [9]. To avoid or reduce shrinkage additives can be added to the adhesive or the adhesive can be modified to cross-link at the heating phase instead of the holding phase. Moreover, adhesives with a low E-modulus, and resulting low G-Modulus, can be used or adhesives with a base polymer that has lower curing temperature to reduce the shrinkage due to the chemical reaction. Instead of changing the adhesive, the bonding process can also be adjusted to avoid shrinkage. By reducing the bond gap and by homogenizing the process temperature of the adherends the shrinkage can also be reduced. Finally, an earlier cross-linking can be achieved not only by adhesive modification, but also by adjusting the process such that the heating rate is decreased and

the holding temperature is increased [9].

Residual Stresses due to Temperature Differences between Adherends and Adhesive

If during the bonding process, especially when using highly exothermic adhesives, the adherends are not heated, residual stresses can be introduced. The highest temperatures will be in the center of the adhesive layer with decreasing temperatures towards the interfaces and the adherends themselves. The temperature differences will cause different degrees of cross-linking during curing introducing the stresses at the interface. Therefore it is advised to heat the adherends to the curing temperature of the adhesive to minimize residual stresses [9].

Residual Stresses due to Temperature Changes and Moisture Absorption

Lastly, residual stresses can be introduced during operation, when the bond ages. Common influences are thermal cycling or moisture absorption. Thermal cycling can cause material expansion or contraction of the adhesive and the adherends. When the bond is heated, compressive stresses act between adhesive and adherends, whereas tensile stresses act when the bond is cooled down. Depending on the $\Delta\alpha$ between adherend and adhesive the introduced residual stresses can vary in magnitude. Moisture absorption can have a similar effect as heating. When moisture is absorbed, the adhesive's volume expands causing compressive stresses at the interface. These stresses result in the same problems as differences in thermal expansion coefficient generate [9].

It can be summarized that residual stresses can be caused by many different effects. It is important to already avoid the generation of residual stresses during the bonding process, because other effects are harder to control. Therefore a proper process control is necessary to especially control the reaction temperature and cooling rate.

Advantages and Disadvantages of Adhesive Bonding

Adhesive bonds have a lot of advantages compared to other joining methods, but they also have their limits [8–10]. Both will be discussed in this paragraph.

Advantages:

1. The stress in an adhesive bond is distributed more uniformly

2. Adhesive bonds are especially good where shear stresses are applied to the joint

3. Similar as well as dissimilar materials can be joined using adhesives, which is extremely good for substrate materials with a large difference in thermal expansion factor

4. Thick, thin and adherends with different thickness can be joined with adhesives

5. Adhesives can be used as an insulator between two materials to avoid heat transfer, electric conduction and corrosion

6. Adhesives are great in terms of fatigue resistance

7. Adhesives can simultaneously be used as sealants

8. Adhesives offer a great specific strength

9. Adhesives are a cheap and quick solution compared to most mechanical fasteners and welding solutions

10. The surfaces of the substrates to be bonded remain unchanged compared to welding or fastening

11. Adhesive joints leave rather smooth surfaces, not disturbing set contours as much as other joint types

Disadvantages:

1. Visual inspection of the bond is extremely difficult or even impossible, which makes inspections elaborate

2. Certification of bonded joints is an elaborate process

3. Adhesives are not well-suited for disassembling and repair, because they cannot be easily removed

4. Adhesive bonds are limited in operating temperatures (commonly $177°C$, unless a more expensive adhesive is used)

5. Proper surface pre-treatment is required before joining

6. Curing times can be long, depending on the adhesive material

7. Adhesives can cause print-through on the outside surfaces of the adherends

8. Adequate process control is necessary

Although bonded joints replace a lot of mechanical fasteners and welds, the main cutback is the certification. The inspection and testing of adhesive bonds is an elaborate process especially for components and modular structures, since the tests are design specific and standard tests cannot be applied. In the automotive industry most testing of bonded joints is performed to qualify new adhesive materials and processes, for which joint elements, specimens, can be used. But the collection of all the data is very time-consuming and expensive, which is why the aerospace industry usually resorts to well-established and tested materials and processes to avoid these expenses [11].

Applications of Adhesive Bonds

The application fields of adhesive bonds follow from their advantages and limitations. Adhesive bonds are often used to join dissimilar materials to prevent corrosion and especially for parts that experience high temperature changes to balance out the difference in thermal expansion. Additionally, adhesive are used as a sealant, if the joint also needs to be air or liquid tight, and to withstand cyclic loading. In a good joint design the adherend fails under fatigue before adhesive failure occurs. And if a smooth surface is required, adhesives are a perfect fit, because they do not disturb the surface as much as some other fastener types. For these reasons adhesives are often used for the joining of rotor blades or for joining of outer parts of the body in white or exterior parts in the automotive industry [8].

2.1.3 Adhesive Categories

A large range of available adhesives makes it necessary to categorize them, which can be done in many different ways. The three most common ways are discussed in this section. Adhesives can be classified by their chemical basis, namely its origin, or by function, whether they have to carry loads or are simply applied to keep two parts together. Additionally, they are often sorted by their type of curing mechanism, whether they bond physically (no chemical reaction) or cure chemically via polymerization, polycondensation or polyaddition.

Categorization by Chemical Basis

The most obvious categorization is done based on the origin of the adhesive. Adhesive materials are either based on ***organic*** or ***inorganic*** bonds [12]. Looking around in the material applications it can be seen that the vast majority is based on organic bonds. The main difference between the two bond types are the processing- and application temperatures, which result from the materials glass transition temperature (T_g). Organic adhesives are usually processed at lower temperatures and therefore also have lower maximum application temperatures as inorganic materials. Typical inorganic materials are silicones, silicates, phosphates and borates [9].

Within organic materials, also called polymeric materials, one can again distinguish between two groups; ***natural*** and ***synthetic*** [8,9,13]. Materials such as natural rubber, natuarl resin and protein- and casein-based polymers are examples of natural adhesives, which make only a small percentage of the organic materials used in industrial applications. Most adhesives are made of synthetic polymeric compounds, like epoxies, polyurethanes and acrylics, to name the most common ones [13]. Synthetic materials can be again be subdivided in thermosets, thermoplastics and elastomers and therewith offer a great application range [8]. Next to their attractiveness due to their great application field, adhesives based on synthetic polymeric bonds are so broadly used because of their great lap shear strength and aging resistance in comparison to natural materials [9]. This is why all structural adhesives are synthetic polymeric compounds.

Categorization by Function

There are two main functions that adhesives can fulfill. An adhesive is either a *structural* adhesive or a ***non-structural*** one, also called holding adhesive. To make a connection to the automotive industry, structural adhesives are usually used in the body-in-white (BIW) of the vehicle and the final assembly. While holding the adherends together, they need to be able to transfer stresses between the adherends and simultaneously keep their structural integrity under their design loads. This structural integrity needs to be kept over its determined lifetime and under all environmental conditions it is meant to experience [14].

The most common structural adhesives are 1-component and 2-component epoxy adhesives, which are mainly used in the BIW, and some 2-component polyurethane adhesives, used mainly in the final assembly. These adhesives they offer a high engineering strength and stiffness, as shown in Figure 2.7, and resulting high crashworthiness. Often a structural adhesive is defined to have a shear strength greater than 7 MPa [8,14].
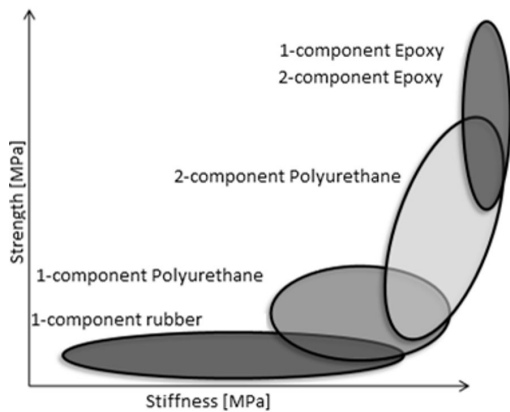
Figure 2.7: Strength and stiffness of common adhesive groups [15]

Epoxy adhesives offer a high strength at a small bond line gap and 2-component polyurethanes are commonly used with a thicker bond line gap and offer a higher elasticity and seal tightness. Polyurethane adhesives are of better use for dissimilar materials, as they better compensate for differences in thermal expansion ($\Delta\alpha$) [8].

Non-structural adhesives however are only used to hold parts in place, which is where the name 'holding adhesive' originates. They are not supposed to carry any higher loads [8] and usually have a shear strength below 10 MPa [9]. Example application fields are tapes, packaging adhesives, underlining, sealants and corrosion protection, which are commonly made of rubber or 1-component polyurethanes [15].

Categorization by Curing Mechanism

There are three main groups of curing mechanisms used to categorize adhesives. They can either cure physically or chemically and one type of adhesives, reactive hot melts, cures a mix of physical and chemical reactions [9, 15].

The major proportion of adhesives cures under a ***chemical reaction***. They can either be ***cold-hardened*** or ***heat-hardened***. Cold-hardened adhesives cure at room temperature or slightly higher temperatures and sometimes need applied pressure. These adhesives are very reactive, which enables them to reach their initial strength fast, but acquiring the final strength takes rather long, resulting in a full processing time of multiple days. The benefits are low processing requirements, as now extra heating or treatment is required. Compared to heat-hardened adhesives cold-hardened adhesives have lower strength, as they have lower degree of cross-linking. Heat-hardened adhesives are cured under the application of heat ($60 - 160°C$), which allows for faster and denser cross-linking. This results in higher strength and a higher thermal stability. Another benefit of heat-hardened adhesives is the longer pot life, because the adhesive components only fully react under the influence of applied heat. Furthermore, this allows for a process where the curing onset can be precisely defined [9,16,17].

Additionally to the grouping in cold- and heat-hardened, chemically reacting adhesives can cure by different reaction types; ***chain-growth polymerization*** and ***step-growth polymerization*** (polycondensation and polyaddition). Chain-growth polymerization needs a reactive end of the growing polymer chain in order to attach more monomers. In order to do so, the first monomer to build the chain is 'activated' in the first step by a reaction with an initiator. An initiator can be UV radiation or heat to start a radical polymerization or ions to start an ionic polymerization. The growth of the chain can be structured in 4 steps: initiation, growth, linking and termination. Chain-growth polymerization always involves the opening of unsaturated carbon-carbon bonds, which in the reaction get saturated to achieve a lower energy state. Polycondensation and polyaddition are both step-growth polymerizations, meaning that both ends of any polymer species in the mix can react step by step. A polycondensation

always includes the separation of a smaller molecule during the reaction of the two monomers to form the polymer. Such molecules are water ($H_2 - O$), acids (such as $H - Cl$) or alcohols (such as $CH_3 - OH$). For this reason the repeat units in the polymer have fewer atoms than present in the monomers. This type of reaction can only happen if the monomers have functional groups, which are of similar reactivity. In comparison polymers made by polyaddition have repeat units that are identical to the monomers that react. In polyaddition atoms are rearranged and electrons moved to build the bonds. The most important polymers made by polyaddition are epoxies and polyurethanes [18, 19].

The second biggest group of adhesives are ***hot-melts***, which are made by physical hardening. These adhesives are usually 1-component adhesives. The majority of adhesives either contain solvents and dry as a result of solvent evaporation or are heated to a liquid state and then consolidate to a solid state during cooling [8, 20, 21]. Some adhesives are also bonded by applying pressure between adhesive and adherend. Further adhesives of this group are contact adhesives, water-based adhesives, dispersion adhesives and plastisols [15]. Usually physically curing adhesives are thermoplastic adhesives. The material properties of physically bonded adhesives are generally lower than of chemically bonded ones, because of the reversible bonding process and low degree of cross-linking [9, 22].

The last group, ***reactive hot melts***, show thermoplastic characteristics since they set physically after application. But instead of reacting reversibly by just consolidating upon cooling like thermoplastics, the molecules crosslink under chemical reaction with the air moisture. This process is therefore a combination of physical and chemical curing and is irreversible. The materials combine the properties of thermoplastics with a better heat resistance due to the crosslinking [23]. The most common ones are Polyurethanes with thermoplastic properties [22, 24].

Polyurethanes

As mentioned in Section 2.1.3 Polyurethanes, abbreviated as PUR's in this document, are cured chemically by polyaddition, a step growth polymerization [20].

The repeat unit of the polyurethane backbone chain, the urethane, is shown in Figure 2.8. The urethane is composed of a diol and a diisocyanate. Polyurethanes can be both, one-component or two-component adhesives. The reaction of one-component polyurethanes is usually much slower (couple of days) than of two-component polyurethanes (seconds to hours) [25]. Depending on the molar mass of the diol the polyurethane can be in a different state. If a polyurethane contains a diol with higher molar mass it is more rubbery and if it contains lower molar mass diols it gets more solid [19].
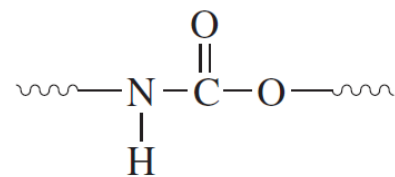
Figure 2.8: Polyurethane repeat unit [19]

The more rubbery or elastic polyurethanes are commonly used for non-structural applications, like bonding windscreens to a cars chassis, whereas solid polyurethanes can also be used for structural applications. Their high degree of crosslinking, which results in a high crystallinity and chain stiffness, makes them particularly suitable to structurally bond parts, especially thermoplastics, composites, rubber and metals [19, 26]. The properties of the material can

be changed in the same way as the state changes with diol and diisocyanate composition. But generally it can be said that polyurethanes have a high strength and a low stiffness (deduced from a low modulus of elasticity), resulting in great shock/impact resistance at low temperatures. The performance at higher temperatures is rather poor. Additionally, some polyurethanes, also influenced by the surface pre-treatment, are prone to moisture absorption, especially if applied to metal adherends. The good properties and tailor ability make polyurethane a good candidate for many different applications [8, 24].

2.1.4   Important Characteristics

This section depicts the most important characteristics, which influence the adhesive behavior. The elastic and shear modulus of an adhesive are used to define its resistance to deformation, while the glass transition temperature to define its operating temperature. The lap-shear strength and peel strength are necessary to determine whether it withstands the design loads and finally the pot life affects the application time of the adhesive.

Elastic and Shear Modulus

For every material a vitally important characteristic is the elastic modulus (E), also known as Young's modulus. It represents the stiffness of linear elastic materials and therewith indicates their resistance to deformation. The elastic modulus is the representation of the material's stress (σ) - strain (ϵ) relation under tensile and compressive loads using Hook's law, visible in Eq. 2.5 [19].

$$E = \frac{\sigma}{\epsilon} \tag{2.5}$$

where $\epsilon = \frac{\Delta l}{l}$ and $\Delta l = \frac{l-l_0}{l_0}$.

Typical stress-strain curves of composites, metals and polymers can be seen in Figure 2.9.
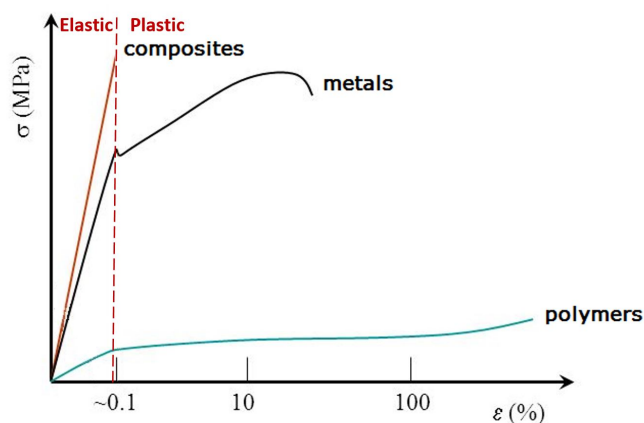
Figure 2.9: Typical stress-strain curves of composites, metals and polymers also indicating the elastic and plastic segments [27]

The elastic modulus gives insight in the deformation behavior of the material. It is very relevant for adhesive bonds, because the adherends usually have a much higher E-Modulus than the adhesive materials. A steep slope in the elastic regime stands for a high stiffness, meaning a lot of force needs to be applied to get a small deformation.

Additionally, metals and composites, common adherend materials, have a very constant Young's modulus, whereas the one of elastomers is very temperature dependent, which is also discussed in the following subsections [9,19,28]. From the Young's modulus another very important material characteristic can be derived, the shear modulus (G) (also vise versa). This is done using Eq. 2.6 [28], where μ is the Poisson's ratio, the ratio of transverse strain to axial strain in a material subjected to uniaxial loading [29].

$$G = \frac{E}{2(1+\mu)} \tag{2.6}$$

The shear modulus, similar to the elastic modulus, describes the resistance to deformation, but in this case due to shear loading. It is also defined as the relation between shear stress (τ) and shear angle (γ), shown in Eq. 2.7 [9,30].

$$G = \frac{\tau}{tan(\gamma)} \tag{2.7}$$

For adhesive bonds this modulus plays an important role, since tensile loading introduces shear stresses in the bond as discussed in more detail in Paragraph 'Glass Transition Temperature'.

Glass Transition Temperature

Because adhesives are polymers, their operating temperatures are limited. It depends on the desired behavior of the adhesive, whether rubbery or solid materials are required for the bond design. As discussed in Section 2.1.3, polyurethanes can be designed to become either, by influencing the degree of cross-linking. An important factor here is the glass transition temperature (T_g), which is the temperature range at which a polymer goes from a glassy/solid state to a rubbery state at increasing temperature because of the beginning of chain movement and the resulting stiffness loss. Figure 2.10 shows this behavior and indicates the T_g of different polyurethanes.

It can be seen that the T_g increases with an increase in cross-linking. A rubbery adhesive is therefore designed to have its operating temperature above its T_g, whereas a solid one is designed to be operated below its T_g. For most PUR's the T_g lies around $-20°C$ [19,26].

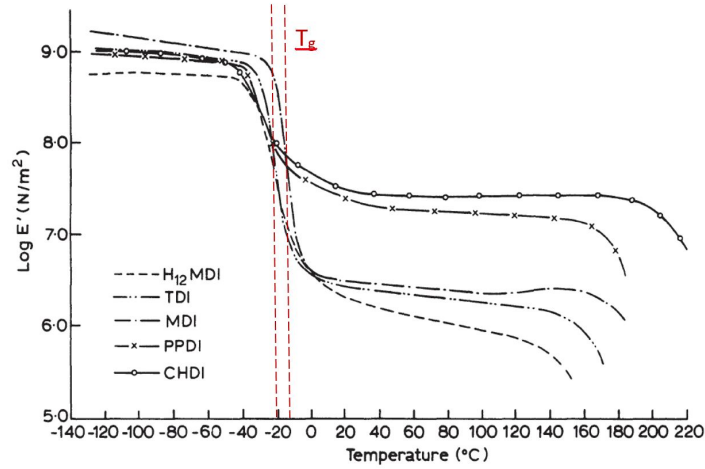**Figure 2.10:** Storage modulus vs temperature indicating the Tg of different polyurethanes [19]

Lap-Shear Strength

If a bonded structure is under tensile loading the bond area does not experience pure tensile loads but a mainly shear loads, because of the axial offset between the two adherends caused by the overlap. Therefore the adhesive requires a so called tensile shear strength, more commonly known as lap-shear strength. For single lap joints as used in a lap-shear test (see Section 2.3.1), the lap-shear strength can be calculated with the maximum recorded force (F_{max}) and the bond area (A) using Eq. 2.8 [9].

$$\tau_B = \frac{F_{max}}{A} = \frac{F_{max}}{l_o w} \tag{2.8}$$

The above describes the ideal case, where infinitely stiff adherends and a fully elastic adhesive deformation is assumed. In real life the adherends do not have an infinitely high stiffness, but also behave elastically under tension. Therefore the deformation of the bond is comprised of the adhesive and the adherend deformation, which are dependent on the elastic modulus (E) of the respective material. Additionally, the adhesive does not only behave elastically but usually shows plastic behavior after the elastic regime is exceeded. Furthermore, the axial offset between the two adherends also creates small bending moments, which act on the bond area and build up normal forces on the bond edges, causing an uneven deformation over the overlap length with the stress maxima at the edges as visualized in Figure 2.2. This results in very complex calculations, which is why in industry adhesive bonds are designed to only be used under elastic behavior. Therefore Eq. 2.8 is a valid equation to estimate the lap-shear strength of an adhesive [9].

The lap-shear strength also varies with temperature in a curvy manner as indicated in Figure 2.11 for various adhesive materials. With increasing temperature the elastic modulus of the adhesive decreases and the strain increases when keeping the stresses constant. The higher strains reduce the stress peaks at the edges and allow for a higher maximum applied force, meaning an increase in lap-shear strength. When the cohesion of the adhesive decreases, which usually happens when the T_g of the material is reached, the strength rapidly decreases again [8, 9].
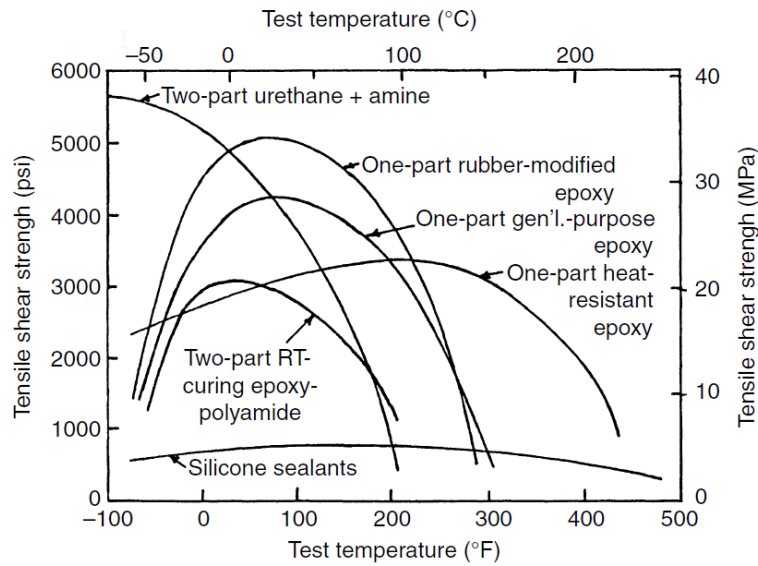
Figure 2.11: Lap-shear strength vs test temperature of various paste and liquid adhesives [8]

In summary, lap-shear strength cannot be seen as an adhesive material property because it is influenced by other factors than the adhesive behavior, but it is vitally important when comparing different adhesives, adherends or surface pre-treatments as well as for the assessment of aging influences [9].

Peel Strength

As already pointed out in the previous section, peel plays another major role in adhesive bonds. Because of the peel stresses acting on the edges of the bond under tensile loading, but also for a bond under pure peel loading, the peel strength needs to sufficiently high to withstand the design peel loads. Peel strength is defined as the average peel force per unit width and is the resistance of the bond to peel forces, acting normal to the bond area. It should actually be called peel resistance, because it is not a property purely dependent on the adhesive material, but dependent on multiple factors. It is influenced by the elastic modulus of the adherends and adhesive, the adhesive thickness, the adherend thickness and the bond width. While the adhesive's stiffness only has a small influence, the peel strength increases rapidly with increasing adherend stiffness. Another way to increase the peel strength is by increasing the adherend thickness or by increasing the thickness of the adhesive layer. Lastly, the peel strength can be increased by increasing the bond width, which is directly proportional to the peel force [9, 30].

Pot Life

For multi-component adhesives the pot life plays an important role. The pot life is the time it takes for an adhesive from mixing of its components until full curing. After mixing the components react to polymers and cross-link. With increasing polymerization the viscosity of the adhesive increases up to the gel point where it becomes fully cross-linked. The more

viscous the adhesive the lower the wettability. Therefore the pot life determines the time available for the adhesive application. It is proportional to the curing time of the adhesive and can take a few seconds up to several hours [30]. For non-reactive adhesives, like hot melts, the application time is also limited but in this case usually defined as open time.

2.2 Pre-Treatments for Composite Substrates

In order to improve the adhesion between the adhesive layer and the adherend different surface pre-treatments should be performed. Different pre-treatments can have different effects on the surface in order to increase the bond strength.

Thermoset composites belong to the group of low-energy surfaces, meaning that they usually have a surface free energy of less than 50 mJ/m^2. Metals in comparison belong to the high-energy surfaces group, because they typically have surface free energies of more than 500 mJ/m^2. Usually surfaces of higher free energy require less pre-treatments and offer great bond strength without any treatment, because an adhesive can only wet a surface well if it overcomes the surface tension. This requires that the surface energy of the adhesive is lower than that of the adherend. But even for those surfaces the bond strength can be improved by pre-treatments. Therefore it is of high importance to pre-treat low-energy surfaces [11, 20]. The three main effects that pre-treatments have on substrate surfaces are [20, 21, 31, 32]:

1. The ***removal of any contaminations*** and lose particles or other substances that create a weak boundary layer on the substrate surface.

2. The ***roughening of the surface*** to create a topology for mechanical interlocking of the adhesive to the adherend.

3. The ***conditioning of the substrate surface*** to facilitate the formation of chemical bonds (hydrogen bonds, dipoles, van-der-Waals forces or even primary bonds) in the adhesion zone. The conditioning can increase the surface free energy and the surface wetting.

These three effects or mechanisms can be assigned to three pre-treatment categories. Many different authors use different categorizations [33,34], but for this document the pre-treatments are separated into cleaning, ablation and conditioning, which are further explained in the following subsections.

2.2.1 Cleaning

The first step of any pre-treatment, basically the prerequisite of bonding, is the cleaning of the surface. This is usually done by the use of a ***solvent***, which does not irritate the surface but removes any kind of grease, particles or other contaminations that could block the adhesive to form a proper bond. If a surface is covered in persistent grease and oil layers it has to be wiped repeatedly with solvent soaked cloths until clean or else the adherends need to be placed in a vapor degreasing chamber, where the solvent is vaporized and 'washes off' the grease [9, 20]. Typical solvents are:

- Halogen hydrocarbons

- Hydrocarbons

- Water-based media

- Biological media

For less contaminated surfaces cleaning with ***water, detergent*** or ***air pressure*** can already be sufficient. It is important to use distilled water when treating CFRP parts. Water containing ions acts as an electrolyte when the CFRP is in contact with metals. Therefore the use of distilled water, which does not contain ions, is used to avoid contact corrosion in CFRP-metal assemblies.

2.2.2 Ablation

Ablating pre-treatments are used to roughen the surface. By doing so additional contaminations are removed and mechanical interlocking is enabled, which improves the adhesion. For composites it is important to use gentle abrasive methods in order to only take off resin and to avoid damaging the fibers. The most common methods for fiber-reinforced plastics are peel-ply, sanding and grit-blasting [35].

Peel-ply is a fabric that is applied as the most outward (and/or inward) layer of a composite layup and undergoes the full curing cycle together with the laminate. Most peel-plies are made of Nylon or Dacron. Their advantage is that they are very repellent towards most resins and therefore easily removable after curing. Once removed they leave a rough surface topology with almost no surface contamination. Some leftover resin particles can be brushed or blown off the surface, which is then bondable straight away. Since this method is the one with the least chance of surface contamination, it is the favored method for most cases [11,35].

If during the manufacturing of the adherend the adhesive bonding was not accounted for or if the composite manufacturing process is not suitable for peel-ply application sanding or grit-blasting are often used for fiber-reinforced plastics.

Sanding can be done by hand or by machine. It is important to use medium grit sandpaper (80- 120 grit) to sand gently without fiber damaging. The surface to be sanded should be large enough to eliminate the edge rounding effect that is common for sanding, even when sanded evenly. Usually machine sanding gives a more even result than hand sanding [9,35].

The least common method is ***grit-blasting***. As the name says, during the process grit is sprayed under high pressure onto the surface to remove a small layer of resin on the substrate surface. It is the most elaborate method, as a trained operator is needed to perform the blasting. Additionally, it is of high importance for composites that the grit is of equal size and free of contaminants in order to leave an even surface topology with no fiber damage [35].

After both, sanding and grit-blasting, some lose particles have to be removed by brushing or blowing. Usually the surface is cleaned once more after ablating treatments have been performed [35].

2.2.3   Conditioning

The last category of pre-treatments is conditioning, the application of media to the adherend's surface to improve the bond strength and to protect the surface from contaminations and corrosion. It is advisable to clean the surface before applying any type of conditioning, especially after abrasive treatments.

For composites the most widely used conditioning pre-treatments are ***primers***, also called 'activator'. A primer is a thinned organic solution that contains the basic adhesive compounds of the adhesive to be applied afterwards. It is applied to the substrate as a thin film of 0.0015-0.05 mm thickness and requires drying before the adhesive is applied. Its main function is to improve the bond strength, the adhesion forces to be exact. A primer can improve the bond strength in different ways. For adhesives with poor wetting properties a primer can be used to improve the wetting of the surface. The adhesive can then adhere to the primer, which is adhered to the substrate surface. The formation of stronger interfacial forces by the use of a primer as an interlink results in a bond with increased strength.

As a second function a primer can be used to increase the bond's durability. It can contain additives that are moisture resistant or corrosion inhibitors. These additives protect the bond interfaces from corrosion and hydration and therewith maintain the adhesion strength. A primer's last function is surface protection. This is particularly important if the pre-treated surface is not adhered right away but undergoes some handling steps before the adhesive is applied. The primer acts as a thin coating that repels contaminations and therewith protects the surface from deactivating again. This way the surface can be stored months before the adhesive is applied [8, 9, 20].

Another way to condition the adherend's surface for bond strength optimization is the application of an ***adhesion agent***. Adhesion agents are very similar to primers. They can be applied to the substrate surface but also be mixed into the adhesive in order to increase the interfacial forces between adhesive and adherend. As shown in Figure 2.12 they are bi-functional; they react with the adherend on one end and with the adhesive on the other.
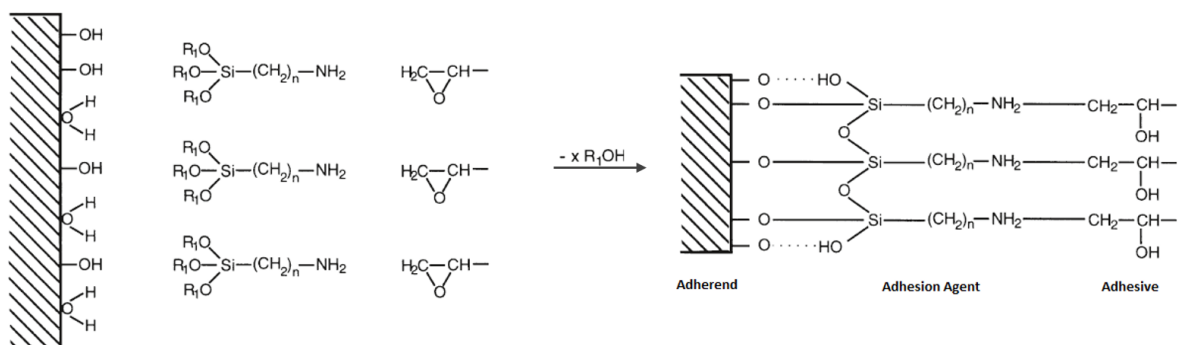
Figure 2.12: Reaction of a silane adhesion agent with adherend and adhesive [9]

In contrast to primers adhesion agents are not chemically reactive to cross-link with the substrate surface but just 'bridge' the adherend and adhesive. Therefore adhesion agents are sometimes also called 'chemical bridges'. Another advantage of adhesion agents is that they improve the aging resistance of the bond [9].

Chemical etching is an additional method for surface conditioning. Here active chemicals, such as acids or oxidizers are applied to the surface in order to activate the surface by changing the physical and chemical characteristics [8, 9].

Lastly, ***electro-chemical processes***, such as Plasma-, Corona-, Flame or Excimer Laser Treatment can be used to treat the substrate surface. Further explanation can be found in [8, 31, 35].

The best solution for low-energy surfaces such as composites is a multi-stage pre-treatment that is built of all three pre-treatment categories. A multi-stage pre-treatment usually results in the greatest bond strength. It is just important to always keep in mind whether the chosen pre-treatment is suitable for the performance requirements of the bond design and whether it is adequately chosen for the manufacturing process and costs of the part [8, 9]. Further information on how to pre-treat a composite or metal surface can be found in [36].

2.3 Test-Methods

This section describes everything related to determining the mechanical properties of the PUR material to be used for the open mold injection bonding process. This entails lap shear and peel tests, including different aging conditions. All of the experiments are performed on flat test specimens, which are manufactured with the same material properties as the actual components. All tests and aging are done in terms of standards to be able to get certification and approval to use the component in a vehicle driving on public streets. All laboratory tests are performed at a technical laboratory at Daimler AG's research site.

2.3.1 Lap-Shear Test

The standard lap-shear test is described in DIN EN 1465 [37]. The purpose of a lap-shear test is to determine the lap-shear strength of the adhesive material and to compare the change in properties due to different aging conditions. Additionally, the failure pattern of the bond area can be analyzed in order to make conclusions with regard to the adhesion of the adhesive on the adherend materials.

The test specimens, as shown in Figure 2.13, consist of two adherends of size $100(\pm 0.25)$ x $25(\pm 0.25)$ x $1.6(\pm 0.1)$ mm, which are adhesively bonded. The bond has an overlap length of $12.5(\pm 0.25)$ mm and a typical thickness of 0.2 mm. For the test the adherends are placed in a tensile test machine using clamping grips. The machine should be set such that it operates at a constant force rate reaching failure after 65 ± 20 seconds. The force input must be parallel to the bond area and the major axis of the specimen. The test result is the highest recorded force at rupture. This force can be translated as the breaking force (F) of the specimen and is used together with the bond area (A) to calculate the tensile lap-shear strength as shown in Eq. 2.8. If a specimen fails under substrate failure, the result is to be discarded. In order to draw valuable conclusions a minimum of five countable tests have to be noted.
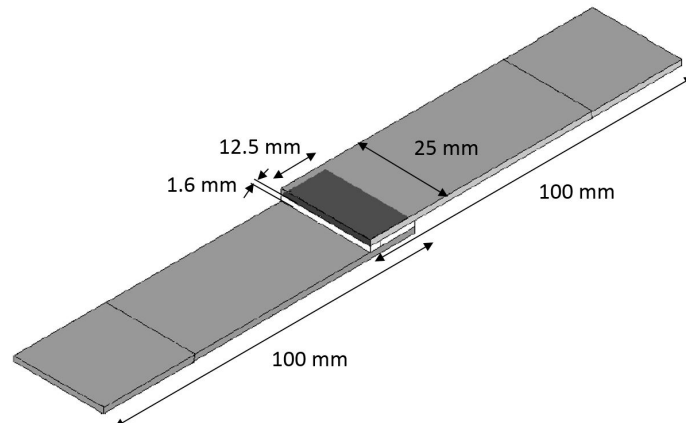
Figure 2.13: Single lap joint specimen as used for lap-shear testing with dimensions according to DIN EN 1465 [38]

It is important to note that this test is not to be used to generate a stress-strain curve and is not applicable for structural bond design calculations. Using the sheets of the above mentioned geometry introduces bending moments to the specimen because of the axial offset of the two adherends and the tendency to create one linear load path. These bending moments cause an overlap with the shear loading, which results in an upward bending of the bond edges and therewith introduces normal forces as shown in Figure 2.14, which causes peel.
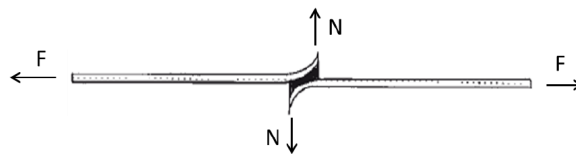
Figure 2.14: Lap-shear specimen under applied load with normal forces acting on the bond edges [28]

To eliminate the peel factor, thick lap-shear specimens have to be used.

2.3.2 Peel Test

A peel test is done to determine the adhesion and failure behavior of the adhesive material on different surface pre-treatments and under different aging conditions. It is not possible to draw any conclusions about the adhesive strength from this test. As depicted in MBN 10518 [39] a 150 x 20 x 5 mm adhesive line has to be applied onto a pre-treated substrate. All adhesive lines are aged in various ways, as listed in Section 2.3.3, to investigate their influence on the adhesion. For the test the adhesive line is cut into just above the substrate and then pulled at a 90° angle with flat nose pliers until adhesion failure. The peel process is demonstrated in Figure 2.15. As soon as adhesion occurs, the adhesive is cut into again and the process is repeated.

Figure 2.15: Peel-off test of an adhesive [39]

After the peel test is done the result will be assessed based on the percentage of cohesive failure. Only an adhesive with more than 95% cohesive failure receives an adhesion grade 5. An adhesion grade 5 (or an adhesion grade 4 with a maximum of 25% substrate failure after aging) is the only grade that counts as a pass for series qualification.

(a) 100% cohesive failure   (b) 50% cohesive failure   (c) 0% cohesive failure
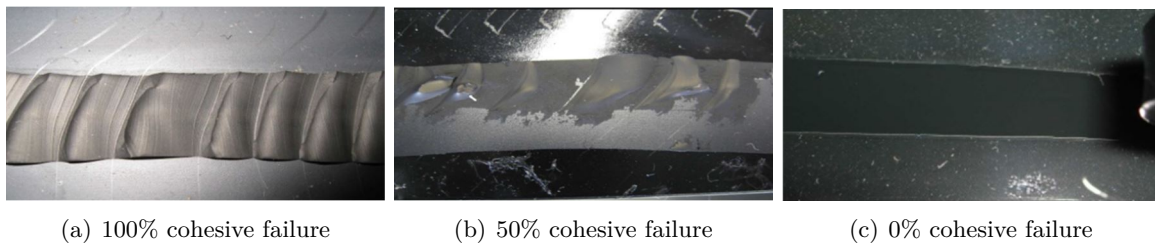
Figure 2.16: Adhesion assessment after a peel test [39]

Figure 2.16 shows typical failure behaviors at different levels of cohesive failure and is used to aid the adhesion assessment.

2.3.3 Aging

An analysis was performed on the most critical aging conditions for a a CFRP automotive roof, based on the test standards necessary for component release. The following standard tests are mandatory according to MBN 10518 [39] condensation atmosphere with constant humidity storage, alternating heat climate storage, cataplasm storage and standard atmosphere. They are all explained in the following sections.

Condensation Atmosphere with Constant Humidity Storage (CCH)

For this aging process the test specimens are stored in a vapor-tight chamber with a constant air temperature of $40 \pm 3°C$ and a constant relative humidity of 98% for 10 days (240 hours), which is depicted in Figure 2.17. It depicts the temperature (T) and relative humidity (RH) over time (t).

Since the surfaces of the specimens are at lower temperatures than the surrounding, the atmospheric humidity condenses on the surfaces. The Condensation Atmosphere with Constant Humidity test is usually used to test the adhesion of coatings, but is also helpful to determine

the adhesion the moisture intake of an adhesive and to that effect the stresses due to adhesive expansion. The detailed storage process is outlined in DIN EN ISO 6270-2 [40].
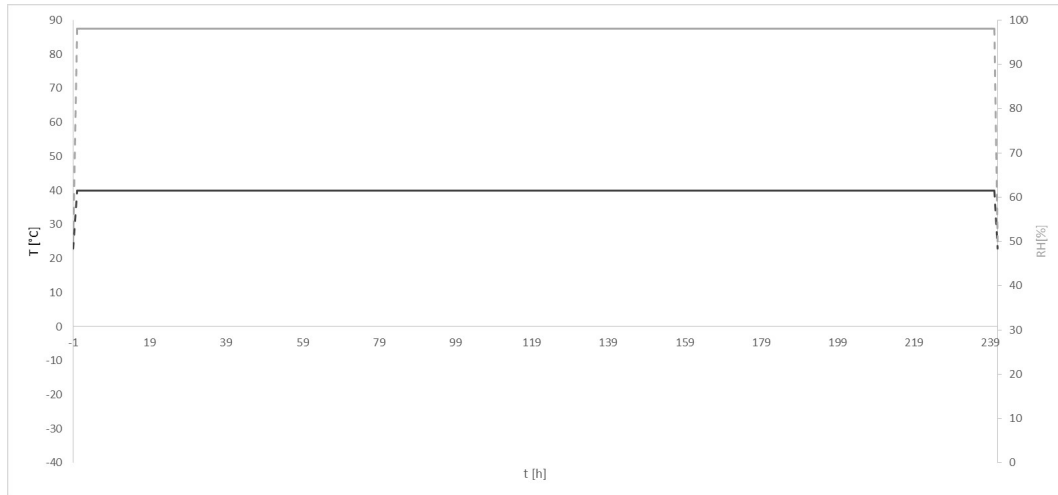
Figure 2.17: Full CCH Aging Cycle

Alternating Heat Climate Storage (AHS)

Figure 2.18 shows the first cycle out of 10 cycles for full AHS conditioning. As described in paragraph 6.7 of MBN 10518 [39] in connection with DIN EN ISO 9142 [41], the alternating heat climate storage is specifically to test the influence of the induced stresses on an adhesive caused by different thermal expansion coefficients of dissimilar adherend materials. For this aging process the specimens are placed in a chamber for ten cycles, in which the temperature alternates between 4 hours of $80°C$, 4 hours of $-30°C$ and 16 hours CCH.
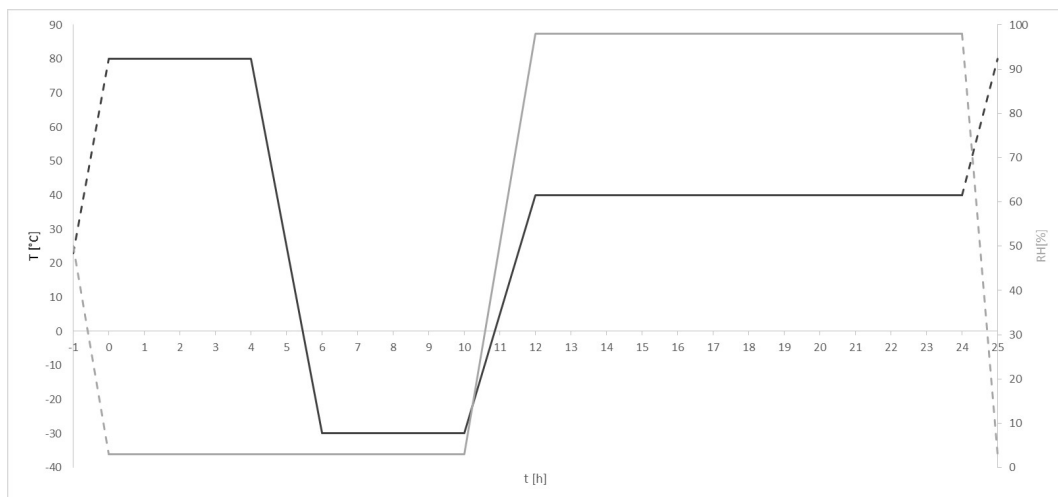
Figure 2.18: The first of 10 repeating AHS Aging Cycles

The times for temperature adjustments is included in the given time frames and should take

no more than 2 hours for each change. The total exposure time results in 240 hours. Between the cycles or stages no conditioning at room temperature should take place.

Cataplasm Storage (Cata)

A common way to test adhesive bonds on glass and e-coats is the cataplasm storage, as depicted in MBN 10518 [39]. During the storage time, as visualized in Figure 2.19, the specimens will first be kept at $70°C$ air temperature and 98% relative humidity for 7 days (168 hours) to experience condensation as described in the cyclic aging of DIN EN ISO 9142 [41]. Immediately after the temperature will be dropped to $-25°C$, which will be kept for 16 hours. The Figure also includes the 72 hours extra time of storage in standard atmosphere, while the specimens in the other storages are still conditioned.
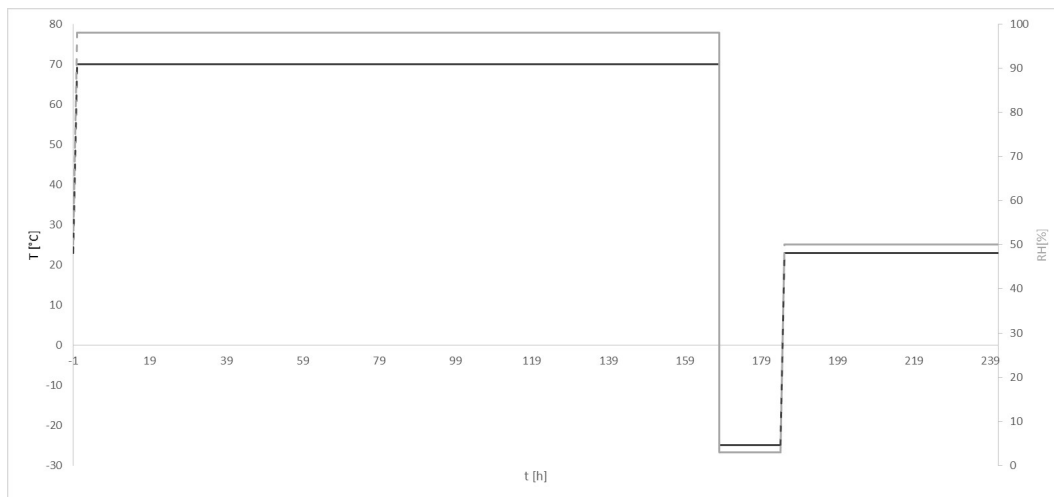
Figure 2.19: Full Cata Aging Cycle

This test is performed to check whether the adhesive bond suffers from frost damage, because the re-drying takes more time than the cooling of the specimen. Another effect of this condition is that the corrosion products which have been created in the meantime can't be dissipated because of the closed test atmosphere and therewith might have an influence on the adhesive properties.
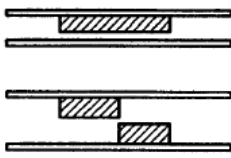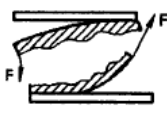
Standard Atmosphere (SA)
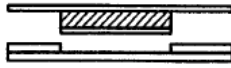
The standard atmosphere, also called normal climate, conditioning is described in DIN EN ISO 291 [42]. This conditioning method is used to expose all specimens to the same standard atmospheric conditions. By doing so all specimens gain the same equilibrium of temperature and moisture and the adhesive can cure fully. This takes out the temperature and moisture factors and gives equal test start conditions for the specimens. The 23/50-2 standard atmosphere is used, which is the condition of non-tropical countries and implies $23° \pm 2°C$ at 50% $\pm 10\%$ relative humidity.

After a minimum of 24 hours in standard atmosphere the specimen can be tested.

2.3.4 Failure Modes of Bonded Joints

Figure 2.20 is an extract from the standard DIN EN ISO 10365 [43], which shows and describes the different failure patterns and the corresponding designations.

Table 1 — Designation of failure patterns

Substrate/Adhesive	Failure patterns	Designation
Substrate	Failure of one or both adherends (Substrate failure)	SF
	Failure of an adherend (Cohesive substrate failure)	CSF
	Failure through delamination (Delamination failure)	DF
Adhesive	Types of cohesion failure — Cohesion failure	CF
	Special cohesion failure	SCF
	Adhesion failure	AF
	Adhesion and cohesion failure with peel	ACFP

Figure 2.20: Failure patterns in adhesive bonds [44]

Adhesive bonds can fail in various ways. One can separate the patterns in failure of the adhesive and failure of the substrate. Usually only the failure in the adhesive layer is of importance, which is why those patterns are commonly subdivided again. One separates between adhesive failure, cohesive failure and mixed failure.

Adhesion failure describes the 'rupture of an adhesive bond in which separation appears visually to be at the adhesive-adherend interface' [43]. It can happen on just one adherend

or on both adherends.

Cohesion failure describes the 'rupture of a bonded assembly in which separation appears visually to be in the adhesive or the adherend' [43]. The rupture can appear right in the center of the adhesive layer or as a special near-substrate failure.

Mixed failure is any combination of adhesion and cohesion failure and can be expressed in a percentage per failure type.

2.4 Process Analysis Tool - Design of Experiments (DoE)

For an experimental research project it is important to optimize the experimental processes to avoid a long trial and error (TAE) or one-factor-at-a-time (OFAT) procedure. The first step is good planning and finding a quick and easy way to properly evaluate the outcome. There are many tools that can be used for process analysis, but the most powerful one and most widely used is the Design of Experiments (DoE). The goal of using DoE is to gather as much information on the relation between input parameters and outputs with minimal test effort. The input parameters as well as the outcomes are deposited in a statistical way in order to quantify the effects of change in parameter [44, 45].
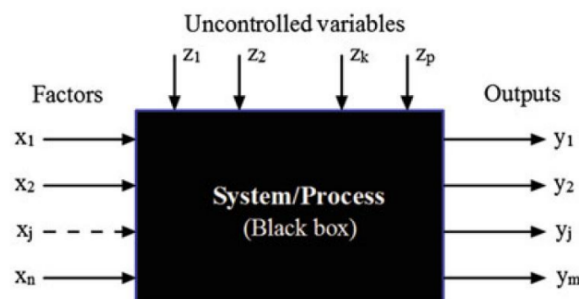

Figure 2.21: Visualization of the formal definition of a DoE [45]

Using TAE many parameters are changed at the same time and using OFAT only one parameter is changed at a time. Both processes are time-consuming and give no insight into the correlation between the inputs and outcomes because the optimum is found by chance. Instead using DoE a set of experiments is conducted in a predefined way where all input parameter adjustment combinations are executed. Because multiple factors are changed at once (factors x_1 to x_n in Figure 2.21), insight in the interactions and influences on the outputs can be identified and the random error is minimized. The minimization of random error using DoE additionally guarantees experiment replication [44–46]. The most common DoE method is the full factorial design as displayed in Figure 2.22. For this design a design matrix is constructed based on all possible input combinations. Therefore each input variable is assigned different test levels dependent on the setting options it is varied upon.

A	B	C	D
-1	-1	-1	-1
1	-1	-1	-1
-1	1	-1	-1
1	1	-1	-1
-1	-1	1	-1
1	-1	1	-1
-1	1	1	-1
1	1	1	-1
-1	-1	-1	1
1	-1	-1	1
-1	1	-1	1
1	1	-1	1
-1	-1	1	1
1	-1	1	1
-1	1	1	1
1	1	1	1

Figure 2.22: Schematic of a full factorial design with 2 levels per variable [44]

This method covers the experiment ground most thoroughly but if many variables and levels are included the matrix rapidly expands to incomputable extent. Therefore many new designs were developed using only a fraction of input variables and levels to decrease the matrix size and still gather useful information on the response behavior [47]. For a well-defined DoE process the following steps need to be taken [45, 46]:

1. Formulation of a clear project objective and the desired outputs essential for the project goal. This also includes the determination of the necessary equipment, processes and people.

2. Diligent definition of the controllable and uncontrollable key input variables to eliminate any unknown influences on the process output. The defined variables should be directly relatable to the output and should not be a function of other variables.

3. Sensible selection of the test levels for every controllable variable in order to cover the extremes or limits as well as means without too much extent.

4. Creating a design matrix with compatible and realizable variable combinations to effectively and efficiently draw conclusions

A well-prepared design of experiments can result in a time- and cost-efficient project analysis even for complex experiments. Because of its special setup it provides insight into the interactions between the different variables and their effect on the output.

Chapter 3

State of the Art

Since the research focuses on an open mold injection process for PUR-adapters on CFRP roofs, this chapter depicts PUR manufacturing techniques that are already used in industry, where the polymer reacts just before injection into the mold and offers fast curing times. First, the most relevant manufacturing and assembly processes and terms for visible CFRP roofs are discussed. As a basis for understanding the working principle of reaction injection molding, a closed-mold injection process, is explained. Finally, the open-mold injection process with its benefits is compared, followed by a presentation of the two mixing and dispensing units usable for the open-mold injection process.

3.1 Visible CFRP Roofs in the Automotive Industry

Automotive OEMs use different manufacturing techniques to get the best CFRP roof quality. Additionally, the roof assemblies to the BIW vary looking at comparable car types between the OEMs. This section discusses the common techniques used for CFRP roof manufacturing and the assembly approach utilized at Daimler AG. Additionally it points out the definition of a Class-A surface finish.

3.1.1 Manufacturing Techniques of CFRP roofs

CFRP roofs for cars can be produced in different ways. The main drivers are the series size, cost and quality of the part. A common technique is Resin Transfer Molding (RTM) [48]. It is known to be used for manufacturing of complex composite parts with high tool parts surface quality for high performance. The process is a closed-mold process with low pressure [49]. The fibers are placed onto the bottom mold and after closing of the molds injected with the resin. For this technique the part size can be small or larger, as long as the tooling is not too big to cause a pressure loss [50]. Another commonly used technique for visible CFRP parts is pre-preg layup with autoclave processing. The pre-impregnated fibers are placed and then bagged and placed in the autoclave, where they are cured under high pressure and

high temperature. This technique is used to have a very low void content and to therefore get high quality parts [51]. The size of the part is dependent on the available autoclaves, which are usually rather limited in size. The major disadvantages of pre-preg in combination with autoclave are the high material and process costs and the relatively low production speed, which is not appropriate for high production series [52]. Experience shows, that the manufacturing technique of the CFRP structure, and whether a two-sided or one-sided tool is used, can have an influence on the print-through to the outside surface.

Because the roof's outside surface is at direct eye-sight of the customer, it is vital that no visible defects can be detected. Such a surface is defined as a Class A surface.

3.1.2 Class-A Surface Finish

The notion Class-A comes from the automotive industry. It describes the quality of the visible surfaces of the exterior or interior. A Class-A surface is curvature constant and has no visible flaws and optical disruptions. Furthermore there are Class-B and Class-C surfaces. A Class-B surface is usually on invisible parts and structural components of the BIW, whereas Class-C surfaces are usually temporary surfaces which are only used for tooling [53]. Since the surface of a visible CFRP roof is so sensitive to defects it is assembled to the chassis after the body-in-white went through all the surface treatments and paint job.

3.1.3 CFRP Roof Assembly

At Daimler AG, to join the CFRP roof to the chassis, a highly viscous assembly adhesive is applied onto the subframe structure, which was previously added onto the inside roof surface. Subsequently, the roof is bonded onto the chassis by pressure application. The application process as well as the placing of the roof onto the chassis is usually automated or at least semi-automated [54].
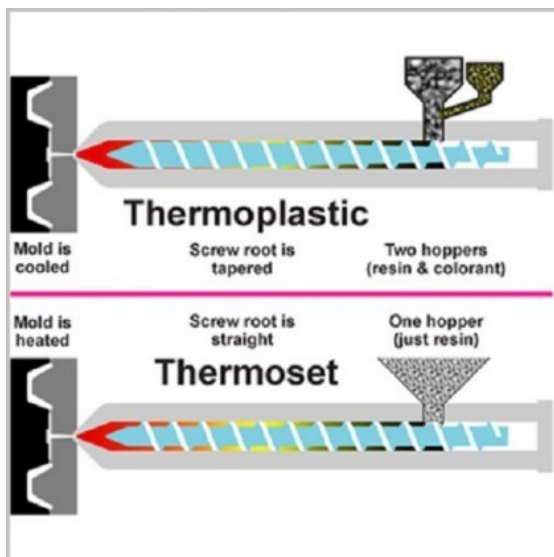
3.2 Polymer Injection Processes

The injection process studied in this thesis is a novel injection process type, an open-mold polyurethane injection process. In this section it is compared to the frequently used closed-mold injection processes; injection molding and reactive injection molding. Moreover, it lines out the the mixing and dispensing unit types that are suitable for the open-mold process.

3.2.1 Closed-Mold Injection Process

The most common closed-mold process is Injection Molding (IM), which is a casting process used to form thermoplastic parts. A similar process for thermoset materials, especially polyurethanes, is called Reaction Injection Molding (RIM). The name comes from the fact that the two thermosetting components both flow into a mixing chamber, where they react under the application of pressure. From there on the process is pretty much the same as for thermoplastic IM. The polymer is directly injected into a closed-mold. Figure 3.1 depicts the RIM process, where polyol and isocyanate react to a polyurethane, which is injected into a closed-mold [55, 56].
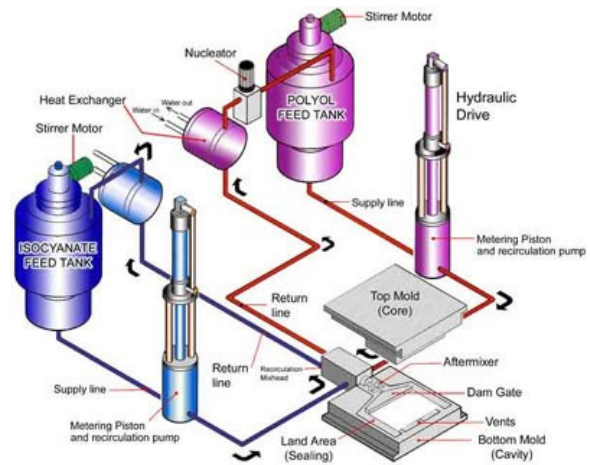
In comparison to IM the mold for RIM is heated instead of cooled and the screw root is straight instead of tapered, as shown in Figure 3.2. RIM can also be used for other 2-component thermosets, such as epoxies or polyesters, but is then called Liquid Reaction Injection Molding (LRIM). Additionally the process can be modified in order to incorporate reinforcements like short fibers or fiber meshes. The first case is called Reinforced Reaction Injection Molding (RRIM) and the latter is called Structural Reaction Injection Molding (SRIM), where the mesh is used to build a solid skin on the outside of the part in order to increase the structural properties, while keeping a low weight [55, 56, 58].

Figure 3.1: Reaction Injection Molding (RIM) process schematic [57]

There are several advantages using RIM. Although the pressure in the mixing chamber is high (up to 21 MPa), the injection pressure into the mold is much lower than of the IM process, because of the lower viscosity of thermosets. This allows for lighter molds and smaller equipment, resulting in 10-20 % lower investment costs [57, 59]. Furthermore, one mixing chamber can be used to feed up to ten molds because of the high pressure in the chamber. This, plus the fact that the curing time is rather low, increases the production rate compared to IM [55, 56, 58].

Figure 3.2: Thermoplastic vs thermoset closed-mold injection process [60]

Other benefits of closed-mold processes are minimal waste, part reproducibility with high accuracy, and low labor costs, because the process is automated and the final parts only need little amount of finishing after demolding [61]. But the process also has a downside. If the complexity of a part increases, casting processes are usually unfavorable. First of all the part always needs demolding after curing. Only if the part does not come with too low radii and angles and a minimum wall-thickness a non-destructive and fast demolding can be assured. With increasing complexity the investment costs increase, since the tool's complexity increases, which might also require higher pressures and more equipment. Moreover, the more complex the part the more labor intensive the application of release agents before the process and the cleaning after the process. The application of release agents to the mold also leaves traces of it on the surface of the final part. This requires additional treatments before the part can be bonded [62]. A less labor intensive option where the bond surface requires no additional treatment could be an open-mold injection process.
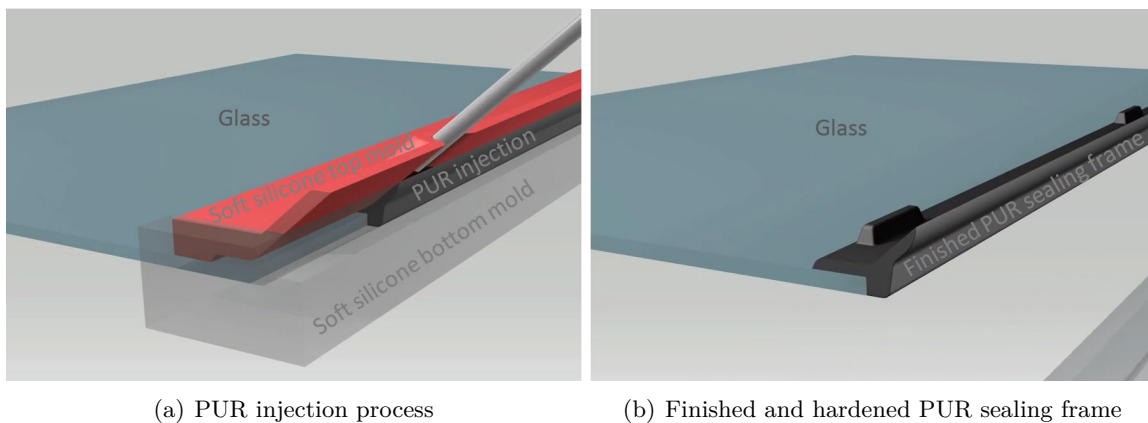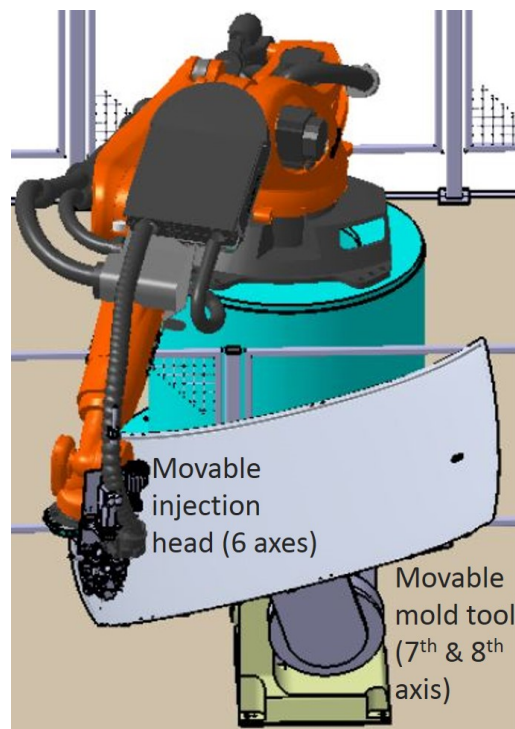
3.2.2 Open-Mold Injection Process

In order to create a multi-functional polyurethane part a good solution is an open-mold injection process. The process is not very common yet. BASF first came up with the idea to use an open-mold process to create 'flush seals' for windscreens without the application of pressure and long curing times. The process is called Window Spray Technology (WST) and originally called 'COLO-Fast WST' by BASF. In 2006 Opel was the first company to use this technology for the panoramic windscreen of the Opel Astra GTC [63]. The Belgian start-up Exypnos carried on BASF's work under the name 'WSTplus' and extended the technology for edge encapsulation and component integration in a single manufacturing step on windscreens and panoramic glass roofs, solar panels and battery systems [64]. Soft silicone cavity profiles are implemented inside solid top and bottom molds. A 6-axes robot injects the PUR into the cavity as shown in Figure 3.3(a). The result presented in Figure 3.3(b)) is a PUR sealing frame, which is directly adhered to the glass without the need of additional adhesive [65].

(a) PUR injection process   (b) Finished and hardened PUR sealing frame

Figure 3.3: Exypnos WSTplus open-mold injection process [65]

Instead of just using the technology for edge encapsulations, the same principle can be applied on different structures and materials to add adapter structures or other functionalities. This is done by placing the main part into a bottom mold and adding one mold or multiple molds on the top to integrate different functionalities, such as inserts, shape changes, insulating mats and many more. The PUR is inserted into a cavity between the molds using a 6-axes injection head. To enable the application of PUR-parts with even higher complexity, the bottom mold can be placed on a movable robot to add a seventh and eighth degree as visualized in Figure 3.4 [1]. The WST process can be seen as a combination of an open-mold, pressure less variation of RIM and adhesive bonding on just one adherend. It facilitates the manufacturing of the PUR part, including the integration of additional objects, and its bonding to the main structure in just one manufacturing step. Two main benefits can be associated with this new technology. Firstly, the investment costs are even lower than for RIM, since no pressure is applied to the molds making them less expensive.

Figure 3.4: Open-mold injection process using 8 axes (6 axes by a movable injection head and 2 axes by a movable mold tool) on a vehicle roof [66]

Furthermore, the molds can be designed such that the contact surface, where an assembly adhesive is supposed to be applied afterwards, is not in contact with the molds and any release agents. This uncontaminated surface can therefore be bonded directly, without the necessity of any pre-treatment [67].

3.2.3 Mixing and Dispensing Units for PUR Injection Processes

Depending on the product's quantity, cycle time, allowed production costs, size and accuracy, a low- or high-pressure mixing and dispensing unit can be used for the mixing and dispensing of the PUR. The working principles, advantages and disadvantages are discussed in the following paragraphs.

Low-Pressure Mixing and Dispensing Unit

A low-pressure mixing and dispensing unit, as the name already gives away, mixes and dispenses the two adhesive components under low pressure. Low pressure in this case means below 20 bar [68]. Both components, polyol and isocyanate for PUR's, are injected into the mixing chamber where they are mixed by a rotor, as depicted in Figure 3.5.

The components are constantly mixed into a homogenous blend while transported to the outlet. This mixing unit can be used for any mixing ratio and gives perfect blends even for small injection quantities that are necessary for very precise applications.

To improve the blending it is advised to eject a small amount before the actual application, such that the first bits which might not be perfectly mixed are discarded [67, 69].

The downside of these types of mixing units is the necessity of a scavenging process between each application to rinse out the left-over adhesive in the mixing chamber that can never be fully emptied. The suppliers offer high-pressure water flush systems for flushing, but the cleaning still increases the process time, which is unfavorable for short cycle times common in the automotive industry. Although the plant investment is relatively low, due to the cleaning necessity the process costs are relatively high. This method is therefore suitable for continuous processes, where the process is started and only stopped after long period of time to minimize the amount of cleaning time [69, 70].
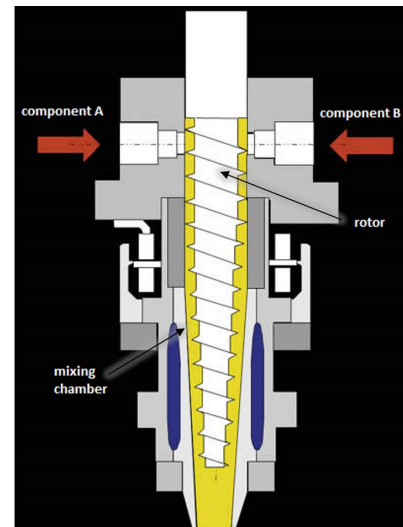
Figure 3.5: Low-pressure mixing and dispensing head

High-Pressure Mixing and Dispensing Unit

As an alternative to low-pressure units, high-pressure mixing and dispensing units can be used to mix and dispense polyurethanes. Using the latter no extra cleaning step is needed between the applications, because the two components are mixed and ejected under high pressure, emptying the mixing chamber fully when the application is stopped.

The control piston is the main piston that applies the high pressure to the mixing chamber. The nozzle needle, a smaller piston, controls the component feed.
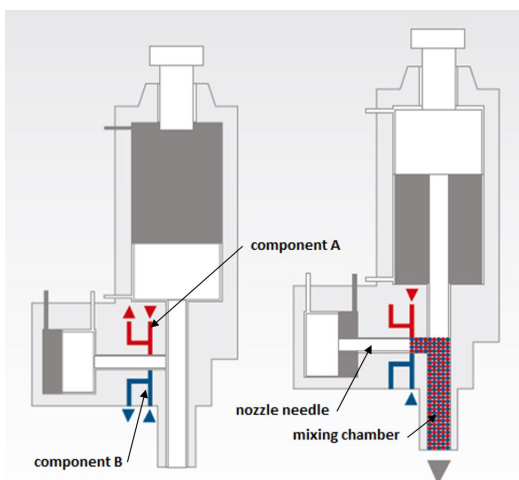
Figure 3.6: High-pressure mixing and dispensing head (closed and open) [71]

If the pressure is applied by the control piston the nozzle needle is simultaneously pushed back and therewith opens the valves of the components. Both components are then mixed together in the mixing chamber by the kinetic energy caused by the high applied pressure. Figure 3.6 shows the high-pressure process described above [69, 70].

Although this mixing unit needs no additional cleaning and offers an increased reaction time to reduce the hardening time, it also comes with disadvantages. The main drawback is that the mixing is not as homogenous as of low-pressure units, which makes it nearly impossible to apply quantities of less than 5 g/s. Additionally, it comes with the downside that the plant invest for this unit is much higher, because of the more complex valve systems and pressure pumps [70].
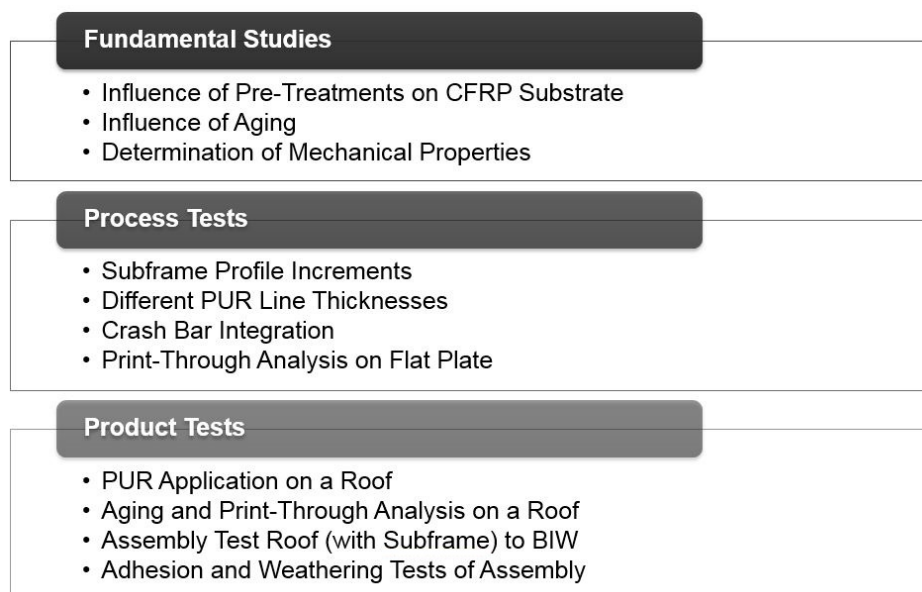
Chapter 4

Research Planning and Preparation

For the research project the PUR material Elastolit R 8919/107 was used and studied. The material in combination with the high-pressure injection process has not yet been tested on CFRP substrates at Daimler AG and AMG. To apply the material and process to a CFRP automotive roof, both material and process have to be qualified and verified. The research objective introduced in Section 1.1 originated from this definition of tasks.

4.1 Experimental Design

Three major experiment steps need to be taken to qualify the production process for the subframe of the CFRP roof, which are visible in Figure 4.1.

Fundamental Studies
- Influence of Pre-Treatments on CFRP Substrate
- Influence of Aging
- Determination of Mechanical Properties

Process Tests
- Subframe Profile Increments
- Different PUR Line Thicknesses
- Crash Bar Integration
- Print-Through Analysis on Flat Plate

Product Tests
- PUR Application on a Roof
- Aging and Print-Through Analysis on a Roof
- Assembly Test Roof (with Subframe) to BIW
- Adhesion and Weathering Tests of Assembly

Figure 4.1: Required Experiment Steps for Series Production Verficiation

The first step contains the fundamental studies. The material itself and its behavior on the CFRP substrate needs to be analyzed, including the influencing factors, such as surface pre-treatments and aging conditions. Secondly, new production processes need to be developed and qualified for subframe applications on different roof designs. And lastly a PUR subframe needs to be applied to a CFRP roof, which is then assembled to a painted body-in-white for the final product examination. This entails assembly and weathering tests. The last set of experiments, from the PUR subframe application onto the CFRP roof onward, is performed by Mercedes-AMG together with the colleagues at Daimler AG Sindelfingen.

To build a strong foundation for the experiments, they were designed using the DoE method as discussed in Section 2.4. The DoE's can be found in Appendix A.

4.2 Design and Constructions

The CFRP roofs at AMG are offered as special equipment, but only if a panoramic glass roof is offered as special equipment. The main reason is a minimization of the development costs. The consequence is that the glass roof needs to be placed on a specific roof frame and as a result, the CFRP roof needs to be assembled to the exact same specific roof frame. Since the CFRP roof is 3 mm than the glass roof, a subframe is required to bridge the distance between roof and roof frame. Presently the solution to the problem is a bonded CFRP subframe, which should now be replaced by a PUR injection bonded subframe to safe time, cost and weight. But before the new subframe can be applied to the CFRP roof, a few construction and design steps need to be taken.

4.2.1 The CFRP Roof

The main implementation focus of the project lies on the AMG GT R roof and the roof of its high-end derivative. The roofs only differ to the extent that the latter possibly gets an embossing along the center line from front to back as shown in Figure 4.2. The process should be possible for both roof types.

(a) AMG GT R CFRP roof design

(b) AMG GT R derivative CFRP roof design with embossing
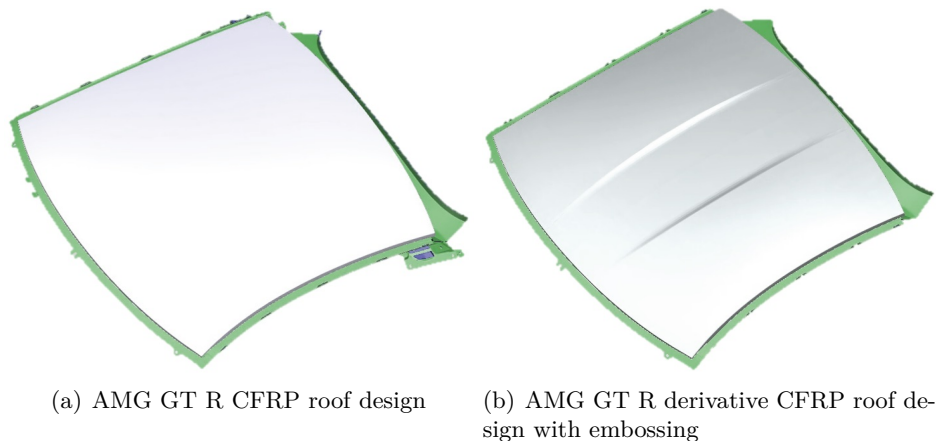
Figure 4.2: CFRP roof design of the AMG GT R and its derivative, including the panoramic glass roof frame

Additionally to the AMG GT R roof, the CFRP roof of another series with different constraints was taken into account, in order to include possible implementations to the process for future vehicles.

(a) AMG GT R CFRP Roof with PUR Subframe (b) AMG four-door vehicle CFRP roof with PUR subframes, crash bar and acoustic inlays
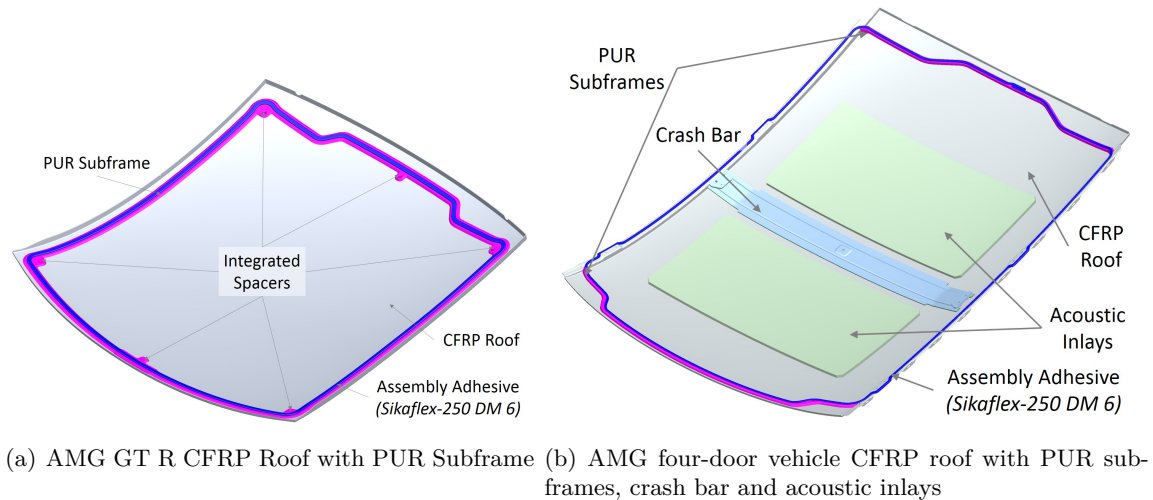
Figure 4.3: Design comparison AMG GT R and AMG four-door vehicle

The major visible difference of this roof is the length extension compared to the GT R roof, since it is a four-door vehicle instead of a two-door one. But with the increase in length come a few additional changes. The longer roof needs an additional crash bar in the middle for vehicle stiffness and crash-worthiness(see Figure 4.3). Additionally, it also requires acoustic fleece inlays to damp out vibrations caused by i.e. rain. Moreover, it has a roof trench with a roof trim on its sides for aeroacoustic reasons and to integrate a water management and roof rack system. For this reason the roof has side flanges which are adhered with direct contact to the painted BIW roof frame. Therefore the CFRP roof of the four-door vehicle only has specific roof bows at the front and rear, which is why no circumferential subframe structure is required, as for the GT R, but a locally applied one at the front and rear of the roof.

4.2.2 The Subframe Structure

As indicated in the previous subsection, the subframe design depends on the design of the roof and the roof frame.

The subframe structures investigated can be categorized in three designs:

1. Circumferential subframe with constant thickness (*GT R*)

2. Circumferential subframe with (local) thickness variations (*GT R Derivative*)

3. Local subframe with (local) thickness variations (*Four − Door Vehicle*)

The AMG GT R PUR subframe was designed based on the current CFRP subframe, but it's volume was reduced to the minimum required to apply the 12 mm wide assembly glue line. The cross-sectional difference can be seen in Figure 4.4.

(a) Original AMG GT R CFRP subframe design   (b) Optimized AMG GT R PUR subframe design
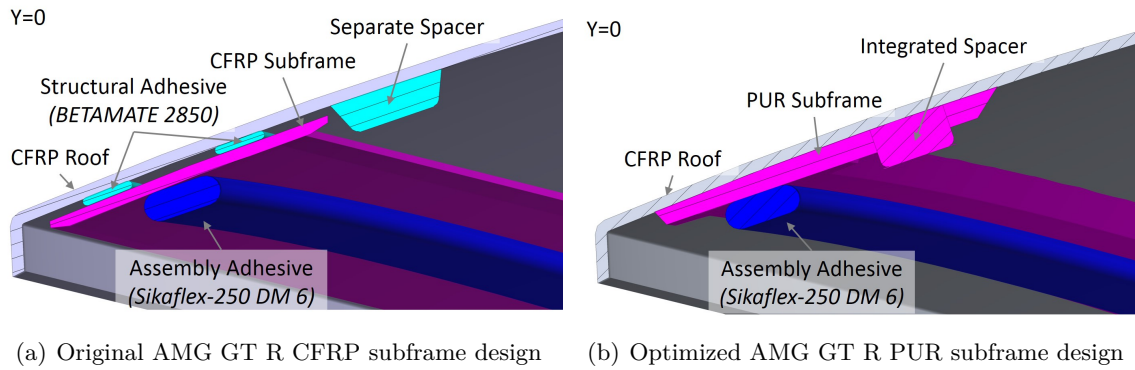
Figure 4.4: AMG GT R CFRP vs PUR subframe design

While changing the material and the dimensions, the PUR subframe still has to meet the requirements, which were already determined for the CFRP subframe. The main requirements to the subframe and its material are as follows.

- The subframe shall bridge the Z-offset between CFRP roof and panoramic glass roof frame.

- The subframe shall supply a rigid surface for assembly adhesive application

- It shall be of hard and tough material to prevent BIW shape deformation during vehicle operation while offering enough energy intake during crash

- The PUR's lap-shear strength shall be above the assembly adhesive lap-shear strength, such that the assembly adhesive is the weak link.

- The PUR has to adhere to the CFRP and the assembly adhesive with a minimum of 95% cohesion failure when peeled.

- The PUR shall not cause print-through on the Class-A roof surface, neither after process application nor due to environmental effects.

The material and slight design change improved the weight of the subframe by 144 g, which is shown in the weight comparison in Table 4.1.

Table 4.1: Weight Comparison CFRP vs PUR Subframe

	Component	Component Weight [g]	Total Weight [g]
CFRP	CFRP Subframe	410	
	Structural Adhesive	85	508
	Spacer	13	
PUR	PUR Subframe	351	364
	Spacer	13	
			- 144

Additionally, it integrates the spacers, which are needed to avoid too low or too high placement of the roof. Using the PUR subframe, the spacers only need to be placed at the correct location (as in CAD) using thin double-sided tape and can then be molded with the PUR in one shot while applying the subframe PUR.

The different influencing factors for the new subframe design and process were evaluated in the experiments, which are discussed in Chapter 5, in order to verify it for series production. The experiments involve verification for all three subframe design categories, testing the adhesion of the PUR on CFRP, determining the maximum profile increment possible in one shot, integrating spacers in the molding process and analysis of print-through due to various thicknesses and $\Delta\alpha$ between crash bar (e-coated steel) and the roof (CFRP).

4.2.3 The Subframe Tool

For the PUR application onto the CFRP roof, a mold tool had to be designed. All parts of the tool are presented in Figure 4.5. To prevent damage of the roofs Class-A surface, the tool consist of a bottom part, which only supports the roof edges. That bottom tool is attached to the tool robot (7th and 8th axis) via a connection plate. It can be seen in Figure 4.5(a).
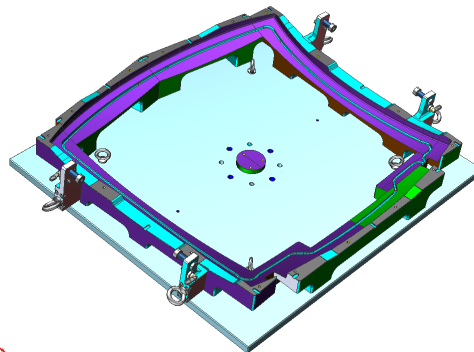
(a) Bottom Tool
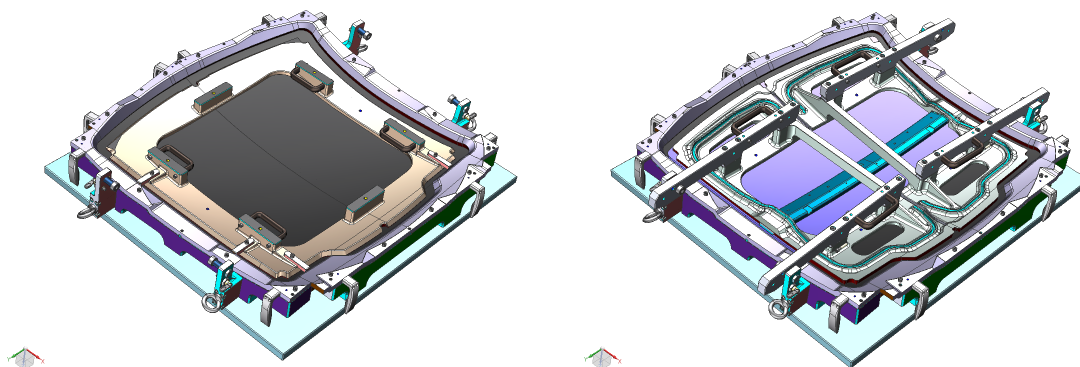
(b) Top Tool for Series Production with CFRP roof   (c) Top Tool for Feasibility Study with CFRP roof

Figure 4.5: Tool Construction for the AMG GT R CFRP Roof

For the top tool two versions were designed; one as for series production (see Figure 4.5(b)) and one for a feasibility study (see Figure 4.5(c)). For both cases an outer aluminum mold is placed around the roof edges, which consists of a total of 5 parts, which create the outer edge of the PUR subframe.

The inner mold of the series production top tool is made of POM material and is placed on the inside of the roof to create the inner edge of the PUR subframe. This tool part also contains the cutouts for the roof spacers. For accurate placement, spacer bars can be applied on two sides, which are removed again after placement such that the robot can apply the PUR freely. For the feasibility study the inner top tool is designed as aluminum flaps. Using these flaps, the overmolding of acoustic (fleece) or stiffness (cardboard) inlays and a crash bar can be tested. It also enables the application of thicker PUR lines and PUR lines of variable thickness. This tool is used for the pre-qualification of part integrations and process variations that could be used in roof types such as the four-door vehicle.

In this research project only the series production tool is used to achieve a fast series production qualification. The tool for the feasibility study will be used by the adhesive research department at Daimler AG subsequently to guide AMG for their future roof concepts.

Chapter 5

Experiments

The experimental research work and its analysis, which forms the main part of the thesis, is discussed in this chapter. It first lists the used test equipment and materials, before the experiments themselves are treated. The experiments are subdivided in fundamental studies, which are performed to determine the bond properties, in sample process and print-through tests and lastly the process application onto an AMG GT R CFRP roof.

5.1 Test Equipment & Material

For the different specimens special equipment was required, which is discussed in this section. The most important part is the polyurethane processing equipment to apply the PUR onto the substrates. Additionally, the used substrate and adhesive materials are characterized.

5.1.1 Polyurethane Processing Equipment

Figure 5.1 shows the PUR high-pressure metering unit PSM 3000 from Isotherm AG. It can be used for *'spraying, casting and injection molding of filled and unfilled PUR-Systems'*. Mixing ratio, temperature and output quantity can be controlled via a touchscreen PC and the metering unit can be used in automatic or manual mode. The PUR application can be done spot-wise or continuously [71].

The high-pressure metering unit is combined with the Isotherm GP 600 L-shaped mixing head, which is displayed in Figure 5.2. Figure 5.2(a) shows a real-life image and Figure 5.2(b) shows a schematic of its working principle. The working principle of this mixing head is the same as for any high-pressure mixing and dispensing unit, as previously described in Section 3.2.3. It

Figure 5.1: Isotherm PSM 3000 PUR high-pressure metering unit

can be used for open and closed molds and is optimized for a clean and laminar discharge. The mixing head guarantees a homogeneous mixing of the components with up to 200 bars, which can even be used for highly reactive PURs with a pot life from 1 second. Additionally, it requires low maintenance due to its automatic cleaning system.

(a) Image of the mixing head

(b) Schematics of the mixing head working principle (left = closed, right = open)
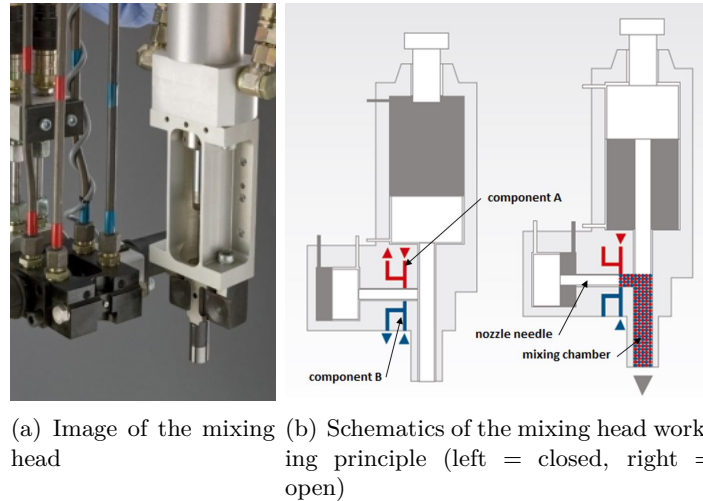
Figure 5.2: Isotherm GP 600 PUR mixing and dispensing head [71]

At the end of every shot the needle is returned to its closing position to block the component outlets and the remaining material in the mixing chamber is pushed out mechanically using a tappet [71].

5.1.2 Tested Materials

For the specimen two substrate materials were used as well as one adhesive material.

Carbon Fiber Reinforced Plastic Prepreg Substrate

The CFRP material and layup choice for the specimens was based on the plybook of the AMG GT R CFRP roof. It is a summetric unbalanced laminate with a layer of glas fiber reinforced plastic (GFRP) along the mid-plane. Figure 5.3 illustrates the layup of the CFRP roof and the specimens used for the research [72].

Stacking Sequence	Ply-Nr.	Orientation	Fiber
	1	0/90°	CFRP
	2	+/-45°	CFRP
	3	0/90°	GFRP
	4	-/+45°	CFRP
	5	90/0°	CFRP

Figure 5.3: Layup of the CFRP roof

For the production of both a Cytec MTM57-CF3202 prepreg is used, which has the material composition as listed in Table 5.1.

Table 5.1: Cytec MTM57-CF3202 Substrate Material Composition

Material Composition	
Carbon Fiber	Cytec CF3202; 3K, 245 g/m^2, 2 x 2 twill
Glas Fiber	600 g/m^2(E- or S-Glass)
Resin	Cytec EP MTM57
Fiber Volume Fraction	58 %
Manufacturing Process	Prepreg Pressing
Overall Thickness	1.75 mm
E-Modulus CFRP Prepreg	57 GPa
E-Modulus GFRP Prepreg	32 GPa
Thermal Expansion Coefficient (α)	-0.41 $\cdot 10^{-6}$ 1/K

Steel Substrate

The used steel is a standard non-alloyed structural steel, S235JR+AR according to EN 10025-2 (old name according to DIN 17100: St 37-2). The norm presents the material properties as depicted in Table 5.2.

Table 5.2: Steel S235JR+AR Substrate Material Properties

Material Properties	
Steel Number	1.0037
Alloy	None
Special Roll and/or Heat Treatments	None, as rolled
E-Modulus	210 GPa
Thermal Expansion Coefficient (α)	$12 \cdot 10^{-6}$ 1/K

For the experiments all steel parts are coated with a thin layer using cataphoresis treatment, also called E-coat. The coating is done according to the Daimler norm for series coating of the body-in-whites using Cathoguard 500 from BASF.

Polyurethane Adhesive

The material properties of the used polyurethane are depicted in Table 5.3. The highly reactive adhesive material used for the OMPURIB process is called Elastolit R 8919/107 and was developed by BASF specially for RIM processes of lightweight automotive systems. All Elastolit R-series materials are advertised by BASF as *'microcellular, almost solid materials'* with *'high impact strength even at extremely low temperatures'* [73].

Table 5.3: Elastolit R 8919/107 Adhesive Material Properties

Material Properties	
A-Component	Polyol, Catalyst, Additives
B-Component	4,4' - Methylene Diphenyl Diisocyanate (MDI) (Iso 134/7)
Curing Mechanism	Polyaddition
Mixing Ratio (A:B)	100:58
Reaction Starting Time at $20°C$	15 s
Characteristics	tough-hard, but elastic
Density	1070 kg/m^3
E-Modulus	25 MPa
Tensile Strength	12 MPa
Shrinkage	1.2 %
Thermal Expansion Coefficient (α)	unknown

The Elastolit PUR material is used for every experiment with the same mixing ratio, pressure and temperature.

5.2 Fundamental Studies for Bond Property Analysis

This section discusses the influences of different pre-treatments and aging conditions on the mechanical properties of the PUR and the interfacial behavior to CFRP, the e-coated steel and the assembly adhesives.

5.2.1 Pre-Treatments

In order to clean the specimen from grease and other substances and to improve the interconnection between substrate and adhesive, different surface pre-treatments can be used. Part of this study is to analyze the effect of a small selection of pre-treatments on the mechanical parameters of the bond and on print-through. The steel specimens are only pre-treated in one way as the preset pre-treatment at Daimler AG is e-coating for all metal parts of the BIW. Additionally, the PUR material is already approved for e-coated steel. Since the CFRP specimens are of major interest and not approved yet, different surface pre-treatments are investigated during the experiments. As mentioned in Section 2.2, there are a lot of different possible pre-treatments for CFRP substrates, but the following ones were selected for this research project for time and cost saving purposes.

1. Cleaning only

2. Cleaning and Primer

3. Cleaning, Sanding and Cleaning

4. Cleaning, Sanding, Cleaning plus Primer

5. Peel Ply and Cleaning

6. Peel Ply and Cleaning plus Primer

The cleaning agent used is Teroson T8850, the same as commonly used by Daimler AG. For the sanded specimens, sanding was done by hand in circular motion using a sandpaper with 120 grit as previously discussed in Section 2.2.2.

Sika 209 D is the primer, which was intended to be used based on a pre-investigations performed by the adhesives department of the Daimler AG. But it was detected during a first peel test that the Elastolit R 8919/107 does not adhere well to the Sika 209 D. Therefore some additional primer tests were performed with the setup as noted in Table 5.4.

Table 5.4: Primer Adhesion Pre-Tests

Primer	minimum drying time	applied drying time	Failure Pattern
Sika 209 D	10 min.	15 min.	AF
Sika 209 D	10 min.	3 min.	AF
Sika 209 D	10 min.	1 min.	AF
Dow BETAPRIME 5404 A	6 min.	6 min.	CF
Dow BETAPRIME 5404 A	6 min.	3 min.	CF

Both primers are based on Polyisocyanate. It was evaluated whether the adhesion between primer and PUR improves when the primer is not fully dried, such that not all isocynates have fully reacted yet and can bond to the PUR. Additionally, another primer, Dow BETAPRIME 5404 A was tested to investigate whether this primer has better adhesion with the PUR.

(a) Peel test Sika 209 D   (b) Peel test Dow BETA-PRIME 5404
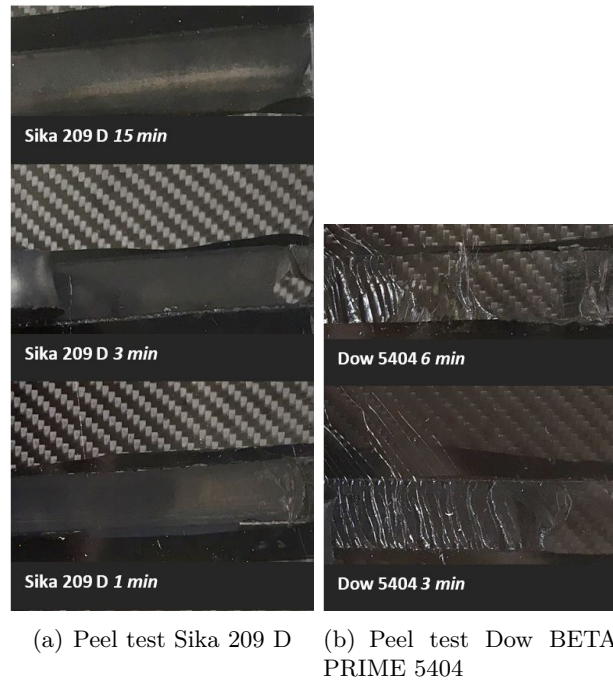
Figure 5.4: Peel test of Sika 209 D and Dow BETAPRIME 5404 at different drying times

It was found, as visible in Figure 5.4, no matter the drying time, the Sika primer (Figure 5.4(a)) cannot bond to the PUR. The Dow primer instead shows cohesive failure (CF), as desired, and was therefore found to be suitable for the subsequent tests. One might argue that Figure 5.4(b) indicates less than 95% CF. But the adhesive failure here is between CFRP and primer, whereas the failure pattern of the primer-PUR interface was of major focus during this test. Moreover, the Dow BETAPRIME 5404 is already approved and used for CFRP structures at Daimler AG. Therefore the decision was made to execute all tests of the fundamental study with Dow BETAPRIME 5404.

5.2.2 Peel Tests

In order to determine the adhesion of the Elastolit on the CFRP and the influences of different pre-treatments on the adhesion, peel tests were performed.

Additionally, the adhesion of two commonly used assembly adhesives on the Elastolit PUR was evaluated on the basis of peel tests.

Sample Preparation and Aging

The CFRP-PUR peel samples were made by placing the CFRP plate on a to $60°C$ heated metal plate and applying the PUR with the in Subsection 2.3.2 described dimensions onto the CFRP plate using simple silicon molds. Figure 5.5 shows the making of the CFRP-PUR peel samples. Although the PUR reacts within five seconds, before they can be aged and tested the samples have to harden for seven days, until full hardening is achieved.

(a) Step 1: Plate and barrier placement

(b) Step 2: PUR application
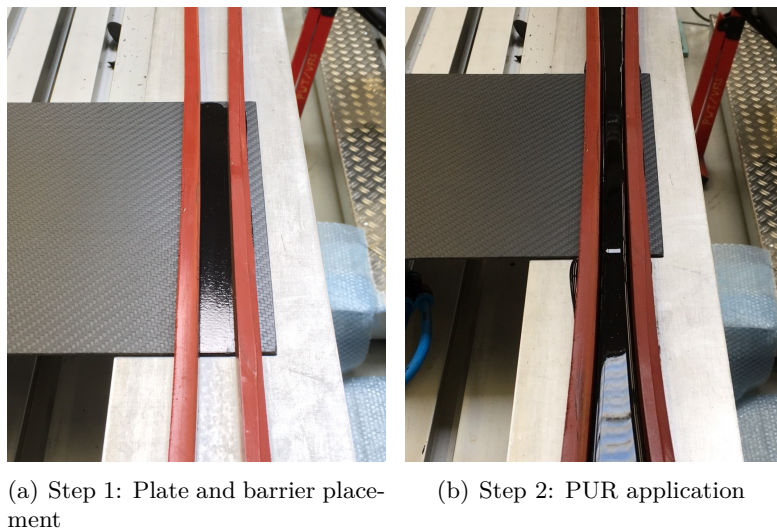
Figure 5.5: Fabrication of a PUR - CFRP peel specimen

For the PUR-Assembly adhesive peel specimens, the PUR was first applied onto e-coated steel plates for better grip while peeling at a later stage. Afterwards, the assembly glues were applied onto the cleaned PUR surface in the way depicted in Figure 5.6. The adhesive line

was applied and then pressed to a 4.5 mm thickness. From there, for 10 days, the specimens have to fully harden before conditioning and testing.

The tested assembly glues are EFTEC EFBOND DA 620 with a higher (>8 MPa) and EFTEC EFBOND DA 217 with a lower ($\sim$ 3 MPa) shear modulus as used in assembly lines at Daimler AG.

(a) Step 1: Assembly adhesive application

(b) Step 2: Spacer placement

(c) Step 3: Foil placement

(d) Step 4: Assembly adhesive grouting
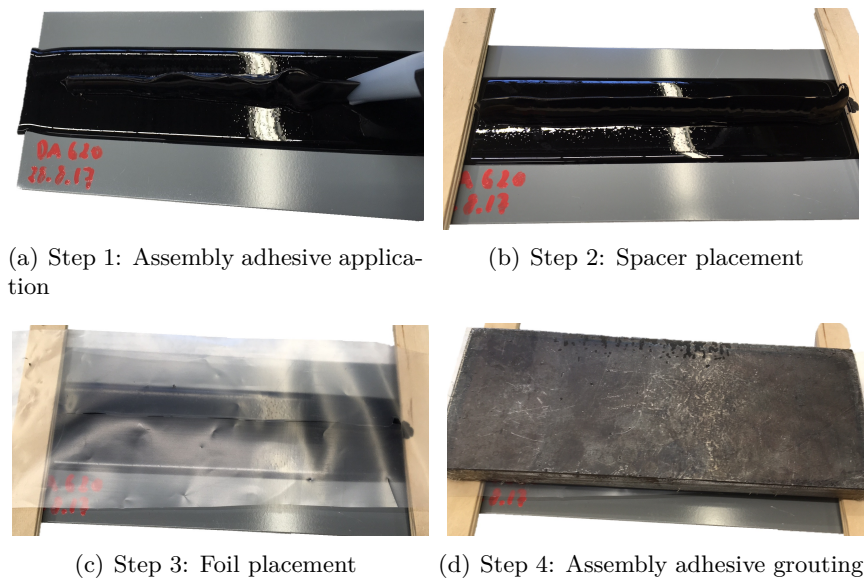
Figure 5.6: Fabrication of an assembly adhesive - PUR peel specimen

The purpose of the assembly adhesive peel tests is to determine whether the assembly glue can be applied directly onto the PUR surface, without any pre-treatments. It is important to minimize the efforts and time required at the assembly to stay within the tact times of the line production at Daimler AG.

Moreover, since the the CFRP roofs can have a transportation time between 1 and 30 days, with a mean of 5 to 7 days, the samples were made at different times after PUR application. It was therefore decided to evaluate the adhesion of the assembly adhesive when applying it after the minimum, maximum and mean of the transportation time. The result is a rather large test matrix, which will be further discussed in the following paragraphs.

After the fabrication of the CFRP-PUR and PUR-Assembly adhesive specimens and their required hardening time, they were placed in the climatic chambers and aged as stated in Subsection 2.3.3.

Test Setup and Execution

The peel tests were performed as described in Subsection 2.3.2. The samples were clamped onto a table and then cut into, piece by piece, using a cutter knife and peeled until adhesive failure. At this point the sample is cut into again to avoid breakage of the adhesive bead.

Test Results and Analysis

The results of the CFRP-PUR peel tests are shown in Table 5.5. From there it can be seen that the adhesion improves when applying a primer independent of the surface topology. Moreover, the best results, adhesion grades of 5, were only obtained if ablative pre-treatments were used in combination with primer application. Another observation, visible from Table 5.5, is that for most specimens only the CCH aging condition deteriorates the adhesion and it seems that AHS and Cata improve the adhesion in most cases.

Table 5.5: DoE of all CFRP-PUR Peel Test Sets

Design of Experiments		
	Factors	**Responses**
Run	**Pre-Treatment**	**Aging**	**Cohesive Failure(%)**
1	Blank + Teroson	SA	65
2	Blank + Teroson	CCH	88
3	Blank + Teroson	AHS	80
4	Blank + Teroson	Cata	90
5	Sanding + Teroson	SA	95
6	Sanding + Teroson	CCH	88
7	Sanding + Teroson	AHS	100
8	Sanding + Teroson	Cata	87
9	Peel Ply + Teroson	SA	98
10	Peel Ply + Teroson	CCH	70
11	Peel Ply + Teroson	AHS	85
12	Peel Ply + Teroson	Cata	95
13	Blank + Primer	SA	90
14	Blank + Primer	CCH	90
15	Blank + Primer	AHS	100
16	Blank + Primer	Cata	100
17	Sanding + Primer	SA	98
18	Sanding + Primer	CCH	95
19	Sanding + Primer	AHS	98
20	Sanding + Primer	Cata	99
21	Peel Ply + Primer	SA	98
22	Peel Ply + Primer	CCH	95
23	Peel Ply + Primer	AHS	98
24	Peel Ply + Primer	Cata	95

The results of the PUR-Assembly Adhesive peel assessments are listed in Table 5.6 for the EFTEC EFBOND DA 620 and in Table 5.7 for EFTEC EFBOND DA 217. The samples are categorized by hardening time of the PUR, aging condition and pre-treatments. The result per pre-treatment and hardening time has to be above 95% for each aging condition in order to qualify for series-production at Daimler AG.

Previous test results, where a similar, but different PUR material by BASF was used in combination with the low pressure metering unit, showed that the assembly adhesives can be applied onto the PUR without any pre-treatments. It was expected that the same would count for the Elastolit 8919/107. During the first set of tests of the samples without any pre-treatments it was detected though that the adhesion is not as expected and most samples fully failed the peel assessment. Therefore a second round of specimens was made, which

were pre-treated before the application of the assembly glue. The downside of pre-treatments is the increase of the tact time at the assembly station , but if no pre-treatment is used the qualification for series production fails.

The investigated pre-treatments were:

1. Sanding

2. Sanding + Primer (Dow BETAPRIME 5404)

3. Primer (Dow BETAPRIME 5404)

Table 5.6: DoE of all PUR-EFBOND DA 620 Peel Test Sets

Design of Experiments				
	Factors			**Response**
Run	**Assembly Glue**	**Hardening Time**	**Aging**	**Pre-Treatment**	**Cohesive Failure(%)**
1	EFBOND DA 620	1	SA	Blank	0
2	EFBOND DA 620	1	CCH	Blank	0
3	EFBOND DA 620	1	AHS	Blank	98
4	EFBOND DA 620	1	Cata	Blank	82
5	EFBOND DA 620	1	SA	Sanded	99
6	EFBOND DA 620	1	CCH	Sanded	100
7	EFBOND DA 620	1	AHS	Sanded	100
8	EFBOND DA 620	1	Cata	Sanded	100
9	EFBOND DA 620	1	SA	Sanded + Primer	100
10	EFBOND DA 620	1	CCH	Sanded + Primer	99
11	EFBOND DA 620	1	AHS	Sanded + Primer	100
12	EFBOND DA 620	1	Cata	Sanded + Primer	99
13	EFBOND DA 620	1	SA	Primer	100
14	EFBOND DA 620	1	CCH	Primer	99
15	EFBOND DA 620	1	AHS	Primer	100
16	EFBOND DA 620	1	Cata	Primer	100
17	EFBOND DA 620	5	SA	Blank	20
18	EFBOND DA 620	5	CCH	Blank	12
19	EFBOND DA 620	5	AHS	Blank	87.5
20	EFBOND DA 620	5	Cata	Blank	90.5
21	EFBOND DA 620	5	SA	Sanded	100
22	EFBOND DA 620	5	CCH	Sanded	100
23	EFBOND DA 620	5	AHS	Sanded	100
24	EFBOND DA 620	5	Cata	Sanded	99
25	EFBOND DA 620	5	SA	Sanded + Primer	100
26	EFBOND DA 620	5	CCH	Sanded + Primer	90
27	EFBOND DA 620	5	AHS	Sanded + Primer	93
28	EFBOND DA 620	5	Cata	Sanded + Primer	99
29	EFBOND DA 620	5	SA	Primer	99
30	EFBOND DA 620	5	CCH	Primer	95
31	EFBOND DA 620	5	AHS	Primer	100
32	EFBOND DA 620	5	Cata	Primer	80
33	EFBOND DA 620	30	SA	Blank	0
34	EFBOND DA 620	30	CCH	Blank	5
35	EFBOND DA 620	30	AHS	Blank	100
36	EFBOND DA 620	30	Cata	Blank	20

Due to time-dependent problems, these tests could only be performed for 1 day and 5-7 days. The outcomes of these tests can also be found in Tables 5.6 and 5.7. It is important to note here, that the cataplasm conditioning did not work. The maximum temperature of $70°C$ and the humidity application were successful, but the minimum temperature of $-25°C$ could not be reached.

Table 5.7: DoE of all PUR-EFBOND DA 217 Peel Test Sets

Design of Experiments					
	Factors				Response
Run	Assembly Glue	Hardening Time	Aging	Pre-Treatment	Cohesive Failure(%)
1	EFBOND DA 217	1	SA	Blank	0
2	EFBOND DA 217	1	CCH	Blank	0
3	EFBOND DA 217	1	AHS	Blank	0
4	EFBOND DA 217	1	Cata	Blank	62.5
5	EFBOND DA 217	1	SA	Sanded	93
6	EFBOND DA 217	1	CCH	Sanded	98
7	EFBOND DA 217	1	AHS	Sanded	100
8	EFBOND DA 217	1	Cata	Sanded	99
9	EFBOND DA 217	1	SA	Sanded + Primer	94
10	EFBOND DA 217	1	CCH	Sanded + Primer	100
11	EFBOND DA 217	1	AHS	Sanded + Primer	99
12	EFBOND DA 217	1	Cata	Sanded + Primer	99
13	EFBOND DA 217	1	SA	Primer	70
14	EFBOND DA 217	1	CCH	Primer	100
15	EFBOND DA 217	1	AHS	Primer	99
16	EFBOND DA 217	1	Cata	Primer	99
17	EFBOND DA 217	5	SA	Blank	0
18	EFBOND DA 217	5	CCH	Blank	10
19	EFBOND DA 217	5	AHS	Blank	0
20	EFBOND DA 217	5	Cata	Blank	88
21	EFBOND DA 217	5	SA	Sanded	99
22	EFBOND DA 217	5	CCH	Sanded	98
23	EFBOND DA 217	5	AHS	Sanded	95
24	EFBOND DA 217	5	Cata	Sanded	99
25	EFBOND DA 217	5	SA	Sanded + Primer	99
26	EFBOND DA 217	5	CCH	Sanded + Primer	100
27	EFBOND DA 217	5	AHS	Sanded + Primer	98
28	EFBOND DA 217	5	Cata	Sanded + Primer	100
29	EFBOND DA 217	5	SA	Primer	96
30	EFBOND DA 217	5	CCH	Primer	98
31	EFBOND DA 217	5	AHS	Primer	100
32	EFBOND DA 217	5	Cata	Primer	100
33	EFBOND DA 217	30	SA	Blank	100
34	EFBOND DA 217	30	CCH	Blank	0
35	EFBOND DA 217	30	AHS	Blank	95
36	EFBOND DA 217	30	Cata	Blank	0

Table 5.6 shows that for the EFTEC EFBOND DA 620 the best results are obtained when sanding the PUR surface before adhesive application, independent of the PUR's hardening time. The primer works better on the PUR surface if it is not hardened for too long, as after 1 day. The reason could be that the isocyanates of the primer can react better with the PUR that has not fully reacted yet.

The outcome for the EFTEC EFBOND DA 217 is slightly different. Generally it can be said that its performance is lower than of the DA 620 and that in contrast to DA 620 its performance improves with increasing hardening time of the PUR. Additionally, it seems that the primer has a better effect used in combination with DA 217 than with DA 620. The primer application after 5 days (also in combination with sanding) results in the highest values of cohesive failure percentage.

Furthermore, in order to avoid pre-treating the PUR surface, it was identified whether a change in mixing ratio of the PUR can improve the adhesion of the assembly glue. Habenicht [9] reports in his work, that an increase of the isocyanate component improves the adhesion, but also comes with the disadvantage that it increases the materials brittleness. He determined the optimal inrease of isocyanate to be 10%. Therefore the PUR mixing ratio was changed from 100:58 to 100:64 to analyze whether improved adhesion to the assembly adhesive can be obtained.

Table 5.8 lists the outcomes of the mixing ratio changes for a PUR hardening time of 1 day and without pre-treatment under the aging conditions used for all experiments. It is clearly visible that both DA 217 and DA 620 show perfect adhesion and guarantee an adhesion grade 5, which approves the Elastolit 8919/107 for series production in terms of adhesion.

Table 5.8: DoE of the PUR-EFBOND DA 620 and 217 Peel Test Sets for a 100:64 mixing ratio

Design of Experiments					
Factors					Response
Run	Assembly Glue	Hardening Time	Aging	Pre-Treatment	Cohesive Failure(%)
1	EFBOND DA 217	1	SA	Blank	98
2	EFBOND DA 217	1	CCH	Blank	98
3	EFBOND DA 217	1	AHS	Blank	98
4	EFBOND DA 217	1	Cata	Blank	95
5	EFBOND DA 620	1	SA	Blank	100
6	EFBOND DA 620	1	CCH	Blank	100
7	EFBOND DA 620	1	AHS	Blank	100
8	EFBOND DA 620	1	Cata	Blank	100

Images of tested peel samples with no adhesion using no pre-treatment, 100% adhesion using primer and 100% adhesion by changing the mixing ratio to 100:64 are depicted respectively in Figures 5.7(a), 5.7(b) and 5.7(c).

Conclusion

From the gathered results it the following can be concluded. The best solutions to obtain the best adhesion of the Elastolit 8919/107 on the CFRP substrate are abrasion pre-treatments in combination with primer. Sanding and peel-ply both resulted in an adhesion grade of 5 and are therefore approved for series-production. Moreover, this result also leaves room for different manufacturing techniques of the CFRP roof. If a method is used that results into a blank, smooth surface, the surface can be sanded, and where the technique allows it, peel-ply can be used to increase the surface roughness and therewith the surface energy.

(a) Peel result of DA 620 on the PUR without pre-treatment

(b) Peel result of DA 620 on the PUR using primer

(c) Peel result of DA 620 on the PUR with mixing ratio 100:64

Figure 5.7: Peel result of DA 620 on the PUR without pre-treatment, with primer and change of mixing ratio

Furthermore, it can be concluded that the addition of heat and humidity, as during the AHS and Cata, mainly does not deteriorate the adhesion between PUR and CFRP, but rather improves it. This is possibly because PUR's react with the moisture, in this case due to the increased humidity, and the reaction is accelerated under heat.

For the PUR-assembly adhesive interface the best adhesion for both tested adhesives was obtained by changing the PUR mixing ratio to 100:64. Another option for the DA 620 is to keep the 100:58 PUR mixing ration and to sand the PUR surface before adhesive application. The adhesion properties seem constant, independent of the PUR hardening time. In terms of pre-treatments of the PUR substrate with a mixing ratio of 100:58 in combination with the DA 217 any pre-treatment can be used. But in contrast to the constant adhesion behavior of the DA 620, the adhesion is only sufficient if the PUR is hardened for a minimum of 5 days.

To keep the handling time and cost low, it is best to avoid pre-treatments where possible. Therefore the recommendation is to use a PUR mixing ratio of 100:64. The disadvantage of this solution though is that further lap-shear and PUR-CFRP peel tests should be performed at least at SA in order to examine whether the mechanical properties are changed against expectation. The print-through is ranked less critical and should not require additional testing. In case of a time restriction, and a lower rating of the cost requirements, it is recommended use the PUR with mixing ratio 100:58 and sand the surface before application of the assembly adhesive. It is important thought that when using EFBOND DA 217 a minimum PUR hardening time of 5 days is ensured.

5.2.3 Lap-Shear Test

Another set of tests done as part of the fundamental studies were lap-shear tests. These tests were performed to determine the adhesion of the PUR on the different substrates, CFRP and e-coated steel, based on the analysis of the lap-shear strength. Moreover, the fracture pattern of the bond area was examined to evaluate the bond quality.

Sample Preparation and Aging

The first step was the preparation of the specimens. All substrates were dimensioned following DIN 1465, as described in Section 2.3.1. For each specimen one e-coated steel adherend and one CFRP adherend were placed in tailor-made tool, which was connected to a heat circulation to heat the substrates to a temperature of $60°C$. This temperature was determined by another Master student at Daimler AG to be the optimal substrate temperature during processing, to achieve the maximum lap-shear strength.

Using the PUR metering unit and the mixing head mentioned in Section 5.1.1 the Elastolit with a mixing ratio of 100:58 was injected into the tool as depicted in Figure 5.8 to fill the overlap area between the two adherends.

Figure 5.8: Injection of the PUR into the lap-shear specimen tool

Because a mixing chamber with a volume of 30 g/s was used, excess material was collected in the funnel of the tool and adhered to the specimen as shown in Figure 5.9(a). This excess material had to be removed to obtain the final specimen dimensions shown in Figure 5.9(b).

168 lap-shear specimens were fabricated, seven for each combination of pre-treatment and aging condition, in order to obtain a reasonable average and to take possible outliers into account. A simplified DoE was generated to summarize the different combinations and to optimize the test execution. The corresponding DoE matrix can be found in Table A.2. A number of six pre-treatments was used, as for all specimens of the fundamental experiments. They are outlined in Subsection 5.2.1.

As a reference, one set of specimens (28 per set) is kept at standard atmosphere conditions, as described in Subsection(reference to lit study). In the mean time the other specimens are aged in the AHS (28 specimens), CCH (28 specimens) and Cataplasm (28 specimens) under the conditions

(a) Lap-shear specimen directly after PUR injection
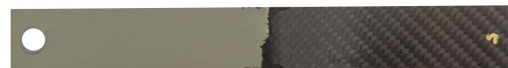
(b) Lap-shear specimen after cutting of the remaining PUR material

Figure 5.9: CFRP-PUR-Steel lap-shear specimen before and after trimming to remove remaining PUR material

as outlined in Section 2.3.1. After aging, all specimen are kept under standard atmosphere conditions for a minimum of 24 hours, to achieve equal test conditions, and are tested afterwards.

Test Setup and Execution
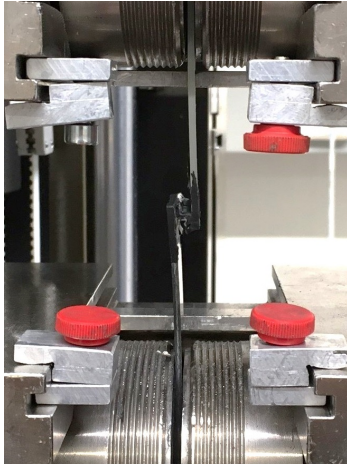
Figure 5.10: Tested sample in test machine

The lap-shear test was performed on a Zwick 1484 RetroLine electromechanic universal-axial test machine. The test machine by Zwick GmbH & Co. KG can be used for tension, compression and bending tests and is commonly used for standard tests to determine material properties. Its nominal force is 200 kN with a maximum travel of 1400 mm at maximum rate of 250 mm/min. Due to the installation of adjustable clamping jaws, the clamp position can be adjusted for the overlap in the specimens. Since it can introduce a parallel force into a specimen with offset axes, the machine is well adapted for lap-shear tests. For the test machine operation and analysis, the test software testXpert III by Zwick was used.

Once the test machine and software were started, the specimen was vertically aligned in the clamping jaws, as in Figure 5.10. At a test rate of 5 mm/min a tensile load was applied to the specimen until failure.

The test specimens were sorted and tested per aging condition and pre-treatment as shown in Table A.2, where the blank samples kept at standard atmosphere are used as the reference samples.

Test Results and Analysis

An extraction of the lap-shear test results is shown in Figure 5.11 and Figure 5.12. Eq. 2.8 was used to calculate the lap-shear strength from the maximum applied force and the average overlap area of 310.856 mm. The bar diagrams in Figure 5.11 compare the influences of the different pre-treatments on the lap-shear strength and sample stiffness. For better understanding of the graphics, Table 5.9 shows a list of the abbreviations used for the different pre-treatments.

Table 5.9: Abbreviations used for lap-shear tests

Abbreviation	Meaning
B	Blank (Cleaning only)
S	Sanded
PP	Peel-Ply
P	Primer

Figure 5.12(a) and Figure 5.12(b) compare the influence of the aging conditions on the lap-shear strength and samples stiffness of the tested samples, in this case the blank samples.

The diagrams showing the influences of the aging conditions on sanded and peel-ply surfaces can be found in Appendix B.

(a) Average lap-shear strength

(b) Average sample stiffness
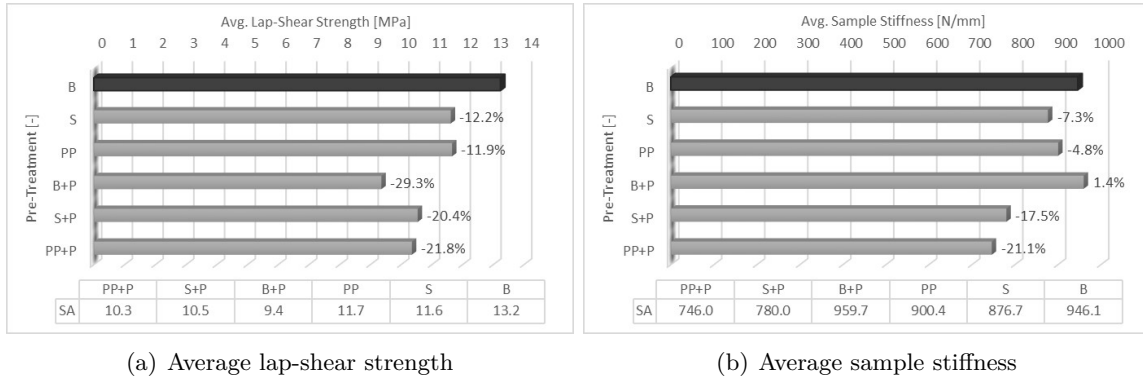
Figure 5.11: Average lap-shear strength and sample stiffness results after different pre-treatments, kept at standard atmosphere

(a) Average lap-shear strength

(b) Average sample stiffness
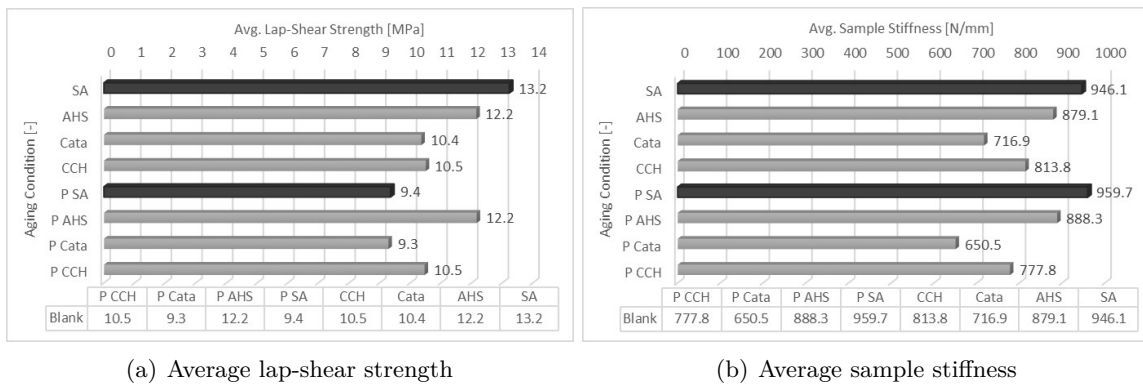
Figure 5.12: Average lap-shear strength and sample stiffness results of blank samples after different aging conditions

From the generated diagrams, comparing the average lap-shear strength and sample stiffness of the specimens a few observations could be made. Sanding and the use of peel-ply have a very similar effect. This result seems reasonable as both pre-treatment methods change the surface topology of the CFRP substrate. A surprising finding was, that contrary to what most literature states, the blank specimens performed best. Without use of pre-treatments the lap-shear strength is highest and the sample stiffness can only be increased by applying a primer onto the blank surface. It seems that it is prejudicial for the used PUR (Elastolit) to abrasively treat the substrate surface. There can be various reasons for this phenomenon. The three most probable ones are:

1. *Batch sensitivity.*
   Per test set (pre-treatment and aging combination) a total of seven repetitions were performed, of which the average (or mean) lap-shear strength and sample stiffness were

calculated. For statistical significance the standard deviation (SD) of the lap-shear strength was calculated for each test set using Eq. 5.1 and it was found that on average only two samples are above or below the mean, and therefore 5 are within.

$$SD = \sqrt{\frac{1}{N-1}\sum_{i=1}^{N}(x_i - \overline{x})^2} \tag{5.1}$$

Statistically speaking the data within the SD is still sufficient for analysis. It could still be a coincidence that the tested batch behaved as stated. To prove or disprove this cause, a minimum of one more batch would have to be made and tested with equal amount of repetitions per test set. Afterwards the SD should be re-calculated and it should be checked whether enough samples still fall within the SD. If again most samples have a lap-shear strength within the standard deviation, the cause is not batch sensitivity.

2. ***Too high viscosity.***
   The viscosity of the PUR during application is too high to flow into the valleys of the roughened surface. Therefore small air pockets are embedded onto the substrate surface, which impede full wetting and therewith reduce the adhesion and as a result also reduce the lap-shear strength. In order to investigate this possibility further, the specimens should be inspected under an electron microscope.

3. ***Introduction of peak stresses.***
   Usually common for high-strength adhesives like epoxies is an introduction of peak stresses due to surface roughening. These peak stresses reduce the transmittable forces and therefore reduce the lap-shear strength of the bond. Most often the peak stresses are caused by bending moment and peel at the overlap ends, by thin and deformation resistant bonds, which inhibit a stress relief through flow, or by an application of adhesives with a high degree of cross-linking and linear stress-strain curve [9]. As mentioned in Subsection 5.1.2, Elastolit R 8919/107 is an almost solid material with a fairly linear stress-strain behavior. In combination with the thin adhesive layer used for the lap-shear specimens and the peel force component acting at the overlap edges in thin lap-shear specimens, as discussed in Subsection 2.3.1, this could be the reason why the peak stresses introduced by surface roughening cannot be balanced out. One possibility to prove or rule out this theory could be to test lap-shear specimens with thicker adhesive layers, to evaluate whether the PUR material is too stiff or whether there is a minimum Elastolit layer thickness required to form a stronger bond.

As a last observation from the data evaluation it was visible that the use of primer does not improve the lap-shear strength. The lap-shear strength increases only after AHS conditioning. From there it can be concluded that the primer needs humidity and elevated temperatures in order to form stronger bonds with the PUR and substrate.

In order to evaluate whether the lap-shear strength of the Elastolit is sufficient for the intended application, and because no lap-shear strength is listed in its data sheet, the values were compared to the structural adhesive (Dow BETAMATE 2850), that was previously used to bond the CFRP subframe to the roof. Since the lap-shear strength of of the structural

adhesive is listed as 11 MPA, the Elastolit's reference value of 13.2 MPa lies above and is therefore fine. Additionally, the lap-shear strengths of the assembly adhesives EFBOND DA 620 and 217 were checked, since they should be the weakest element in the assembly. The values are 8 MPa and 3 MPa respectively. Therefore the Elastolit's lap-shear strength is again higher, which rates it as applicable for the roof application.

Furthermore, it is important that the lap-shear strength does not decrease too much, after aging. MBN 10518 states, that the value should not be lower than 25% of the initial value, after room temperature curing and storage at standard atmosphere. In case of the blank specimens the initial value is the reference value of 13.2 MPa. The initial value varies, depending on the pre-treatment, which can be seen in the diagrams depicted in Appendix B. It can also be spotted from these diagrams and the one in Figure 5.12(a), that none of the outcomes falls below the corresponding initial value. Therefore this check also verifies the use of the PUR material for the tested pre-treatments.

Looking at the failure patterns after testing, it can be seen that without primer, at standard atmosphere, the blank samples show the most amount of cohesive failure. The overall tendency though goes toward adhesive failure and mainly detachment of the e-coat from the steel substrate. After conditioning, a tendency of slight cohesion improvement can be noticed for all specimens. For the specimens with primer application it can be noted that on most specimens the primer fails at the primer-CFRP interface. And as for the specimens without primer, the cohesive failure percentage of the PP+P and B+P samples increases after conditioning. For the S specimens an increased detachment of the e-coat from the steel can be observed. All observed failure patterns are illustrated in Table 5.10. Looking back at Figure 2.20, it can be said that all common failure patterns of adhesives are present in the table.

Conclusion

From the previously discussed results a general conclusion can be drawn that the application of humidity and heat improves the adhesion of the PUR and the primer, since both are based on isocyanate. Isocyanate reacts with the water molecules as found in the atmospheric humidity. This reaction is additionally accelerated under elevated temperatures.

The lap-shear strength investigation proved that the strength of the PUR is high enough for the CFRP roof application, as compared to the assembly glues and the structural adhesive of the CFRP subframe the PUR offers the highest lap-shear strength.

The low amount of cohesive failure patterns on the testes lap-shear samples is usually a negative outcome. But since most failure patterns indicate a detachment of the e-coat from the steel or a detachment of the primer from the CFRP, which are both approved treatments, it can be said that the Elastolit is not the weakest element.

One might argue that the results of the peel tests and lap-shear tests are contradictory, since the lap-shear strength results are highest without any abrasive pre-treatment or primer, whereas the peel tests result in highest adhesion using abrasive pre-treatments plus primer.

These results can not be compared directly, since different load cases and conditions (e.g. different PUR thicknesses) are applied during testing and the lap-shear tests additionally have the influencing factors of the steel adherend.

Table 5.10: Lap-shear test failure patterns

Failure Pattern	Images		
Adhesive Failure	CFRP	E-coat	
Cohesive Failure	PUR		
Mixed Failure	PUR, KTL		
Substrate Failure	CFRP	E-coat	Primer

When deciding about a pre-treatments for series-production one should focus on the adhesion, since the lap-shear strength is sufficient for any tested pre-treatment. The recommendation is therefore the use of both abrasive pre-treatment (sanding or peel-ply) and primer, even though handling time and cost will slightly increase.

5.3 Process and Print-Through Tests

For the Class-A surface of the CFRP roof it is of high importance that the process of the PUR application as well as environmental effects, such as humidity and extreme temperatures in the operating temperature range of the part ($-40°C$ to $105°C$), do not cause any print-through. Additionally, special additions to the PUR injection bonding process, such as thickness increments of the subframe and crash bar integration have to be tested in order to qualify the process for future AMG sportscars. Therefore this section treats the process and print-through related tests for series production qualification and verification.

5.3.1 Subframe Profile Variations

The profile variation tests are done for proof-of-principle. Vehicles, which have a CFRP roof that requires subframe cross-sections other than of constant thickness and width, need a fitted application process. Possible cross-sectional profiles that might be required in the near future are presented in the sketches of Figure 5.13.
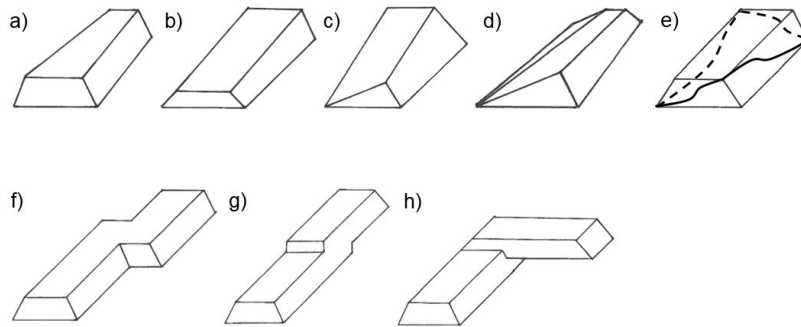
Figure 5.13: Sketches of possible profile variations required for future subframe designs

From the top left to the bottom right the complexity of the design increases. Further combinations of the displayed profiles might be necessary at a later stage.

For a four-door vehicle and the GT R Derivative the most important profiles to consider are profile a), b), d) and f). The profiles either have variations in width, height or combination of both. Therefore it is tested whether the process is feasible for such design types or whether changes need to be implemented to make it suitable. The primary focus lies on the process to create thickness increments at the ends of a PUR line. The other variations are discussed theoretically without further testing.

Test Setup and Execution

The thickness increment tests were done in a steel channel, as shown in Figure 5.14 of 40 mm height and 20 mm width, similar to the design of the actual subframe for the four-door vehicle. In order to investigate the maximum slope that can be applied in one shot the channel was kept horizontal or tilted 10°, 15° or 20°. Afterwards the maximum height and length of the thickness increment, as well as the starting height were measured and compared.

Figure 5.14: Test setup for subframe thickness increments

This test was done first by filling a minimum constant thickness in horizontal position and then tilting the channel to fill the end for the thickness slope. Secondly it was examined whether tilting first and filling the corner and a subsequent tilt back into the horizontal position leads to the same results.

For the different samples the material injection rate was kept constant at 30 g/s. The variables were the application speed, inclination and fill time at each end.

After the first round of experiments in the small channel were performed, it was attempted to replicate the dimensions of the four-door vehicle rear subframe CAD design (Figure 4.3(b)), since it has a steeper slope than the front subframe. For this experiment a slightly wider channel (30 mm width) was used to allow for better fine tuning with the large amount of material ejected from the mixing head. The subframe has a thickness increment at the ends towards the roof trim as sketched in Figure 5.15 and is symmetric over the x-axis.
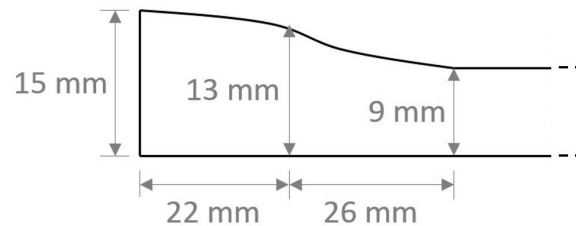
Figure 5.15: Sketch showing the dimensions of the four-door vehicle subframe

Test Results and Analysis

The results obtained for the thickness increment experiments are listed in Table 5.11. The influencing factors are shown on the left columns. v_1 and α_1 represent the speed and inclination for the horizontal part and v_2 and α_2 represent the inclination part of runs 1-7. For run 8 and 9 the setup is vise versa, because it was inclined first and then continued horizontally. The fill time is the time for how long the mixing head was kept at the end to build up the slope material. The responses, listed in the right columns are the length over which the slope ranges, the starting height which build the base of the slope, the maximum height achieved and finally the resulting slope.

Table 5.11: Test results of the thickness increment tests

Design of Experiments									
Factors						**Response**			
Run	v_1 [m/s]	α_1 [°]	v_2 [m/s]	α_2 [°]	**Fill time [s]**	**Length [mm]**	**Start height [mm]**	**Max. height [mm]**	**Slope [°]**
1	0.3	0	0.3	0	1	315	4	12	3
2	0.3	0	0.3	0	3	340	5	21	4
3	0.3	0	0.3	10	2	145	4	30	12
4	0.3	0	0.5	10	2	145	5	30	11
5	0.3	0	0.5	15	3	135	4	39	15.5
6	0.3	0	0.5	20	3	110	4	40	21
7	0.3	0	0.5	20	2	115	4	35	15
8	0.3	10	0.3	0	3	215	8	30	6
9	0.3	15	0.3	0	2	205	9	23	9

From the table and the images in Figure 5.16 it is visible that the creation of a thickness increment in one shot is possible. A slope of up to 21° is feasible when inclining the channel to 20°. It can also be observed that the resulting slope is related to the inclination angle.

With no inclination a maximum slope of 4° can be achieved when filling the end for 3 seconds, which equals 90 g (considering that the injection rate is 30 g/s). This is due to the fact that most material flows away from the injection spot, but since it hardens within 5 seconds it still builds up a small hill. Under inclination the resulting slope is about 1° more than the inclination angle.

Moreover, it can be seen that when first tilting down and filling the end and subsequently tilting horizontally the material still flows downstream if it has not hardened yet. The resulting slope is lower than the inclination angle it was tilted to at the beginning. This effect needs to be taken into account when trying to achieve the same results as with the tilting as the last step. Additionally, since the injection nozzle was closed for 3 seconds before tilting horizontal and then open again, it causes a small ridge as visible in Figure 5.16(b) where the liquid material flows over the already hardened material. This ridge needs to be avoided in order to prevent a possible gap between PUR and assembly adhesive, which could lead to a moisture bridge during vehicle operation. The elimination of the ridge can be done by fine tuning, by tilting the tool backward, against the flow direction.

(a) Slope created by tilting at the end

(b) Slope created by tilting at the beginning
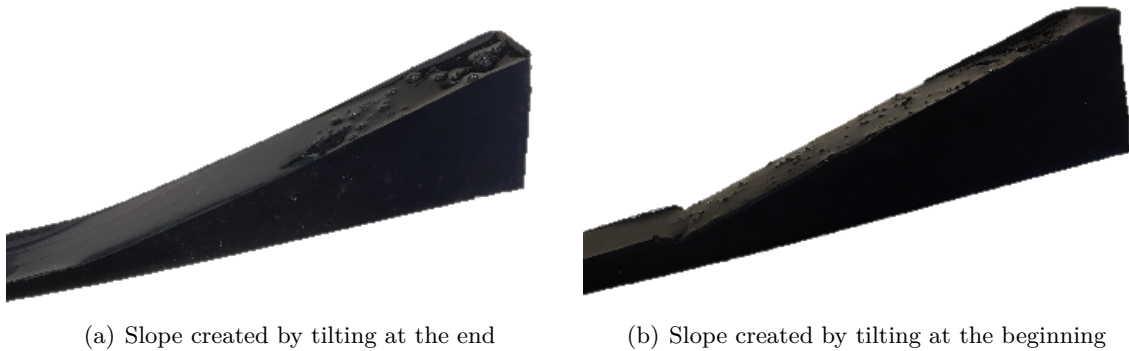
Figure 5.16: Resulting slopes created by tilting at the end or beginning of the process

If a thickness increment is required along the mid-section of the subframe the build up is only possible by using a second shot at the desired location after waiting for five seconds for the material to harden. The same should be considered if a plateau is required at the end slopes towards the roof trim. A positive characteristic of the Elastolit is that it allows for a second application directly on top of the first, without any treatment in between.

One of the additional observations made during the experiments was the formation of blisters on the surface of the PUR. This occurrence was only visible in the areas of the thickness increments, where large amounts of material were applied. Most probably these blisters are caused by the exothermic reaction of the PUR, whose effect is larger when applying larger amounts of material. Additionally, they could be air inclusions from the fast injection into material which is still liquid (similar to filling a glass of water).

A final finding was that to fast tilting of the channel allows the bulk of the material to flow away, while the material in contact with the heated substrate already hardens. The result is a small brink on each side. The brink does not cause problems unless it gets higher than the pressed thickness of the assembly glue. It can be avoided by implementing slower, smoother movements of the tool and the use of a mixing head with a lower injection rate.

Following the thickness increments in the small channel, as a second step it was tested whether the slope, as indicated in the CAD subframe design of the four-door vehicle, can be reproduced in real-life.

Figure 5.17: Result of a simplified PUR subframe based on the CAD data of a four-door vehicle

Since the programming of the CAD reproduction is done by hand and not by machine, it is a rather long an delicate process. But as Figure 5.17 shows, after 2 days of programming a relatively symmetrical subframe can be produced, which almost maps the dimensions of Figure 5.15. The biggest difference is still in the increment length. Both sides are 15 mm apart and also more than 12 mm away from the design. In the end the goal is to achieve a tolerance of $\pm 1mm$, which should be feasible after further teaching.

Next to the thickness increments the cross-sectional profile can also vary in width and combinations of both. The width variation is easily done by the tool design. The inner and outer part of the top tool (Figure 4.5) define the inner and outer edge of the PUR subframe. The height and angle can be changed circumferential or be varied in defined areas. Combinations of thickness increments and width variations are therefore influenced by the tool and the way the tool and mixing head are moved during PUR application. These possibilities allow for subframe shapes of high complexity.

Conclusion

The performed thickness increment experiments proved that the principle of creating a smooth slope at the subframe ends is possible. More drastic thickness jumps, plateaus at the ends or changes along the mid-section of the subframe can be done by adding a second application shot locally after 5 seconds, once the PUR is hardened to touch.

A controllable issue is that the top surface still entails three major imperfections ; ridges in the transition zone, blisters in the thick areas and brinks on the edges. These issues can cause problems for the adhesion of the assembly adhesive, as discussed below. A process adjustment is therefore required.

1. The blisters on the surface material need to be prevented, as they can act as moisture bridges and impair the adhesion of the assembly adhesive, especially at higher temperatures when the air in the voids expands. This problem could be solved by locally applying two or multiple shots of PUR instead of one in order to decrease the effect of the exothermic reaction.

2. Where the injection nozzle is closed for a few seconds and then opened again, the transition area still contains a small ridge. This imperfection needs to be eliminated, because it can again cause moisture bridges between PUR and assembly glue. A solution is to tilt the tool against the flow direction while the material is still liquid to create a smooth transition.

3. On some samples there are small brinks along the sides, which mainly appear when using a high material injection rate and fast tool movements. These edges could be prevented if a mixing head with lower material injection rate is used (i.e. 10 g/s), which allows for a slower material application and slower tool movements.

Once the remaining problems are solved and the process is fine tuned, the subframe design as of the four-door vehicle can be reproduced using the OMPURIB process. This is proven by the result in Figure 5.17, which after two days of teaching is already very close to the CAD design.

Lastly, further profile variations, such as changes to the edges of the subframe are done by the tool design. The definite angle or maximum height of the edges is defined by the inner and outer top tool. Therefore only the variations in thickness along the flow direction and the increments from one edge to the other are process-dependent. The same counts for the shape of the adhesion zone of the subframe. Whether it is smooth or entails modifications like steps is dependent on the adherend, because the PUR is directly applied onto the adherend's surface and follows its shape. The adherend acts as the bottom tool.

5.3.2 Flat Plate with different adhesive thicknesses

In order to analyze the print-through (Section 2.1.1) due to shrinkage effects caused by the application of PUR subframes of different thicknesses, four different thicknesses were tested. These thicknesses were determined from recent and potential subframe designs and set to 5, 10, 15 and 20 mm. The corresponding DoE can be found in Table A.3.

Sample Preparation and Aging

As for the CFRP peel specimens, the CFRP plates were placed on a heating plate to heat the substrate. As boundaries 2 steel molds were placed on the sides at a 15 mm width and a small metal plate at each end was used to close the molds and prevent the PUR from flowing out. This setup is shown in Figure 5.18(a). The thickness was adjusted by changing the speed with which the mixing head is moved along the line, because the material flow rate is constant at 30 g/s. This means that for the 5 mm thickness the head had to move the fastest and for the 20 mm thickness the slowest. The sample plates were blank CFRP plates and CFRP plates to which peel-ply was applied on one side during manufacturing, in order to investigate whether there is a difference in print-through behavior. The resulting PUR lines can be seen in Figure 5.18(b).

A first print-through analysis was performed directly after the application process, as soon as the samples were cooled down.

(a) Production of the PUR bond lines

(b) Top and front view of the four lines of different thickness
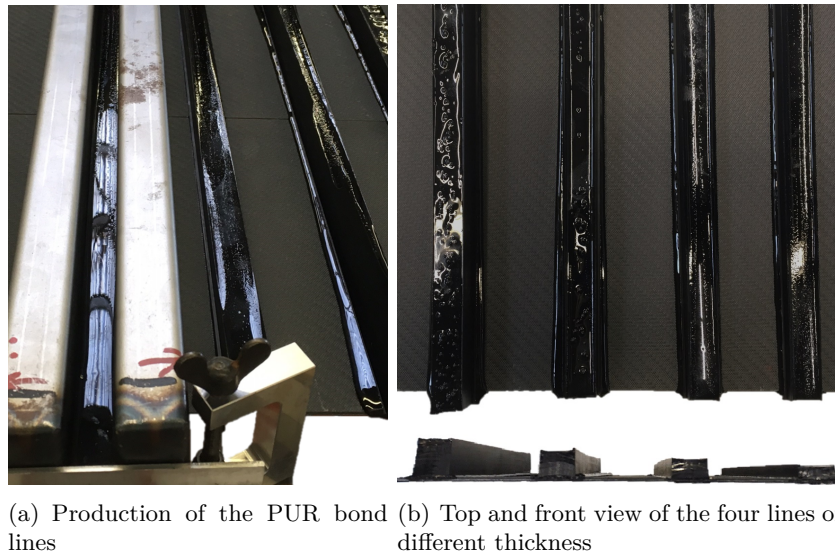
Figure 5.18: Production and results of the applied PUR lines of different thicknesses

After the required hardening time of 7 days, the samples were placed in the climatic chambers (AHS, CCH, Cata) and analyzed again afterwards to investigate the print-through after simulated environmental influences. For the print-through analysis they were held under a light beam in a light booth (xrite Macbeth SpectraLight III), which is commonly used for visual assessment of smaller items under different lighting conditions.

Print-Through Analysis

All print-through examinations on plate level were done together with Mr. Bernd Uwe Kettemann, a senior expert of surface assessments at Daimler AG. As stated before, they were performed in a light tunnel for post-process examination and a light booth after aging. Both, tunnel and booth, are equipped with straight light bars. The light emitted by those bars is a long linear light beam, which bends where irregularities are within or on the reflecting surface, such as indentations and print-through.

The first evaluation showed no print-through for 5, 10 and 15 mm thick PUR lines. However, the 20 mm ones showed slight print-through lines along the sides of the bond line. The print-through was not strong enough to capture in pictures, which is why schematics are shown in Figure 5.19 to visualize the effect for better understanding.

After aging, the samples were examined again at room temperature and it was found that all samples still showed print-through for the 20 mm PUR line. The blank sample that was kept in AHS was the only one, which showed slight print-through at 15 mm thickness.

It makes sense that the print-through effect is greater where more adhesive material is used, because a shrinkage factor of 1.2% results in a higher total shrinkage for thicker material applications. The resulting shrinkage for 20 mm thickness is 0.24 mm, whereas for 5 mm it is only 0.06 mm, which is $1/4^{th}$. As mentioned in Section 2.1.2 shrinkage causes residual stresses within the bond, which result in print-through on the outside surface. The stresses

due to shrinkage can be calculated using Eq. 2.4, if the strain caused by the reaction and cooling is known.

(a) Isometric view indicating the print-through lines visible on the top of the plate surface

(b) Zoomed-in front view showing the trench effect on the PUR edges, which causes the print-through lines
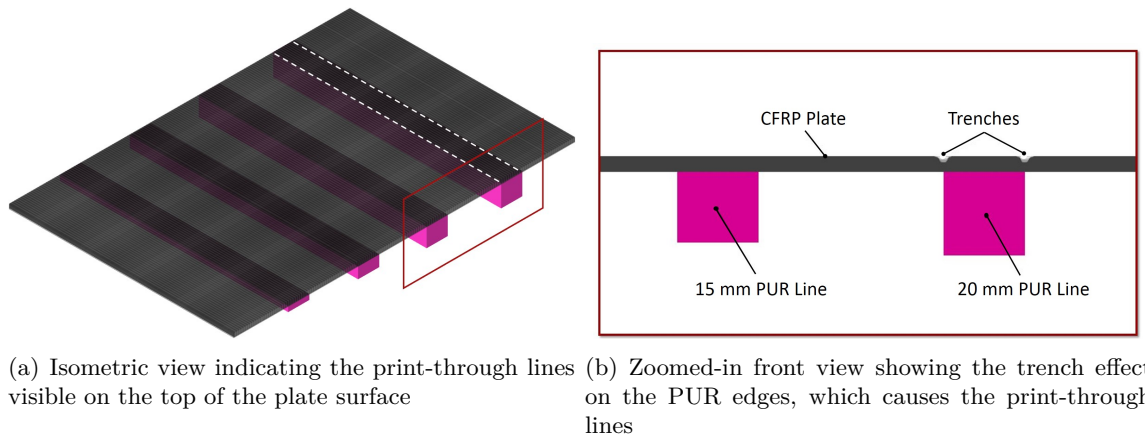
Figure 5.19: Visualization of the print-through effect (dashed lines and trenches) on the plates with four applied thicknesses in isometric and front view

Additionally, in order to also consider the upper operating temperature limit of the CFRP roof and subframe, the samples were placed in an oven for two hours and subsequently went through their final print-through check. This final check indicated that the temperature increase does not increase print-through. Only the plate with peel-ply showed an additional slight print-through for the 15 mm thickness, as was the case for the one blank sample kept in AHS.

The lower limit of the temperature range was not investigated, because the CFRP's stiffness increases and the CFRP expands when cooled down to $-40°C$, such that it does not allow for print-through due to shrinkage of the PUR. Therefore the minimum operating temperature was not rated as critical.

Also noticeable was the fact that where the tool was not sealed well and some PUR spilled at the edges, as visible in Figure 5.20, the print-through disappeared.

Figure 5.20: Image of a plate with spilling on the PUR edges without print-through on one side and sharp edge with print-through on the other

The reason is that the spilled material reduces the stress jump created at the 90° edge between PUR and CFRP plate. From this observation it can be concluded that smaller angles (i.e. 45 °

instead of 90 °) decrease the thickness jumps and therefore the stress jumps and consequently reduces the print-through effect.

Conclusion

On a flat CFRP plate the print-through results are very good, since only the thick bond lines show slight print-through. None of the recent subframe designs actually extends a thickness of 15 mm yet. But even though the thick bond lines indicate print-through, these effects are so minor that only an expert can spot them. They would be invisible to a customers eye, which is not trained to detect these slight flaws.

In theory the print-through should be even less on a curved structure, like the CFRP roof, since it has a higher bending resistance and therefore flexes less. This should make it harder for the PUR to pull CFRP material to the inside. But to ensure no print-through visible to a customer's eye, the tests have to be repeated on the actual component.

Lastly, the examination should not only be done after the samples reached room temperature again, but also at the minimum and maximum operating temperature. This is to assure that even in the desert or tundra at a petrol station the customer is guaranteed a Class-A roof surface.

5.3.3 Flat Plate with a Simplified Crash Bar

This experiment was used to qualify the crash bar overmolding process and to analyze possible print-through caused by $\Delta\alpha$ between crash bar and roof. A DoE was used to design the experiments and can be seen in Table A.4.

Sample Preparation and Aging

The crash bar is simplified to a hat profile without any beading or cut-outs, as indicated in Figure 5.21.

(a) Real-life crash bar of a four-door vehicle   (b) Simplified crash bar design for experiments
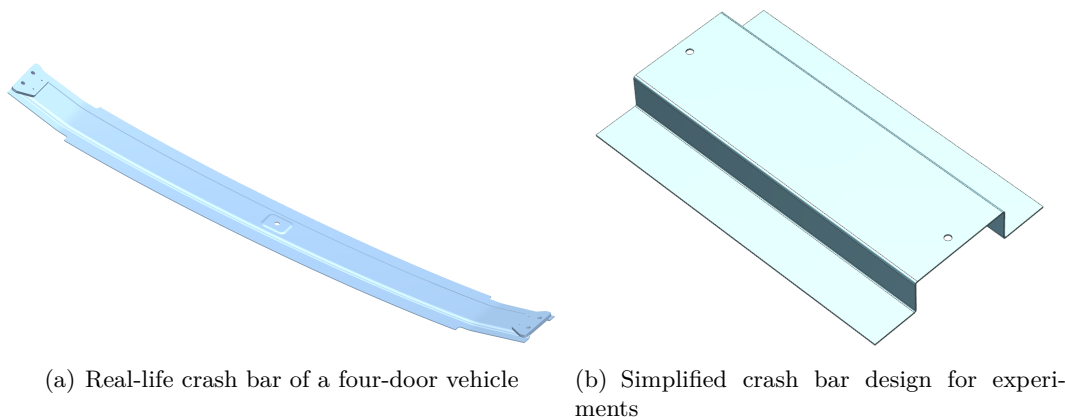
Figure 5.21: Comparison of a real-life to the simplified crash bar

For the crash bar tests near-net shape samples are used. To simplify the CFRP roof, a simple 200 x 300 mm CFRP plate with the roof's layup is used as for the previous experiments. These come in two versions again, with and without peel-ply, and are both examined.

It should be noted here that due to a dimensioning mistake during manufacturing of the simplified crash bars, they were slightly oversize. The stiffness is therefore lower than originally intended.

Test Setup and Execution

For the PUR injection the simplified crash bar and the CFRP plate were connected using spacers on the inner edge and on the sides of the flanges. The spacers held the two parts together with the required bond gap distance and additionally sealed the bond gap from PUR leakage. A bond gap of 4.5 mm was chosen in order to investigate print-through of the adhesive thickness when applying the commonly used assembly adhesives at Daimler AG. Images of the assembly of the two parts can be seen in Figure 5.22.

(a) Attachment of the spacers onto the simplified crash bar

(b) Connection of the two parts

(c) Side view showing the resulting bond gap of 4.5 mm
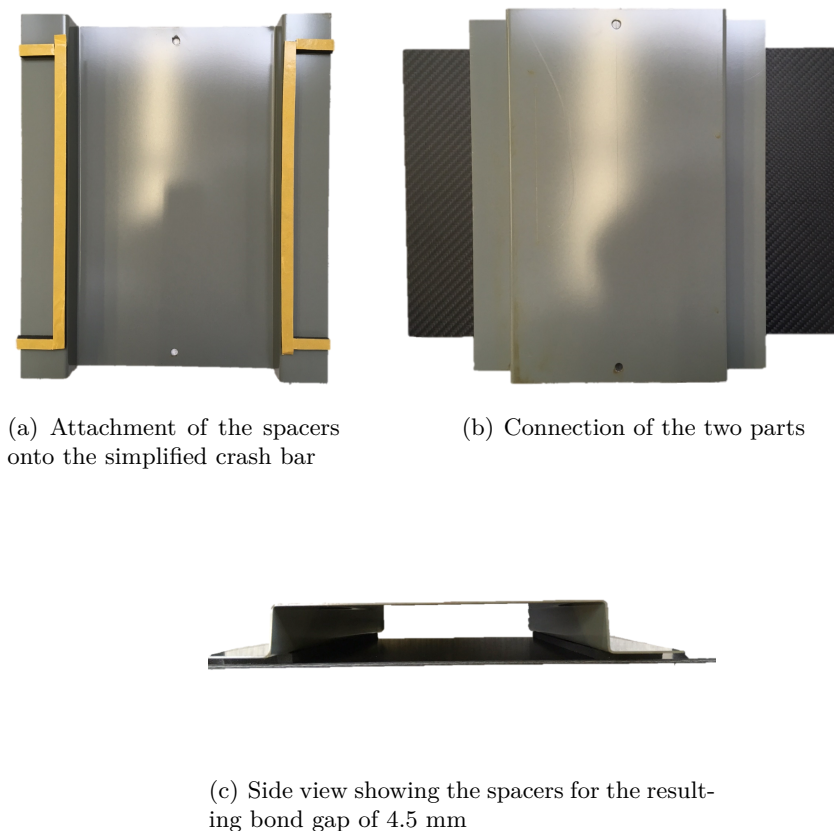
Figure 5.22: Assembly of the two simplified crash bar with the CFRP plate

Once the samples were assembled, they were placed and fixed onto a heated ($60°C$) item construction at an angle of $20°$ as depicted in Figure 5.23.
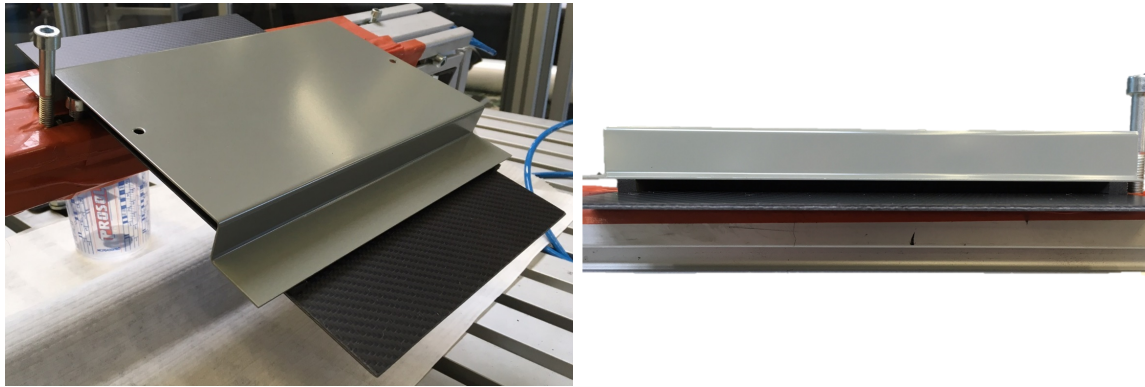
(a) Isometric view of the sample fixed onto the heating plate

(b) Front view showing the bond gap

Figure 5.23: Positioning of the crash bar sample for PUR injection

The PUR is then injected into the bond gap with a speed of 0.6 m/s and hardens to touch within 5 seconds.

The original intention was to extent the test range to 1.5 mm and 3 mm bond gaps, as commonly used when applying structural adhesives, but with a 30 g/s mixing head it was not possible to program the injection properly, because within the possible speed ranges too much material was injected.

After a first inspection in a light tunnel, which is usually used to inspect surface flaws of Class-A automotive surfaces, and full curing, the samples were aged under the conditions described in Section 2.3.3.

Following the aging the samples were re-examined under a light booth again, as was done for the plates of Subsection 5.3.2.

Test Results and Analysis

As previously stated, the specimens were analyzed for print-through directly after the application process and after aging, same as done for the different applied PUR thicknesses discussed in Subsection 5.3.2.

After the application process and some cooling down time, all samples showed no sign of print-through, the surfaces were undisturbed.

Looking at them again after aging showed some changes. There was still no bond line print-through visible, but the assembled specimens were slightly deformed. This deformation was basically a small bending one each side over the crash bar flanges, which caused changes in the optics of the CFRP in terms of fiber orientation. Instead of straight lines, the fibers followed a slight curvature. The majority of results indicated a slight S-shaped warping transverse to the longitudinal axis of the crash bar, as shown in Figure 5.24(a). The samples, which were stored in Cata, also showed S-shaped warping, but diagonally to the transverse axis, which is depicted in Figure 5.24(b). Lastly, one CCH specimen exhibits dishing at the center of the plate, illustrated in Figure 5.24(c).

(a) Transverse S-shaped warping   (b) Diagonal S-shaped warping   (c) Dishing in the plate center
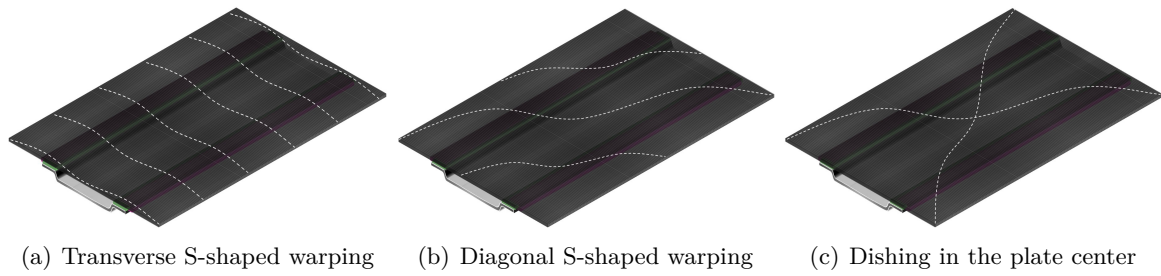
Figure 5.24: Schematics of the detected print-through effects on the simple crash bar specimens

The most probable cause for the deformations is a combination of low flexural rigidity of the adherends and the large difference between thermal expansion coefficients. A simple thin plate, with no curvature, can flex a lot in the out-of-plane direction. The same holds for the simplified crash bar. Even though the flanges create some rigidity, the wider the web or the higher the flanges, the more the bar's bending resistance, its flexural rigidity, decreases. At elevated temperatures the steel expands (mainly in 2 directions), whereas the CFRP contracts (mainly in 1 direction), since it has a negative CTE. The opposite happens at minus temperatures. The differences in CTE cause residual stresses in the bond, which the PUR tries to balance out, while it also expands or contracts with the temperature changes. The stresses that the PUR experiences due to thermal expansion can be calculated using Eq. 2.2, but because neither the CTE nor the Poisson ratio is known for the Elastolit, the calculation could not be done. At a certain point, the adhesive encounters too high stresses, which it cannot counterbalance anymore. It pulls on the material of lower rigidity and causes a small local bending, which can be visually observed as local print through lines along the bond line edges, similar to the thick bond lines described in section 5.3.2, or, if the stress jumps are more distributed it can result in a warping of the adherend. The adhesive lines both pull the adherend towards their bulk, causing shear stresses between the two flanges, which then cause warping of the adherend along the direction of the highest stress, in this case transverse to the bar's longitudinal axis. For an adherend with low flexural rigidity, like a flat plate, this effect is much stronger than for an adherend with higher flexural rigidity, like a roof which is cambered. This is due to the fact that the flexural rigidity is related to the material stiffness as well as the cross-sectional area of the part. It therefore depends on the Young's Modulus E and the second moment of area I. The formula to calculate the resulting curvature under an applied bending moment M_B as shown in Figure 5.25 is shown in 5.2. The higher the E-Modulus and second moment of area, the lower the curvature κ for a constant bending moment.
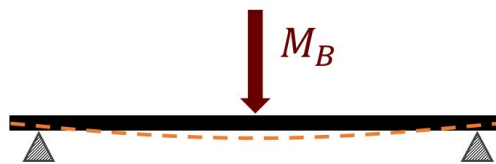
Figure 5.25: Deflection of a supported plate with an acting bending moment M_B

$$\kappa = \frac{M_B}{EI} \tag{5.2}$$

During aging the bending moment is not a result of an applied force, but a result of the residual stresses in the bond due to expansion or contraction of the materials.

During Cataplasm storage the temperature control was not functioning correctly, such that the samples could not be exposed to minus temperatures. Usually during the Cataplasm conditioning the sample is exposed to $70°C$ at 98% humidity for 7 days before the temperature is rapidly dropped to $-25°C$ (see Section 2.3.3. While the sample is exposed to heat and humidity the plastic materials, both the PUR as well as the epoxy, absorb the humidity and are re-dried again when rapidly cooled (frost effect). If the minus temperatures are not reached the plastics constantly absorb humidity without emitting any. This results in a drop of E-Modulus for the plastic materials (the E-Modulus of the PUR is effected more than the E-modulus of the epoxy). The carbon fibers and the e-coated steel do not absorb humidity and therefore do not experience a decrease in mechanical properties. Due to the decrease in material stiffness of the plastic components, the stresses caused by the difference in thermal expansion coefficient have a larger impact on the CFRP plate's deflection. Warping is caused along the path of maximum stress, which in this case is under a $45°$ angle to the bond line. The direction is possibly dependent on the CFRP laminate, which is effected by the epoxy's humidity absorption.

The dishing of the plate could be a result of the combination of diagonal and transverse warping or two opposite diagonal warps.

For vehicles a crash bar structure is optimized for high flexural rigidity, but simultaneously for certain folding patterns during crash. Therefore the assembly with the chambered roof, which has adherends of higher second moment of area and therefore higher flexural rigidity, should be able to withstand higher residual stresses and therefore be less prone to print-through. This theory should be tested before it can be verified for series production by repeating the print-through tests on a crash bar and roof assembly.

The fabrication of the samples was also used as a pre-examination, whether the crash bar overmolding process is usable. It can be said that the process proved possible and can be applied to components. Though the programming is rather time-consuming when using the mixing head with an ejection rate of 30 g/s, especially for even smaller bond gaps.

Conclusion

The outcomes of the print-through tests with a near-net shaped crash bar and 4 mm bond gap to the CFRP plate were useful for a preliminary valuation of possible print-through effects on a CFRP roof. A positive outcome was that the bond lines themselves were not visible on the outer surface of the CFRP plate, neither directly after the process nor after aging. The less fortunate finding was the warping of the plates after aging due to the difference in α. This outcome could change though once the test is repeated on a roof, which is chambered, and a curved and stiffened crash bar is used. The components have a higher bending stiffness and should therefore have higher resistance to the residual stresses inserted during aging.

Again, as stated by the expert, the print-through is visible for an expert's eye, but should be invisible for customers. In case the higher bending stiffness of the roof does not eliminate

the print-through, it might be possible that the effect seen over a larger area could become visible to the customer. This is another reason why a test on the actual component should be performed.

In order to give more leeway to future roof concepts it is advised to also test bond gaps of 1.5 mm and 3 mm. These bond gaps are closer to the ones used for structural adhesives in automotive part production and could also be suitable for the semi-structural Elastolit. For theses bond gaps the print-through effect could worsen on the samples, but it could be usable for the roof. When applying PUR to smaller bond gaps using the OMPURIB process it is recommended to use a 10 g/s mixing head for better applicability (higher accuracy and more leeway for the application speed).

Moreover, it is also possible to test thicker bond gaps in order to investigate the interference of the $\Delta\alpha$ effect and shrinkage of the adhesive. While the $\Delta alpha$ effect should decrease with the increase of PUR material, the shrinkage becomes more relevant for thicker bond lines, as discussed in Section 5.3.2.

Additionally, further process experiments could be performed. For the assembly it might be easier to place the crash bars with small local spacers and seal the gap from the outside. The PUR injection could then be done using the holes in the crash bar, which are already inserted for specific crash behavior anyway. Here it is important to check the flow length of the PUR per bond gap in order to determine the required maximum distance between the injection holes to achieve a continuous bond.

Further process and component tests for crash bar overmolding on a roof will be continued by the colleagues at Daimler AG Sindelfingen subsequent to this study.

5.4 Process Application onto an AMG GT R CFRP Roof

As the final experiment the OMPURIB process was applied to the AMG GT R CFRP roof as a final prove of concept. The applied subframe was made based on the CAD design shown in Figure 4.3(a) of Section 4.2.

Test Setup and Execution

From the constructions done at the beginning of the research project, which is discussed in Section 4.2, the tool was manufactured and setup at Daimler AG Sindelfingen. The CAD construction as well as the manufacturing of the tool was done by f.u.n.k.e. MOLDS & SPECIAL PARTS GmbH.

The CFRP roof was placed in the bottom tool, after which the outer top tool was placed on the roof edges and held in place by fasteners. Subsequently the POM tool was placed in the center of the roof and aligned using spacer bars on two edges. Inside the cutouts of the inner tool the spacers were placed for integration using thin 0.2 mm thin double-sided tape. This tool setup and spacer placement can be seen in Figure 5.26(a).

The PUR application was programmed to create a 3 mm thick subframe and to simultaneously enclose the spacers. This was done by using all 8 axes, as explained in Section 3.2.2. The thickness is, as for the test specimens of Sections 5.2 and 5.3, depedent on the speed with

which the robot head moves along its path. The start and end point are at the rear right corner, which was chosen arbitrarily.

Figure 5.26(b) shows the finished PUR subframe adhered to the CFRP roof without the top tool as a result of the open-mold polyurethane injection bonding process. It presents the overall result as well as a zoomed-in view of the integrated spacer at the front right corner.

(a) Mold tool for the PUR subframe   (b) Finished subframe with integrated spacers
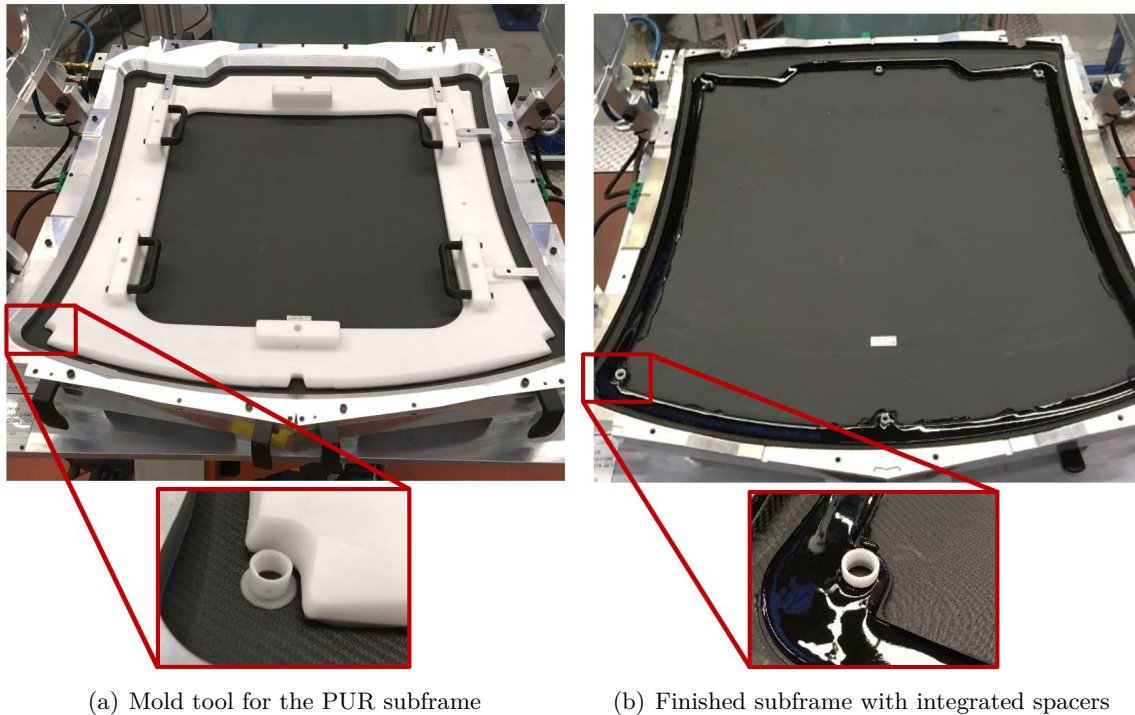
Figure 5.26: Process of the subframe PUR application including spacer integration

Test Results and Analysis

Since the complexity of the AMG GT R subframe design is rather low, the programming is rather easy and fast. The resulting subframe was programmed within 1.5 days. Though for series production some adjustments still need to be made. The start and end point needs to be smoother in order to guarantee proper sealing after the application of the assembly glue and to prevent moisture bridges. Furthermore, the thickness is not yet of constant 3 mm with $\pm 1mm$ tolerance. One small, but changeable problem is, that the POM inner tool is too light to prevent some spilling. Even though it includes a seal, the PUR still flows underneath and leaves unaesthetic edges, which are also visible in Figure 5.26(b). The above mentioned issues are all treatable with some more time invest and an adaptation of the inner top tool.

Very positive though is the fact that no print-through can be detected on the outside surface of the roof. The roof was analyzed in a light tunnel, with the help of a quality engineer and no traces of print-through caused by the PUR application could be detected.

Conclusion

It can be concluded that the process, for the previously discussed roof and subframe design, still guarantees a Class-A surface finish. Additionally, with some adjustments to the tool and to the application program, the subframe should get the intended $3\pm1mm$ constant thickness. Therewith the subframe for series production could be produced using the OMPURIB process.

For final series production qualification, a roof with an optimized PUR subframe should be aged and examined for print-through in order to guarantee a Class-A surface at the roof's operating temperatures.

Furthermore, the roof should be assembled to a GT R body, either by hand or better in the assembly line using the exact system (assembly adhesive, gripper and tact time) as in series production. This should be done for 3-5 vehicles in order to to get a first impression on the ability to incorporate the changed roof component. These vehicles should subsequently be exposed to weathering and driving dynamics. Moreover, the roofs should be cut out again after the real-life tests to examine the adhesion and whether any sealing or unforeseen issues could be detected. If all those tests are passed the PUR subframe can be implemented in the next generation GT R.

Chapter 6

Industrialization and Cost Analysis

An industrialization and cost analysis was performed for the AMG GT R Derivative to summarize the financial and supplier strategy as well as the application field of the OMPURIB technology.

The AMG GT R Derivative will be introduced as a limited edition of 750 vehicles. Every vehicle will be equipped with a CFRP roof. Therefore 750 subframes are required, plus an additional 250 spare parts, resulting in a total of 1000 units.

The goal of the research project is the achievement of a more flexible subframe technology, that is also a cheaper solution with reduced required handling.

Using the OMPURIB technology, the profitability of AMG's CFRP roof can be improved and the technology can create a competitive advantage towards other OEM's and suppliers. The reasoning for the positive assessment of this investment is given in the following sections.

6.1   Market Analysis

In order to identify the technologies that are already on the market and to rule out that the technology is already used, together with the patent lawyers and innovation managers, the market was analyzed based on benchmarking criteria.

It was investigated how other OEM's join the CFRP roofs to their vehicles and whether they or suppliers already patented such a system. The finding was that no other OEM or supplier is using this type of OMPURIB technology or has patented it. An investigation of competitor OEMs' roof attachments showed that the roofs are directly bonded and/or fastened to body-in-white to increase the BIW stiffness. The only action taken in the direction of the OMPURIB technology was a disclosure for the roof trim system by Daimler AG in 2015 [2] as described in 3.2.2 and the WST technology developed by BASF and applied by Exypnos [64, 74].

Considering that no such technology is on the market or even registered at the european patent office yet leaves room for a patent or disclosure of the OMPURIB technology for the application of a PUR subframe to a CFRP roof.

6.2   Technology Transfer

To increase the value of the technology application it is important to determine further areas of application. Such areas of application could be other automotive parts or even utilization in other industries. The technology can be used for any application where open mold PUR injection is used to directly form and bond a solid structure simultaneously, such as the subframe of the roof.

The previously mentioned and in Figure 1.3 visualized roof trim system is an example of an exterior automotive part application. The application is very similar to the subframe structure with an integrated sealing lip.

The OMPURIB process can be used for exterior parts or any flexible structural part with a one-sided PUR application. Additionally, the same technology can be used for other structural and non-structural parts as an injection process to bond two parts together and simultaneously seal the joint.

Examples of other exterior structural parts could be the hood and the trunk lid. Both hatches usually consist of an outer surface shell and an inner shell, which are bonded together. For an accelerated process the shells could be joined using the PUR injection process developed at Daimler AG.

If in any other industries parts similar to the previously described ones are used, the OM-PURIB or the PUR injection process can be applied to replace complex bonding or even fastener and welding solutions. It is very attractive for multi-material modular parts, where thermal joining techniques cannot be applied.

6.3   Supplier Strategy and Tactics

For the series production of the AMG GT R derivative it is important to discuss and trade-off the different potential supplier strategies. Together with one of the purchasers for carbon fiber BIW parts and the adhesives team colleagues at Daimler AG six potential strategy options and seven trade-off criteria were determined, which are traded off as indicated in Figure 6.1. The strategy options are shown in the columns and the criteria in the rows. For each strategy option the criteria were rated from strong positive to strong negative, the legend is indicated in the top left corner of Figure 6.1. For this trade-off all criteria were weighted as equally important, since for each department another criterion is the most critical one.

The clear winner of the trade-off is the last strategy option listed, a production at the 'PWT' (Produktions- und Werkstofftechnik) department of the Daimler AG. This strategy can work for a single small series production like for the AMG GT R derivative, but can not be done for any further applications, since it can only be done as a trial run for the qualification of the technology. Even though it has the highest potential, it has to be ruled out.

++ strong positive
+ positive
o neutral
- negative
-- strong negative

Criteria	Strategy Options					
	Availability of plant on free market	CFRP roof supplier buys plant	CFRP roof supplier leases plant	AMG buys plant and provides it for supplier	Seperate PUR subframe supplier buys/leases plant	Internal production at the 'PWT' as a trial run
Costs for AMG	++	+	+	-	++	++
Risk for roof assembly (responsibility matrix)	--	+	+	+	--	++
Length of transport path, minimum amount of points of intersection	-	+	+	+	-	++
Speed knowledge transfer and technology implementation	+	-	-	-	-	++
Dependence of AMG on supplier, supplier monopoly	+	-	+	--	+	o
Appeal for supplier (low cost, order guaranty, etc.)	+	--	+	++	+	o
Utilization for other projects possible	+	-	-	--	+	o

Figure 6.1: Trade-Off of the possible supplier strategies

On second place, with a tie, are the strategies 'Availability of plant on free market' and 'CFRP roof supplier leases plant'. The first one has to be ruled out as well, because no supplier was discovered yet that has the ability to perform the OMPURIB process directly. Therefore the best option is to have the supplier, who also manufactures the CFRP roof, lease an OMPURIB plant and apply the subframe straight after roof production to deliver it to the Daimler plant as an assembly. This strategy will bear the lowest risk in terms of quality liability because additional transportation stages and handling are avoided, and the leasing does not make AMG and the supplier interdependent. If the supplier does not provide the required quality, AMG is not tied to the supplier for the next projects because he made a large investment for the PUR plant, but can find another supplier, who also leases the PUR plant. But most importantly this strategy will involve relatively low plant investment cost for AMG.

6.4 Financial Forecast

In order to analyze whether the new process optimizes the resource requirements and the manufacturing and material cost, the cost comparisons depicted in Table 6.1 and Table 6.2 were done together with the division's quantity surveyor. The optimized PUR subframe, as shown in Figure 6.2(b), is compared to the current solution, a CFRP prepreg pressed

subframe which is bonded to the CFRP roof, as shown in Figure 6.2(a). The calculations are approximations based on reduced and confined assumptions. The break down was based on prices previously offered by suppliers. For reconciliation the costs were compared to the CFRP subframe overall costs reduced from the total roof price of the AMG GT R roof.

(a) AMG GT R CFRP roof with CFRP subframe   (b) AMG GT R CFRP roof with PUR subframe
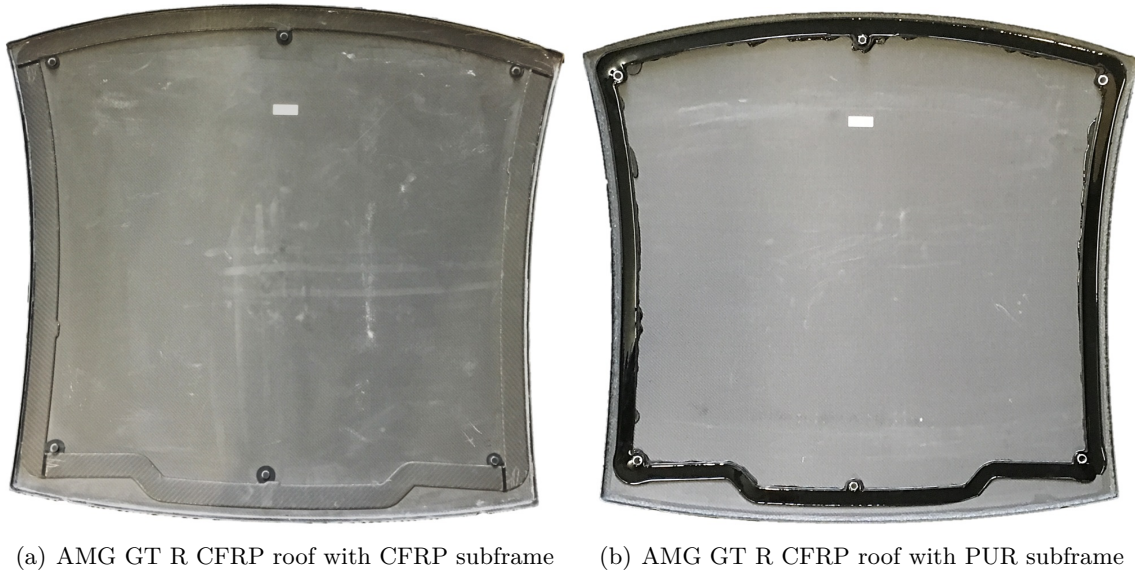
Figure 6.2: AMG GT R CFRP roof with a CFRP and PUR subframe

The cost comparison is done for the resource requirement and manufacturing and material cost separately. The resource requirement is usually paid up front as a total plant invest and not added to the unit price. It summarizes all the equipment payment necessary for quantitative and qualitative execution of the production [75]. At AMG this includes the cost for the mold tools, jigs and supplier development.

Table 6.1: Resource Requirements Comparison of a CFRP Pressed Prepreg and a PUR Subframe

Type of Cost	CFRP Pressed Prepreg (+Adhesive)	PUR
Mold Tools	80,000.00 €	50,000.00 €
Jigs		
Milling Jig	25,000.00 €	-
Bonding Jig	20,000.00 €	-
	45,000.00 €	**0.00 €**
Supplier Development Cost	18,000.00 €	50,000.00 €
Total	**143,000.00 €**	**100,000.00 €**
Per Unit	**143.00 €**	**100.00 €**

The manufacturing and material cost in contrast are broken down to the unit price, in this case per subframe. Material cost include raw material, production material and consumables.

The hourly rate of the appliances and machines as well as labor cost are comprised in the manufacturing cost.

Table 6.2: Manufacturing and Material Cost Comparison of a CFRP Pressed Prepreg and a PUR Subframe

Type of Cost	CFRP Pressed Prepreg (+Adhesive)	PUR
Machine Hourly Rate		
Press	80.00 €/h	-
Prepreg Cutting	40.00 €/h	-
Bonding	35.00 €/h	-
Low Pressure Metering Unit	-	30.30 €/h
Robots for PUR Application	-	17.05 €/h
	155.00 €/h (x 0.3 h)	**47.35 €/h (x 0.3 h)**
Avg. Labor Cost (GER)	**35.00 €/h (x 0.3 h)**	**35.00 €/h (x 0.3 h)**
Material		
Prepreg (12K, 300 g/m^2, 2 x 2 twill)	64.48 €	-
Adhesive (Dow BETAMATE 2850)	6.00 €	-
PUR (BASF Elastolit R 8919/107)	-	0.88 €
	70.48 €	**0.88 €**
Consumables	**4.00 €**	**2.00 €**
Production Overhead (20% of net product)	**26.30 €**	**5.52 €**
Per Unit	**157.78 €**	**33.10 €**

For simplification the production time for each production step of both subframes was assumed to be 0.3 hours. It can be seen that for both, the required resources as well as the manufacturing and material cost, the cost are lower using the new PUR subframe solution. € 43,000.00 can be saved in required resources and broken down to the value per unit, the PUR subframe is € 43.00 cheaper. In the category 'manufacturing and material cost' another € 124,68 is saved when using the PUR subframe. Altogether changing from a CFRP to a PUR subframe results in a total **saving per roof of approximately € 168.00**, which is about half the cost of the CFRP subframe.

The greatest financial benefit of the OMPURIB process becomes clear as soon as the complexity of the subframe increases, similar to the sketches in Section 5.3.1. If, for example, the thickness increases towards the ends or even in center of the subframe, or if an inclination towards one of the edges is required, the production of a CFRP subframe becomes much more complicated and therefore more expensive. More layers will have to be added locally to increase thickness, which extends the production time and material cost. Another option for sideways inclinations could be the use of different adhesive line thicknesses, which comes with a long print-through and adhesion qualification process each time the adhesive gap design is adjusted or the adhesive material is changed. Together with the weight optimization the OMPURIB process definitely optimizes the time and cost for complex subframe systems of CFRP roofs.

Chapter 7

Conclusion and Recommendations

For Mercedes-AMG it is important to develop a long term solution for the CFRP roof subframe that can be used for various designs, regardless of whether a local or circumferential adapter frame is used. For this case it is important to make a smart material choice to find the most flexible and cost-effective solution.

According to the project definition the OMPURIB technology was partially verified for the application of a PUR subframe onto the inside surface of a CFRP roof. The problem at hand was the bridging of the Z-offset between roof and roof frame caused by the thickness difference between panoramic glass and CFRP roof. Currently this offset is bridged by a bonded CFRP subframe, which has its limits when it comes to more complex subframe designs and therefore quickly becomes a time consuming and expensive process, as soon as small variations need to be included. Therefore a PUR subframe was chosen, which is formed and adhered to the roof in one step by using the in-house open-mold polyurethane injection bonding process. This process was invented by BASF and used by Exypnos to apply seals to car windows and to solar panels. It was then further refined by the adhesives team at Daimer AG Sindelfingen to replace the roof trim with a shadow gap. And now the research shows that the process can also be used to replace the CFRP subframe as used in the AMG GT R to bridge the Z-offset between the CFRP roof and the roof frame.

The requirements of the subframe are the above described bridging of the Z-offset, using a hard and tough material that can keep its structural integrity without causing print-through on the CFRP roof with Class-A surface finish. Furthermore, it is important that the PUR adheres well to the CFRP roof as well as to the assembly adhesive used to bond the sub-assembly to the BIW. It was concluded from the peel tests that the best adhesion between PUR and CFRP is achieved by combining abrasive and conditioning pre-treatments. First the surface topology should be changed by sanding the substrate surface or by applying peelply onto the laminate side to be adhered, when producing the CFRP adherend. In a second step a primer should be applied onto the abrasively treated surface to activate the surface. For the PUR-assembly adhesive interface the best result, independent of the type of assembly adhesive used, was obtained when changing the mixing ratio of the PUR from 100:58 to 100:64. Since a change of mixing ratio comes with a partial repetition of the performed verification

process, the quicker solution is the pre-treatment of the PUR surface before application of the assembly adhesive. The best overall outcome here is sanding of the PUR surface, although dependent on the adhesive type, the PUR requires different minimum hardening times before the adhesive application to achieve optimal adhesion. Moreover, pre-treating the PUR surface is an additional production step, which will increase the cost of the subframe.

Next to the adhesion, the lap-shear strength of the PUR is of high importance. It should be above the lap-shear strength of the assembly adhesive (4-8 MPa at standard atmosphere) to guarantee that the weakest link is the assembly glue. Additionally, it should offer a lap-shear strength that is close to the one of the structural adhesive (11 MPa at standard atmosphere) used to bond the CFRP subframe. With a maximum observed lap-shear strength of 13.2 MPa at standard atmosphere, the PUR strength lies above both the strength of the assembly as well as the structural adhesive and therefore meets the requirement. This value was obtained when using no pre-treatments. Since the peel test analysis suggests the use of an abrasion-primer combination for pre-treatment, the lap-shear strengths for those conditions were also considered. Sanding plus primer as well as peel-ply plus primer show values of 10.5 MPa and 10.3 MPa respectively. Even though the strength for both cases is 20% less than for the untreated surface, the values deviate less than 10% from the strength of the structural adhesive and are still far above the strength of the assembly adhesives. Therefore the lap-shear strength is still sufficient.

Subsequently to the fundamental studies on material and bond properties, the process and print-through tests gave insight into the subframe design possibilities. Print-through tests were performed in order to analyze possible print-through on the Class-A outside surface of the substrate. The influence of the PUR line's thickness was investigated, as well as the influence of the $\Delta\alpha$ between an integrated steel crash bar, the CFRP part and the PUR at a bond gap size of 4.5 mm (typical thickness of an assembly adhesive bond gap). In terms of PUR line thickness it was detected that only very thick bond lines (15-20 mm) cause print-through, due to the greater shrinkage effect where more material is applied. This effect is barely visible to an experts eye, but it can be reduced by tapering the edges to avoid 90° angles between substrate and PUR to take out the localized stiffness jumps. Looking at the crash bar specimens right after the PUR application no bond line print-through could be detected, but the examination after aging showed that the CFRP plate warped over the crash bar in a transverse or diagonal S-shape. This behavior is introduced by residual stresses which are caused by the difference in thermal expansion between the different materials, which the PUR cannot fully balance out. Again the effect is very minimal and not visible for a customer's eye. The technology therefore still passes theses pre-tests, but further testing should be performed on the actual roof and crash bar components for validation, because the print-through effect is not only dependent on the material properties, but also on the adherends' flexural rigidity.

The previously stated design flexibility of the PUR subframe was examined using a proof-of-principle test on the process for thickness variations. It was found that it is easily doable in one shot to create a slope at the ends of a non-circumferential subframe. It was even possible to reproduce the CAD design of a subframe to a few millimeters. Variations in the mid-section or the build-up of plateaus and rapid jumps can be achieved by applying multiple shots. Since the PUR hardens to touch within 5 seconds, a next layer can be applied directly onto the first after 5 seconds without moving material of the first layer. Other variations, such as the variations in width, height and angle of the edges are process-independent and only determined by the tool design. The same counts for the bottom shape of the subframe

which solely depends on the shape of the adherend. This test pointed out that the application of thick layers still comes with the downside that blisters appear on the PUR surface. These air inclusions could cause moisture bridges between PUR and assembly adhesives as well as a reduced adhesion of the assembly adhesive on the PUR. The solution to this problem could be to apply multiple layers of PUR in order to build up the thickness variation. This theory could reduce the exothermal expansion effect of the material, but this theory still needs testing. Additionally, the use of a mixing head with a lower injection rate (10 g/s) could allow a smoother injection to reduce the air inclusions. Two more process related issues were observed during this test set, a small ridge where two PUR ends overlap and brinks on the sides of the frame. Both issues can be solved by fine tuning the process and using a mixing head with lower injection rate.

As a concluding test a PUR subframe was applied onto an AMG GT R roof including the integration of spacers. This proved the feasibility of the OMPURIB process to create a 3D subframe structure, since a subframe with $\pm 1mm$ can be applied that shows no print-through effect after process application. It also showed that functional integration, such as the spacer integration, can be done. The PUR application onto the AMG GT R roof itself was done within 30 seconds. Considering the time for the roof placement in the tool and the fixing of the top tools, the cycle time to produce one subframe should take no more than 20 minutes.

The major influencing factors for the subframe design are the injection rate, application speed and the tilt direction and speed of the robot head and the tool. The adhesion of the PUR is mainly influenced by the PUR mixing ratio and the substrate material.

After the experimental examination of the material and process, a closer look was taken at the industrialization possibilities of the technology. The market was analyzed for similar technologies and for potential applications of the OMPURIB technology. Moreover, the cost and possible supplier strategies were analyzed for Mercedes-AMG. The decision was made that the best supplier strategy for Mercedes-AMG is to have the CFRP roof supplier lease the OMPURIB plant to apply the subframe directly after the roof is manufactured, without any intermediate transport stages. Of course, this involves a negotiation process with the CFRP roof supplier. When comparing the PUR subframe cost to the CFRP subframe cost, a total saving in plant invest (resource requirements) of € 43,000.00 and a saving in manufacturing and material cost of € 124.68 per unit can be obtained. Splitting the costs of both categories into a price per unit, the result saving are € 167.68. This high difference in expenses makes the implementation of the technology even more appealing.

Recommendations

To use this technology in the next-generation AMG car, a few steps still have to be taken.

A repetition of the print-through tests in cataplasm storage have to be repeated, because of the malfunctioning of the chamber, which did not reach the minus temperatures. This counts for both the different bond line thickness samples and the simplified crash bar samples. Only if the test set is repeated, the tests are complete.

It is also recommended to repeat the full crash bar test, which was performed with a 4.5 mm bond gap, with bond gaps of 1.5 mm and 3 mm to investigate the impact it has on print-through and possibly include another design variable for more flexibility in roof concepts.

Further experiments can be performed on the thickness increments topic. The tests could be

repeated with a 10 g/s mixing head to inspect whether it can solve the issue with the brinks on the edges and the blisters on the thick surfaces. Additionally, the thickness increment tests could be repeated with the application of multiple layers instead of one to determine the impact on the blister formation and to expand the possibilities for different designs.

In case the decision is made to change the mixing ratio of the PUR material to improve the adhesion to the assembly adhesive, the lap-shear tests and print-through tests should also be redone, in order to examine whether the change in mixing ratio changes the material properties or influences the print-through effect.

For the application of the PUR onto the CFRP roof, the first required step is to fine tune the process to get continuous $3 \pm 1mm$ thickness of the subframe and to avoid the small ridge at the start-end point. To do so it is also necessary to increase the weight of the POM inner top tool to create defined edges without spilling. Once the process is optimized, about 10 roofs with PUR subframes should be produced and their outside surfaces should be coated. Four of these roofs should be aged under the same conditions as the samples and analyzed for print-through and adhesion afterwards. The other roofs should be assembled to a BIW either by hand or better in the final vehicle assembly under the real-life circumstances in order to see whether assembly works smoothly and within the designated tact time. Finally, the vehicles with the PUR subframe should be test driven in different climates to examine if it withstands the dynamic loads experienced during driving and the different environmental conditions. This test will also give insight in the print-through under real-life conditions. After a view weeks (determined by the developer based on company standards) the roof should be cut out again to analyze the adhesion once more. If the subframe passes all these tests, it is verified and validated for the implementation in series production.

From the experiments it can be observed that the OMPURIB technology offers a great alternative for the subframe production to the current CFRP design. It provides the required material properties and enables a great design flexibility. The industrialization and cost analysis also showed that the PUR subframe is very profitable. It saves a total of € 167.68 per unit, which is 56% of the cost of a CFRP subrame.

A great result of the market analysis is that the OMPURIB technology does not exist on the open market in this form yet, but can be used for many other applications. Anywhere where a one-sided bonded structure is required, no matter if for structural or non-structural parts, the technology can be used. Moreover, it can also be used for a injection process to bond two parts together and simultaneously seal the bond.

List of Figures

List of Tables

References

[1] Christian Stasch and Tim Zanker. Innovatives Dachkonzepte mit Schattenfuge. Technical report, Daimler AG, Sindelfingen, 2015.

[2] Reiner Jost, Thomas Disse, Christian Stasch, and Mark Wolf. Dachmodul für einen Personenkraftwagen, 2015.

[3] Deutsches Institut für Normung e.V. DIN EN 923 - Adhesives: Terms and definitions, 2016.

[4] Souheng Wu. Polymer Interface and Adhesion. Technical report, Marcel Dekker, New York, 1982.

[5] Adhesives.org. Adhesives & Sealants.

[6] Cameron Tracey, Ling Xie, and Irene Ly. Cohesive and Adhesive Forces. Technical report, LibreTexts library, 2015.

[7] S. Durso, S. Howe, and M. Pressley. Adhesive Bond-line Read-through: Theoretical and Experimental Investigations. *SAE 1999 Transactions - Journal of Materials & Manufacturing*, 108(5), 1999.

[8] Arthur H. Landrock. *Adhesives Technology Handbook*. William Andrew Inc., Norwich, 2nd edition, 2008.

[9] Gerd Habenicht. *Kleben - Grundlagen, Technologien, Anwendungen*. Springer, Berlin Heidelberg, 6th edition, 2009.

[10] G. McGrath. Adhesives - An Introduction, 2003.

[11] D. A. Dillard. *Advances in Structural Adhesive Bonding*. Woohead Publishing Limited, Cambridge, 2010.

[12] J. Shields. *Adhesives Handbook*. Butterworths, London, 1984.

[13] Michael J. Troughton. *Handbook of Plastics Joining: A Practical Guide.* William Andrew, Norwich, 2nd edition, 2008.

[14] S.R. Hartshorn. Introduction. In *Structural Adhesives - Chemistry and Technology*, pages 2–3. Plenum Press, New York, 1986.

[15] Michael Zürn. Klebetechnik im Automobilbau, 2016.

[16] A. Matting. *Metallkleben: Grundlagen Technologie Prüfung Verhalten Berechnung Anwendungen.* Springer, Berlin Heidelberg, 2013.

[17] Alfred Böge and Wolfgang Böge. *Handbuch Maschinenbau: Grundlagen und Anwendungen der Maschinenbau-Technik.* Springer, Berlin Heidelberg, 2017.

[18] Giles F. Carter and Donald E. Paul. *Materials Science and Engineering.* ASM International, Materials Park, OH, 1991.

[19] R. J. Young and P. A. Lovell. *Introduction to Polymers.* Taylor & Francis Group, Boca Raton, USA, 2011.

[20] A.J. Kinloch. *Adhesion and Adhesives.* Springer Science+Business Media B.V., Berlin Heidelberg, 1987.

[21] C. Whysall. Adhesive bonding of composites. Technical report, Composites UK, Hemel Hempstead, 2007.

[22] A.V. Pocius. *Adhesion Science and Engineering: Surfaces, Chemistry and Applications.* Elsevier, Amsterdam, 2002.

[23] TKH. Schmelzklebstoffe TKH-Merkblatt 4. Technical report, Industrieverband Klebstoffe e.V., Düsseldorf, 2015.

[24] Covestro. Product Center Adhesives - Reaktive Schmelzklebstoffsysteme, 2016.

[25] Adhesives Toolkit Co-ordinator. The Adhesives Design Toolkit, 2017.

[26] C. Hepburn. *Polyurethane Elastomers.* Elsevier, Essex, 2nd edition, 1992.

[27] Hillary Hampton. ME 330 Engineering Materials - Presentation, 2016.

[28] A.V. Pocius. *Adhesion and Adhesives Technology - An Introduction.* Hanser Publishers, Cincinnati, 3rd edition, 2012.

[29] H. Gercek. Poisson's ratio values for rocks. *International Journal of Rock Mechanics and Mining Sciences*, 44(1):1–13, 2007.

[30] L. F. M. da Silva. Failure Strength Tests. In *Handbook of Adhesion Technology*, pages 443–472. Springer, Heidelberg, 2011.

[31] J.R.J. Wingfield. Treatment of composite surfaces for adhesive bonding. *International Journal of Adhesion and Adhesives*, 13(3):151–156, 1993.

[32] A. Baldan. Review Adhesively-bonded joints and repairs in metallic alloys, polymers and composite materials: Adhesives, adhesion theories and surface pretreatment. *Journal of Materials Science*, 39(1):1–49, 2004.

[33] D.M. Brewis. *Surface Analysis and Pretreatment of Plastics and Metals.* Applied Science Pub., London, 1982.

[34] R.C. Snogren. *Handbook of Surface Preparation.* Palmerton, New York, 1975.

[35] Sina Ebnesajjad. *Surface Treatment of Materials for Adhesive Bonding.* Elsevier, Oxford, 2nd edition, 2014.

[36] R. F. Wegman and T. R. Tullos. *Handbook of Adhesive Bonded Structural Repair.* Noyes Publications, Park Ridge, New Jersey, 1992.

[37] Deutsches Institut für Normung e.V. DIN EN 1465 - Adhesives - Determination of tensile lap-shear strength of bonded assemblies, 2009.

[38] D.N. States and K.L. DeVries. Geometric Factors Impacting Adhesive Lap Joint. *Journal of Adhesion Science and Technology*, 26(1-3):89–107, 2012.

[39] M. Schmücker. MBN 10518 - Test Specifications for Ensuring the Adhesion of Assembly Bonds. Technical report, Daimler AG, Sindelfingen, 2015.

[40] Deutsches Institut für Normung e.V. DIN EN ISO 6270-2: Paints and varnishes âĂŞ Determination of resistance to humidity - Part 2: Condensation (in-cabinet exposure), 2016.

[41] Deutsches Institut für Normung e.V. DIN EN ISO 9142 - Adhesives - Guide to the selection of standard laboratory ageing conditions for testing bonded joints, 2003.

[42] Deutsches Institut für Normung e.V. DIN EN ISO 291: Plastics -Standard atmospheres for conditioning and testing, 2008.

[43] Deutsches Institut für Normung e.V. DIN EN ISO 10365 - Adhesives- Designation of main failure patterns, 1995.

[44] B. Giger. DESIGN OF EXPERIMENTS - Einführung in die statistische Versuchsplanung (DoE). Technical report, TQU AG, Winterthur, Switzerland, 2016.

[45] V. P. Astakhov. Screening (Sieve) Design of Experiments in Metal Cutting. In J. Paulo Davim, editor, *Design of Experiments in Production Engineering*, pages 1–38. Springer Switzerland, 2016.

[46] S. Roy, J. Paulo Davim, S. Bhowmik, and K. Kumar. Estimation of Mechanical and Tribological Properties of Epoxy- Based Green Composites. In *Green Approaches to Biocomposite Materials Science and Engineering*, pages 96–124. IGI Global, 2016.

[47] K. Griendling and D. Mavris. A Systems Engineering Approach and Case Study for Technology Infusion for Aircraft Conceptual Design. In *Advances in Systems Engineering*, pages 219–268. American Institute of Aeronautics and Astronautics, Inc., Reston, USA, 2014.

[48] Dr.-Ing. Lars Herbeck. Anforderungen an eine Faserverbund-Produktionstechnik. Technical report, Voith Materials, Braunschweig, 2009.

[49] K.-T. Hsiao and D. Heider. Vacuum assisted resin transfer moulding (VARTM) in polymer matrix composites. In *Manufacturing Techniques for Polymer Matrix Composites (PMCs)*, pages 310–347. Woodhead Publishing, 2012.

[50] C. F. Johnson and N. G. Chavka. Resin transfer molding core, preform and process, 1988.

[51] F. Y. C. Boey and S. W. Lye. Void reduction in autoclave processing of thermoset composites: Part 1: High pressure effects on void reduction. *Composites*, 23(3):261–265, 1992.

[52] C Soutis. Fibre reinforced composites in aircraft construction. *Progress in Aerospace Sciences*, 41(2):143–151, 2005.

[53] R. Blien. Class-A-Fläche, 2006.

[54] Jim Camillo. Adhesives Aid Body-in-White Assembly at VW. *Assembly Magazine*, 2014.

[55] K. Ashida. *Polyurethane and Related Foams: Chemistry and Technology*. Taylor & Francis Group, Boca Raton, 2007.

[56] Jan W. Gooch. Reaction Injection Molding, 2011.

[57] PURMOLD. PURMOLD Technology, 2017.

[58] J. H. Eckler and T. C. Wilkinson. Processing and designing parts using structural reaction injection molding. *Journal of Materials Shaping Technology*, 5(1):17–21, 1987.

[59] F.A. Shutov. Reaction Injection Molding Process. In *Integral/Structural Polymer Foams - Technology, Properties and Applications*, pages 92–109. Springer, Berlin Heidelberg, 1986.

[60] PlasticsU. Lessons, 2017.

[61] J. Wang, Q. Mao, and J. Chen. Preparation of polypropylene single-polymer composites by injection molding. *Journal of Applied Polymer Science*, 130(3):2176–2183, 2013.

[62] D. V. Rosato and Et Al. Specialized Injection Molding. In *Injection Molding Handbook*, pages 1197–1269. Kluwer Academic Publishers, 2000.

[63] BASF. COLO-Fast®WST® creates flush seals around panorama windscreens - Innovative PU glass encapsulation technology from BASF for Opel Astra GTC. Technical report, BASF Polyurethanes Europe, Lemförde, 2011.

[64] BASF. WST Presentation. In *BBG Innovation day*, Wien, 2014.

[65] J. van Dyck. Chemistry for better Engineering. Technical report, VKC-Centexbel, Kortrijk, 2016.

[66] Daniel Adis. WST PU-Anlage. Technical report, Daimler, Sindelfingen, 2015.

[67] Gerrit Conermann. *Qualifizierung eines PU-Umspritzungsprozesses für Leichtbaudächer in der Fahrzeugendmontage.* PhD thesis, Karlsruhe Institute of Technology, Sindelfingen, 2015.

[68] Sonderhoff. Sonderhoff - Engineering - Mischköpfe, 2015.

[69] Ch. Decker and B. Dormann. High Tech im Niederdruck - PU-Elastomerverarbeitung. *Fachmagazin für Polyurethanindustrie*, 32, 2005.

[70] Maschinenbau-Wissen.de. PUR-Mischkopf zur Verarbeitung von Polyurethan, 2017.

[71] Isotherm. PUR-Mixing heads, 2011.

[72] Fabio Utzeri. Carbondach C190 - Lieferantenanfrageunterlagen. Technical report, Daimler AG, Sindelfingen, 2013.

[73] BASF. Elastolit D/K/R - Rigid Integral- and RIM- Systems. Technical report, BASF Polyurethanes Europe, 2014.

[74] Exypnos. WSTplus.

[75] REFA. *Methodenlehre der Betriebsorganisation : Lexikon der Betriebsorganisation.* Hanser Fachbuchverlag, 1993.

Appendix A

Remaining DoE's

Lap-Shear Tests

For every test set in Table A.2 seven repetitions were performed. Therefore the outcomes listed are the averages. The abbreviations of the failure pattern are listed in Table A.1.

Table A.1: Abbreviations used for lap-shear tests

Abbreviation	Meaning
AF	Adhesion Failure
CF	Cohesion Failure
MF	Mixed Failure
SF	Substrate Failure

Table A.2: DoE summarizing all Lap-Shear Test Sets

Design of Experiments					
	Factors		**Responses**		
Run	**Pre-Treatment**	**Aging**	**max. Force [N]**	**Displ. [mm]**	**Failure Pattern**
1	Blank + Teroson	SA	4114	4.3	SF, MF
2	Blank + Teroson	CCH	3265	4.0	MF
3	Blank + Teroson	AHS	3779	4.3	MF
4	Blank + Teroson	Cata	3220	4.5	MF, SF
5	Sanding + Teroson	SA	3611	4.1	AF
6	Sanding + Teroson	CCH	2817	3.7	AF, SF
7	Sanding + Teroson	AHS	3327	4.0	MF
8	Sanding + Teroson	Cata	2872	4.3	AF, MF
9	Peel Ply + Teroson	SA	3624	4.0	AF
10	Peel Ply + Teroson	CCH	2906	3.9	AF, MF
11	Peel Ply + Teroson	AHS	3620	4.1	MF
12	Peel Ply + Teroson	Cata	2886	4.2	AF, MF
13	Blank + Primer	SA	2909	3.1	MF, SF
14	Blank + Primer	CCH	3254	4.2	MF
15	Blank + Primer	AHS	3782	4.3	MF, SF
16	Blank + Primer	Cata	2886	4.4	AF, MF
17	Sanding + Primer	SA	3276	4.2	SF
18	Sanding + Primer	CCH	2903	4.2	MF, SF
19	Sanding + Primer	AHS	3701	4.6	CF, SF
20	Sanding + Primer	Cata	2827	4.6	CF, SF
21	Peel Ply + Primer	SA	3217	4.3	AF
22	Peel Ply + Primer	CCH	2671	4.1	MF
23	Peel Ply + Primer	AHS	3527	4.5	MF
24	Peel Ply + Primer	Cata	2706	4.6	MF

Bond Line Thickness Tests

The print-through (PT) test DoE for different bond line thicknesses is shown in Table A.3.

Table A.3: DoE summarizing all print-through tests on bond line thickness

Design of Experiments				
	Factors			**Response**
Run	**Pre-Treatment**	**Aging**	**Bond line thickness [mm]**	**Print-through**
1	Blank + Teroson	after process	5	OK
2	Blank + Teroson	after process	10	OK
3	Blank + Teroson	after process	15	OK
4	Blank + Teroson	after process	20	slight PT
5	Blank + Teroson	SA	5	OK
6	Blank + Teroson	SA	10	OK
7	Blank + Teroson	SA	15	OK
8	Blank + Teroson	SA	20	slight PT
9	Blank + Teroson	CCH	5	OK
10	Blank + Teroson	CCH	10	OK
11	Blank + Teroson	CCH	15	OK
12	Blank + Teroson	CCH	20	slight PT
13	Blank + Teroson	AHS	5	OK
14	Blank + Teroson	AHS	10	OK
15	Blank + Teroson	AHS	15	slight PT
16	Blank + Teroson	AHS	20	slight PT
17	Blank + Teroson	Cata	5	OK
18	Blank + Teroson	Cata	10	OK
19	Blank + Teroson	Cata	15	OK
20	Blank + Teroson	Cata	20	slight PT
21	Blank + Teroson	2h at $105°C$	5	OK
22	Blank + Teroson	2h at $105°C$	10	OK
23	Blank + Teroson	2h at $105°C$	15	OK
24	Blank + Teroson	2h at $105°C$	20	slight PT
25	Blank + Teroson	after process	5	OK
26	Blank + Teroson	after process	10	OK
27	Blank + Teroson	after process	15	OK
28	Blank + Teroson	after process	20	slight PT
29	Peel-Ply + Teroson	SA	5	OK
30	Peel-Ply + Teroson	SA	10	OK
31	Peel-Ply + Teroson	SA	15	OK
32	Peel-Ply + Teroson	SA	20	slight PT
33	Peel-Ply + Teroson	CCH	5	OK
34	Peel-Ply + Teroson	CCH	10	OK
35	Peel-Ply + Teroson	CCH	15	OK
36	Peel-Ply + Teroson	CCH	20	slight PT
37	Peel-Ply + Teroson	AHS	5	OK
38	Peel-Ply + Teroson	AHS	10	OK
39	Peel-Ply + Teroson	AHS	15	slight PT
40	Peel-Ply + Teroson	AHS	20	slight PT
41	Peel-Ply + Teroson	Cata	5	OK
42	Peel-Ply + Teroson	Cata	10	OK
43	Peel-Ply + Teroson	Cata	15	OK
44	Peel-Ply + Teroson	Cata	20	slight PT
45	Peel-Ply + Teroson	2h at $105°C$	5	OK
46	Peel-Ply + Teroson	2h at $105°C$	10	OK
47	Peel-Ply + Teroson	2h at $105°C$	15	OK
48	Peel-Ply + Teroson	2h at $105°C$	20	slight PT

Crash Bar Tests

For the print-through tests on a crash bar sample, the DoE used for the test setup and result recording is presented in Table A.4. Since the test sets for the 1.5 mm and 3 mm bond gap could not be performed yet, the response entries are empty.

Table A.4: DoE summarizing all print-through tests on the crash bar samples

Design of Experiments				
	Factors			Response
Run	Pre-Treatment	Aging	Bond line thickness [mm]	Print-through
1	Blank + Teroson	after process	1.5	-
2	Blank + Teroson	after process	3.0	-
3	Blank + Teroson	after process	4.5	OK
4	Blank + Teroson	SA	1.5	-
5	Blank + Teroson	SA	3.0	-
6	Blank + Teroson	SA	4.5	OK
7	Blank + Teroson	CCH	1.5	-
8	Blank + Teroson	CCH	3.0	-
9	Blank + Teroson	CCH	4.5	S-shaped warping (transverse)
10	Blank + Teroson	AHS	1.5	-
11	Blank + Teroson	AHS	3.0	-
12	Blank + Teroson	AHS	4.5	S-shaped warping (transverse)
13	Blank + Teroson	Cata	1.5	-
14	Blank + Teroson	Cata	3.0	-
15	Blank + Teroson	Cata	4.5	S-shaped warping (diagonal)
16	Blank + Teroson	2h at 105°C	1.5	-
17	Blank + Teroson	2h at 105°C	3.0	-
18	Blank + Teroson	2h at 105°C	4.5	S-shaped warping (transverse)
19	Peel-Ply + Teroson	after process	1.5	-
20	Peel-Ply + Teroson	after process	3.0	-
21	Peel-Ply + Teroson	after process	4.5	OK
22	Peel-Ply + Teroson	SA	1.5	-
23	Peel-Ply + Teroson	SA	3.0	-
24	Peel-Ply + Teroson	SA	4.5	OK
25	Peel-Ply + Teroson	CCH	1.5	-
26	Peel-Ply + Teroson	CCH	3.0	-
27	Peel-Ply + Teroson	CCH	4.5	Dishing towards crash bar
28	Peel-Ply + Teroson	AHS	1.5	-
29	Peel-Ply + Teroson	AHS	3.0	-
30	Peel-Ply + Teroson	AHS	4.5	S-shaped warping (transverse)
31	Peel-Ply + Teroson	Cata	1.5	-
32	Peel-Ply + Teroson	Cata	3.0	-
33	Peel-Ply + Teroson	Cata	4.5	S-shaped warping (diagonal)
34	Peel-Ply + Teroson	2h at 105°C	1.5	-
35	Peel-Ply + Teroson	2h at 105°C	3.0	-
36	Peel-Ply + Teroson	2h at 105°C	4.5	S-shaped warping (transverse)

<div align="right">

Appendix B

</div>

Lap-Shear Result Diagrams

Figures B.1 and B.2 summarize the lap-shear strength and sample stiffness results of the sanded and peel-ply samples.

(a) Average Lap-Shear Strength

(b) Average Sample Stiffness
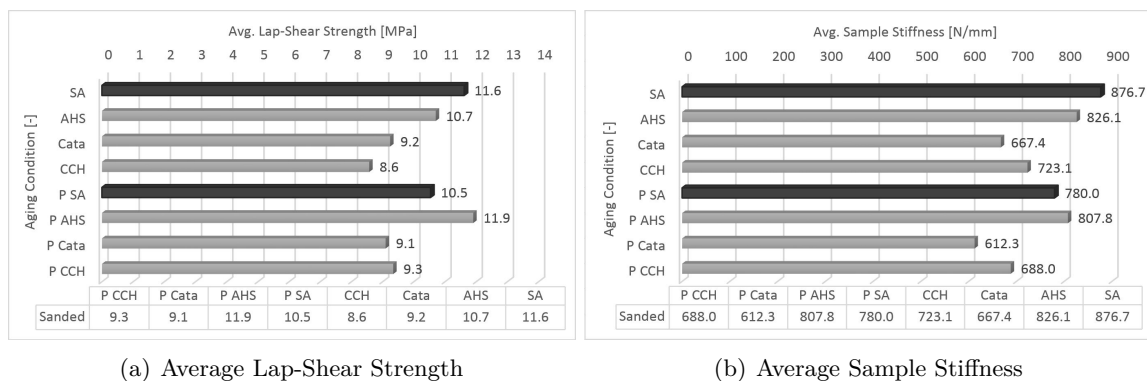
Figure B.1: Average Lap-Shear Strength and Sample Stiffness Results of Sanded Samples after Different Aging Conditions
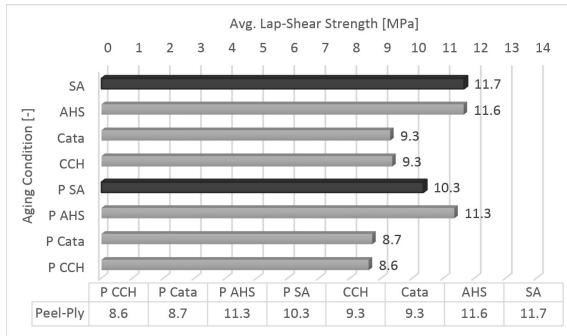
(a) Average Lap-Shear Strength
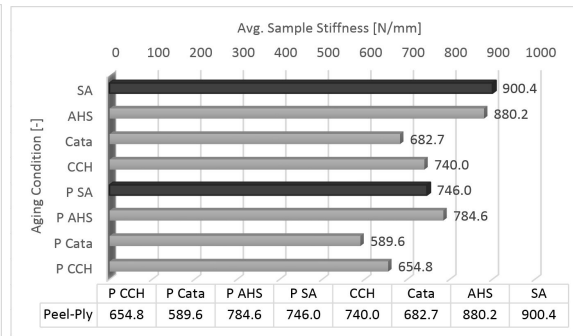
(b) Average Sample Stiffness

Figure B.2: Average Lap-Shear Strength and Sample Stiffness Results of Sanded Samples after Different Aging Conditions

Appendix C

Data Sheets

This appendix includes the data sheets of the Elastolit R 8919/107, the PUR used for all experiments, and the data sheets of the tested assembly adhesives, EFTEC EFBOND DA 217 and DA 620. Moreover, it contains the data sheets of the structural adhesive that is currently used to bond the CFRP subframe to the roof, Dow BETAPRIME 2850, and the primers Sika 209 D and Dow BETAPRIME5404, of which the latter was chosen to use for the experiments after the primer pre-test.

□ ▪ BASF

We create chemistry

Anwendung:

Dieses System ist eine Prozess-optimierte Version von Elastolit R 8919/101/OA48 und dient zur Herstellung von zähharten, elastischen Formteilen im Dichtebereich von 900-1200 kg/m³

Chemischer Aufbau:

A-Komponente: Zubereitung auf Basis: Polyol, Katalysator, Zusätze
B-Komponente: Zubereitung auf Basis: 4,4'-Methylenediphenyl Diisocyanate; Diphenylmethane-4,4'-Diisocyanate
= Iso 134/7

Lieferform:

Die Art der Anlieferung der Komponenten erfolgt in Absprache mit unserem Verkauf.

Lagerung, Aufbereitung:

Polyurethan-Komponenten sind feuchtigkeitsempfindlich. Sie sind daher stets in dicht verschlossenen Gebinden aufzubewahren. Die A-Komponente muss vor der Verarbeitung durch gründliches Aufrühren homogenisiert werden. Nähere Informationen sind dem gesonderten Informationsblatt „Verarbeitungsvorschläge für die aromatischen Scheibenumguß-Systeme" zu entnehmen.

Mögliche Gefahren:

Die B-Komponente (Isocyanat-Komponente) reizt die Augen, Atmungsorgane und die Haut. Sensibilisierung durch Einatmen und Hautkontakt ist möglich. MDI ist gesundheitsschädlich beim Einatmen. Bei der Verarbeitung sind die in den Sicherheitsdatenblättern beschriebenen Vorsichtsmaßnahmen zwingend zu beachten. Dies gilt auch für mögliche Gefahren der A-Komponente (Polyol-Komponente) sowie weiterer Zusatzkomponenten. Siehe auch unser gesondertes Informationsblatt "Sicherheits- und Vorsichtsmaßnahmen bei der Verarbeitung von Polyurethan-Systemen.
Nutzen Sie unser Trainingsangebot "Sicherer Umgang mit Isocyanaten".

Abfallbeseitigung:

Nähere Informationen sind den länderspezifischen Druckschriften zu entnehmen.

Bedarfsgegenstände, Medizinprodukte:

Ist beabsichtigt, aus den Produkten der BASF Polyurethanes GmbH Bedarfsgegenstände (z.B. Gegenstände mit Lebensmittel- oder Hautkontakt, Spielzeug) oder Medizinprodukte herzustellen, sind nationale und internationale Gesetze und Regelungen zu berücksichtigen. Wo solche nicht existieren, sollten die Bedarfsgegenstände bzw. Medizinprodukte den in der Europäischen Union geltenden gesetzlichen Anforderungen genügen. Rücksprache mit unserer Vertriebsabteilung und der Abteilung Ökologie und Produktsicherheit wird dringend empfohlen.

,

Elastolit® R 8919/107

BASF
We create chemistry

Komponentendaten:

Merkmal	Einheit	A-Komp.	B-Komp.	Vorschrift
Dichte (25°C)	g/cm³	1,03	1,20	G 133-08
Viskosität (25°C)	mPa·s	1080	125	G 133-07
Mindesthaltbarkeit	Monate	6	6	

Becherversuch

Merkmal	Einheit	Wert	Vorschrift
Komponenten-Temperatur	°C	20	
Einwaage (Index 105)	Gewichtsteile	A : B = 100 : 58	G 132-01
Startzeit	s	15	
Steigzeit	s	25	
Rohdichte (freigeschäumt)	kg/m³	950	

,

Elastolit® R 8919/107

□ ▪ BASF

We create chemistry

Typische Physikalische Eigenschaften:

Merkmal	Einheit	Meßwerte	Vorschrift
Rohdichte	kg/m³	1070	DIN EN ISO 1183-1
Shore-Härte	A	89	DIN ISO 7619-1
Zugfestigkeit Stab S1	MPa	12	DIN 53504
Zug-Modul	MPa	25	DIN 53504
Bruchdehnung	%	185	
Weiterreißfestigkeit (Graves)	N/mm	25	DIN ISO 34-1, B (b)
Weiterreißfestigkeit (Graves)	N/mm	42	ASTM D 624
Schwund	%	1,2	-

Die Eigenschaften wurden an maschinell hergestellten Prüfplatten (Dicke 4mm) ermittelt. Die Prüfplatten wurden in einer temperierten Alu-Form (Formtemperatur 75°C, Entformzeit 45 sec.) hergestellt.

EFBOND DA 217

General description

EFBOND DA 217 is a humidity-curing, one component, polyurethane adhesive for the direct glazing of automotive glasses. The adhesive shows

- low conductivity: the product is a low conductive product, which minimises the risk of contact corrosion between the adhesive and the car body.
- high shear modulus: the product has a high shear modulus which increases the stiffness of the car body significantly.
- very good direct adhesion to paints.

Application

The application is done by extrusion out of drums, hobbocks or cartridges. The recommended application temperature is 35 - 60°C. For uniform extrusion rates and application conditions, the application temperature of the adhesive has to be kept constant.

Storage / Transport

Store between 0 and 35 °C, in closed packaging.
During transport the storage temperature may shortly (2-4 days) go below or above these limits. When this happens, the material has to be climatized at room temperature before application: Drums, hobbocks and packed cartridges need 1-2 days. Single cartridges need 3-4 hours or may directly be heated to application temperature, when heating time is extended by up to 30 minutes.

EFTEC AG
Hofstrasse 31
CH-8590 Romanshorn

Phone   +41 (0)71 466 43 00
Fax   +41 (0)71 466 43 01

Mail   info@eftec.ch
Internet   www.eftec.ch

EFBOND DA 217

Technical properties

Binder	reactive polyurethane prepolymer	
Colour	black	
Density	1'300 - 1'350 kg/m^3	
Hardness (Shore A)	70 - 80	
skin building time	30 – 60 min	(23°C / 50 % r.h.)
Tensile strength	6 - 14 MPa	
Elongation at break	> 300 %	
Shear modulus (10% gliding)	2.5 - 3.5 MPa	
Lap shear strength	> 3.0 MPa	(23°C / 50 % r.h.)
Specific electrical resistance	> 10^8 Ω·cm	

EFTEC AG
Hofstrasse 31
CH-8590 Romanshorn

Phone	+41 (0)71 466 43 00
Fax	+41 (0)71 466 43 01
Mail	info@eftec.ch
Internet	www.eftec.ch

EFBOND DA 620

General description

EFBOND DA 620 is a polyurethane adhesive for semi-structural bonding in automotive industry. The adhesive has a high shear modulus. Therefor the product increases the stiffness oft he car body significantly. **EFBOND DA 620** shows very good direct adhesion, even after overburning, on different electro coatings and OEM clearcoats. It may be ued as single component adhesive or accelerated with EFBOND BA pastes.

Application

The application is done by extrusion out of drums, hobbocks and cartridges. The recommended application temperature is 40 – 70°C. For uniform extrusion rates and application conditions, the application temperature of the adhesive has to be kept constant. The adhesive cures even at 30°C and 80% r.h. without forming bubbles or tunnels.

Repair

A freshly cutted bead of **EFBOND DA 620** may be bonded with itself or, after testing, with other polyurethane adhesives.

Storage / Transport

Store between 0 und 35°C in closed packaging.
During transport the storage temperature may shortly (2-4 days) go below or above these limits. When this happens, the material has to be climatized at room temperature before application: Drums, hobbocks and packed cartridges need 1-2 days. Single cartridges need 3-4 hours or may directly be heated to application temperature, when heating time is extended by up to 30 minutes.

EFTEC AG
Hofstrasse 31
CH-8590 Romanshorn

Phone   +41 (0)71 466 43 00
Fax   +41 (0)71 466 43 01

Mail   info@eftec.ch
Internet www.eftec.ch

EFBOND DA 620

Technical properties

Binder	reactive polyurethane prepolymer
Appearance	black paste
Flow, 23°C - 4mm / 4bar	25 – 35 g/min
Density	1'250 – 1'350 kg/m^3
Open time (23 ºC / 50 % r.h.)	20 – 30 min
Hardness Shore A	75 – 90
Elongation at break	> 300 %
Shear modulus (10 % gliding)	> 8 MPa
Lap shear strength after 7 days (23 ºC / 50 % r.h.)	> 8.0 MPa
Curing rate 23°C / 50% r.h.	> 3 mm / 24 h
Tear resistance	> 5 N/mm

EFTEC AG
Hofstrasse 31
CH-8590 Romanshorn

Phone	+41 (0)71 466 43 00
Fax	+41 (0)71 466 43 01
Mail	info@eftec.ch
Internet	www.eftec.ch

Dow

Preliminary Technical Data Sheet
PUR Semi Structual Adhesive

Dow Automotive

BETAMATE 2850

Description / Application:

BETAMATE 2850 is a semi-structural two component polyurethane adhesive with moderate curing speed at room temperature. **BETAMATE 2850** is designed for hybrid application where bigger differences are expected in the thermal expansion of dissimilar materials and a long open time is required. **BETAMATE 2850** integrates unique properties like high modulus, high strength and high elongation properties in one system.

All Dow Automotive products are primarily developed in co-operation with the automobile manufacturers, according to their needs and their specifications; they are approved for the specific applications as defined by the customer.

The use of the product other than approved application have to be released in written form by the Technical Service of Dow Automotive.

Technical Data:

The data are based on laboratory results, climate 23°C / 50% r.h.
The results represent typical data and not specifications

Basis	Isocyanate, PU prepolymers Polyol, Polyol
Colour	Hardener: black Resin: white
Density	Isocyanate: 1.17 g/cm^3 Polyol: 1.42 g/cm^3
Viscosity **Extrusionrate (Ballan) 4bar/2mm nozzle**	Isocyanate approx 25g/min. Polyol: approx 30g/min.
Mixing Ratio (by Volume A:B)	1:1 +/- 0.10
Application temperature	18 - 28°C Please note: The temperature has a strong influence on the curing speed / open time
Open time	10-15 minutes
Handling strength at RT **(>0.25MPa Lap Shear strength) reached within**	approx. 90min.
Handling strength at 80°C **(>0.25 MPa Lap Shear strength) reached within**	approx. 20min.

More details relating to curing behavior are

available via our sales force

Tensile Strength (DIN 53 504)	approx. 10 MPa
Elongation at Break (DIN 53 504)	approx. 250%
Lap Shear Strength	11 MPa (bond line height 2.0mm)
E-Modulus (DIN 53504)	24MPa
G-Modulus (According to DIN EN 6721-2/Torsion-pendulum)	9 MPa after 7 days
Glas transition temperature (DSC)	approx. -45℃
Shore A Hardness (DIN 53505)	70 +/- 5
Heat Resistance	-40℃ to 100℃, short term up to 160℃ (0.5h)
Chemical Resistance	Good against aqueous chemicals, gasoline and alcohol. Fairly good against ester, ketones and aromatic and chlorinated hydrocarbons.
Surface preparation	All surfaces must be free from dirt, dust, grease and oil. In certain cases it could be necessary to use an adhesion promoter. Preliminary tests are recommended.
Cleaning	Uncured BETAMATE 2850 can be removed with BETACLEAN 3000. Cured BETAMATE 2850 can only be removed mechanically. Immerse tools in BETACLEAN 3000.
Shelf life	6 month for BETAMATE 2850 at +5℃ to +25℃, in unopened containers.
Containers	a) Cartridges of 2 x 290 ml: the material can be extruded by using the BETAPOWER pneumatic gun and a static mixer.
	b) Pails of 22 l and 200l content: application with usual closing pumps provided with a static mixer. We would be pleased to assist you in constructing and choosing your pump equipment.
Protection measures	See health and safety data sheet.

Attention

Following should be taken in consideration when BETAMATE 2850 is being processed together with our primer systems:

The opentime of the primer BP 5404, 5500 and 5061 Is between 30s and 10min at 23℃/50%rh. If the primer open time has exceeded >10min, a single time reactivation with the same primer is possible.

Prior to the bonding it is important to control the open time of the adhesive

Technical Data Sheet

BETAPRIME 5404

Description / Application:

Primer without toluene for plastic and paint substrates. Undercoat as bonding surface for all BETASEAL and BETAMATE E products.

All Dow Automotive products are primarily developed in co-ordination with the automobile manufacturers, according to their needs and their specifications; they are approved for the specific applications as defined by the customer.

The use of the product other than approved application have to be released in writing by the Technical Service of Dow Automotive.

Technical Data:

Basis	Polyisocyanates
Colour	Black
Pigments	Carbon black
Density	0.91 +/- 0.02 g/cm^3 at 23°C
Viscosity (DIN-cup 4)	< 16 s at 23°C
Flash Point	-8°C
Processing temperature	Ideal 10 - 40°C
Evaporation time	Min: 30 s at 23°C/50% rh depending on the application method - the film must be touch-dry.
	Max: 8-24 h, depending on the type BETASEAL used, an reactivation with BETAPRIME 5404 or BETAWIPE 4000 is possible.
Instruction for use	Shake container well before opening. Continue to shake for at least 60 sec after steel balls inside the container are released.
	Caution! The product is extremely hygroscopic! Close containers immediately to preserve remaining contents. Use up remainder within a few days
Bonding surface preparation	Clean contaminated areas with BETACLEAN 3350. Verify compatibility or consult our technical service department.
Processing equipment	Primer applicator, primer application unit (container with primer application head and felt).
Cleaning	Clean equipment with BETACLEAN 3000
Shelf life	6 months at +5 - +25°C in unopened containers (see the "use before" date printed on the container)

,

Sika® Primer-209 D

Polyurethane-Based Black Primer

Technical Product Data

Chemical base	Black pigmented solvent-based polyurethane solution
Color	Black
Density (CQP[1] 006-3 / ISO 2811-1)	8.35 lb/gal (1 kg/l) approx.
Viscosity[2] (CQP 029-3 / ISO 3219)	15 cps approx.
Flash point (CQP 007-1 / ISO 13736)	-4°C (25°F)
Solid content	30% wt. approx.
Application temperature	15° - 35°C (59° - 95°F)
Application Method	Felt or foam applicator
Coverage	150 ml/m^2 approx.
Drying Time[3] minimum	10 min.
maximum	24 hours
Storage	Store in sealed container in a cool dry place
VOC	704 g/l
Shelf life	9 months

[1] CQP = Corporate Quality Procedure   [2] 23°C / 50% r.h.   [3] Drying time dependant on temperature and application specifics

Description

Sika® Primer-209 D is a black, moisture-curing low viscosity primer specifically formulated for the treatment of painted surfaces or plastics prior to the application of Sikaflex® direct-glazing adhesive.

This product is suitable for experienced professional users only. Tests with actual substrates and conditions have to be performed to ensure adhesion and material compatibility.

Areas of Application

Sika® Primer-209 D is suitable for application to the following substrates:

- Paints   Acrylics
              Alkyds/Melamine
              Powder coatings
              Baking varnishes
- Plastics   Acrylic (PMMA)
              Polycarbonate
              Polystyrene
              PES-FRP
              EP-FRP
              ABS
              PVC

Due to the individual chemical composition of the formulations and specific furnace conditions, we recommend doing adhesion tests for each paint and plastic. Always seek the paint or plastic manufacturer's advice before using the primer on plastics that are prone to stress cracking, such as acrylics, polycarbonates or ABS.

Industry